Available online at www.ilcpa.pl

International Letters of Chemistry, Physics and Astronomy

16 (2014) 1-85 ISSN 2299-3843

M O N O G R A P H

Probability of Solar Flares Turn Out to Form a Coronal Mass Ejections Events Due to the Characterization of Solar Radio Burst Type II and III

Zety Sharizat Hamidi

2014

Probability of Solar Flares Turn Out to Form a Coronal Mass Ejections Events Due to the Characterization of Solar Radio Burst Type II and III

Zety Sharizat Hamidi

School of Physics and Material Sciences, Faculty of Sciences, MARA University of Technology, 40450 Shah Alam, Selangor, Malaysia

E-mail address: zetysh@salam.uitm.edu.my

ABSTRACT

The solar flare and Coronal Mass Ejections (CMEs) are well known as one of the most massive eruptions which potentially create major disturbances in the interplanetary medium and initiate severe magnetic storms when they collide with the Earth's magnetosphere. However, how far the solar flare can contribute to the formation of the CMEs is still not easy to be understood. These phenomena are associated with II and III burst it also divided by sub-type of burst depending on the physical characteristics and different mechanisms. In this work, we used a Compound Astronomical Low-cost Low-frequency Instrument for Spectroscopy in Transportable Observatories (CALLISTO) system. The aim of the present study is to reveal dynamical properties of solar burst type II and III due to several mechanisms. Most of the cases of both solar radio bursts can be found in the range less that 400 MHz. Based on solar flare monitoring within 24 hours, the CMEs that has the potential to explode will dominantly be a class of M1 solar flare. Overall, the tendencies of SRBT III burst form the solar radio burst type III at 187 MHz to 449 MHz. Based on solar observations, it is evident that the explosive, short time-scale energy release during flares and the long term, gradual energy release expressed by CMEs can be reasonably understood only if both processes are taken as common and probably not independent signatures of a destabilization of pre-existing coronal magnetic field structures. The configurations of several active regions can be sourced regions of CMEs formation. The study of the formation, acceleration and propagation of CMEs requires advanced and powerful observational tools in different spectral ranges as many 'stages' as possible between the photosphere of the Sun and magnetosphere of the Sun and magnetosphere of the Earth. In conclusion, this range is a current regime of solar radio bursts during CMEs events.

***Keywords*:** Solar flare; Coronal Mass Ejection; solar burst; type II; type III; space weather

Reviewer

Prof. Aleksy Patryn
Koszalin University of Technology, Koszalin, Poland

TABLE OF CONTENTS

INTRODUCTION

1. 1. INTRODUCTION

The main theme of this work is to investigate the dynamical structure of solar radio burst type III and II burst in the low frequency radio region. The region from 45 - 870 MHz will be focused. In this case, how large solar flares can relate to the Coronal Mass Ejections (CMEs) events will be highlighted through statistical data and selected events. Our data analysis concentrated on solar burst images and spectra observed by e-CALLISTO (Compound Astronomical Low-frequency, Low-cost Instrument for Spectroscopy in Transportable Observatories) network during the phase of the solar flares and CMEs events.

An extensive experimental and theoretical work has succeeded in elucidating many observational and characteristics of radio bursts in understanding their physical nature. Radio observations have been carried out since 1944 when J.S Hey discovered that the Sun emits radio waves [1]. This method reveals us to study energy release, plasma heating, particle acceleration and particle transport in solar magnetized plasma. However, the dynamics of the solar corona is still not understood, and new phenomena are unveiled every year. This region covers from 15 – 30 GHz. Thus, the radio spectrum is limited at the low frequency side of the ionosphere and at the high frequency region by the troposphere.

One major finding in solar radio emission is the understanding of thermal radio emission of the large scale structure and physical state of the chromospheres and corona with a rapid transition between them from hot plasma. In the beginning 1960s, radio observations played a central role in establishing the long-standing view. A full characteristic of metric radio bursts and their classification were presented by [2]. In their contribution, they have proved a strong correlation between bursts and solar flares and successfully determined two possible phases of particle acceleration. At the first phase, this region has combined with observations by Hard X-ray (HXR) emission, microwave (centimetre wavelengths) emission and m-λ type III bursts. It was found that during large flares, a second phase occurs within 10 minutes after the first. In this phase, most observations carried out at meter wavelengths [3,4].

There are two solar activities that will be highlighted in this study (i) solar flares and (ii) Coronal Mass Ejections (CMEs). It is generally accepted that solar flares provide as one of the most suitable laboratories to study particle acceleration and related high-energy processes, because of the proximity of the Sun and abundant observations available. Solar flares were first observed by William Carrington in England in 1859. In this case, the electron, proton and heavy nuclei are heated and accelerated in the solar atmosphere as the magnetic energy released.

Meanwhile, Coronal Mass Ejections are well known as one of the most enormous eruptions of magnetized plasma expelled from the Sun into the interplanetary space, which potentially create major disturbances in the interplanetary medium and trigger severe magnetic storms when they collide with the Earth's magnetosphere. These two phenomena are associated with type III and II burst respectively. It should be noted that an individual flares and CMEs are widely different. In general and how these mechanisms operate in solar flares and CMEs in particular based on solar radio burst characteristics.

Until now, there has been an increasing interest in the space weather program has stimulated interest in this issue. A new experiment approach by e-CALLISTO with 24 hours

monitoring and further development of a model of the theory are hoping to meet the current knowledge about the Sun behaviour.

1. 2. BACKGROUND THEORY

The existence of a clear correlation between the observed radio flux and solar activity was found since the first observations of solar radio emission in the late 1940's [1]. The study of solar flares and CMEs variations from the corona magnetic region is the most active manifestation of solar activity and one of the main solar activities is of scientific interest because it reveals the furthering knowledge of the Sun. Interestingly, among different types of observation, the ground-based by using optical and radio telescope still give the best result in monitoring the solar activities.

This study concerned about Coronal Mass Ejection related with solar flares. The solar flares and CMEs are usually accompanied by solar radio bursts and the signals are usually can be characterized by background levels of radiation upon which are superimposed bursts. Solar flares and CMEs monitoring in radio region is very important in order to identify the active flares sources based on their nature and emission mechanisms and to relate their properties with plasma parameters in flaring regions [5]. These bursts originate by bremsstrahlung, gyrosynchrotron and plasma radiations.

It is well known that the characteristics of the bursts vary with wavelength. Bursts in the meter – wave range (12 m to about 50 cm) are classified by spectral type. They almost invariably occur at sharp inversions of the sign of the longitudinal field, in places where the magnetic field gradient is so steep that only a force-free field, with strong currents flowing along the field lines could obtain. The surface migration of magnetic elements (in particular sunspots) builds up these currents and through the flare events. A sunspot or active region motions are believed to contribute a complicated interaction of magnetic field, convection and solar rotation [6]. This field can fall to a much lower energy potential field, usually by means of magnetic reconnection. The emission of the spikes usually occurring on very short time small spatial scale is very significant to correlate the elementary processes of the magnetic field annihilation in the energy release region of the solar flare [7,8] while second fragmentation of the magnetic fields directly in radio source [9,10].

With higher temporal resolution, radio apparatus with a complex interrelated analysis could offer a high quality data concerning small and short scale physical processes as well as the main properties of the area involved [11-13].

A new solar cycle of 24^{th} has started since 4 January 2008. It is believed that the 24^{th} solar cycle will be less energetic than the last maximum in 2002 – 2003. Overall energetic eruptions seem to be less frequent in cycle 24 as shown by the lower number of type II radio bursts, full halo CMEs, and interplanetary shocks [14]. The profile of cycle 24 was determined by the maximum phase of cycle 23 and the deep minimum of preliminary phase of cycle 24 [15]. Decade observations have also revealed that solar protons could sometimes be accelerated up to tens of GeV in some intense solar energetic process. The latest observations are extremely deficient in the radio and X-ray synoptic and diagnostic influence on these coronal phenomena rich of physics they could reveal.

In this work, the study on the radio bursts type II and III from solar active regions is proposed. The most important results of this study are to find out the current correlations between total duration, peak, flux and total energy of extended meter of radio emission and compare with an X-ray observation.

1. 3. PROBLEM STATEMENT

The origin and persistence of solar activity are one of the basic problems of solar physics. Solar activities are not a stationary or temporally homogenous process, and therefore, the behaviour of various solar indices depends on the time interval under study. Generally, solar activities will base on solar indices such as flares, plages and sunspot and the measurement of solar radiation at different wavelengths. Although solar radio observations have been made for more than six decades, there is an increasing concern on results from the observations because it is very limited. This is due to the observation is only during the day there is no continuity data for 24 hours daily. Moreover, their short time behaviour is generalized for a long period of solar activity which is inappropriate in the non-stationary process developed on the Sun.

Though there are many studies individually on burst associated with CMEs and flares, a comprehensive study of the important characteristics are still rare. Questions have been raised about to what extent solar flares and CMEs form. In order to achieve these objectives, several key research questions that need clarification are addressed throughout this study. However, an acceleration of charged particles as an internal property of energy release in solar flares and CMEs are not yet been fully understood in spite of the significant progress achieved recently [16,17].

One major theoretical issue that has dominated the field for many years' concerns and the most interesting problem of solar radio astrophysics is the study of the generating mechanisms of radio bursts. The most relevant observations for such studies are the measurements of dynamic spectra and positions of radio burst sources as a function of frequency and time. So far, however, at a meter and decametre wavelength, the phenomena of most interest, burst and storms vary rapidly from second to few hours. Therefore, the observations must be made with high time resolution over the entire frequency range of interest.

The other most outstanding problems are in understanding the microphysical nature driving solar bursts. In solar atmosphere layer very dynamic magneto plasma on various time scales from hours to tens of milliseconds, which reflect different magneto plasma processes connected to the energy release driving the bursts. However, this process is believed to be homogenous at large scale. Such elementary process is very difficult to be detected directly due to the limitation of observational resolution of telescope and instrumentation.

Since there remain many unsolved processes for particle acceleration and radio emission of these solar radio bursts, monitoring of their observation is significant and the most relevant in solar coronal physics.

1. 4. OBJECTIVES

The solar radio burst type II and III components are the subject to be investigated further in this study. The aim of the present work is to make a comprehensive and detailed analysis of this event and then put forward an idea about the relation between the solar radio burst and CMEs mechanism.

In general, this research is aimed at:

1. To investigate the tendencies of solar radio burst type III form solar radio burst type II based on statistical properties.

2. To evaluate the correlation between total duration, distribution of frequency, occurrences total energy of both radio burst in meter region.
3. To correlate and comprehend other parameters that might contribute the behaviour of both solar radio bursts associated with solar flare and Coronal Mass Ejections (CMEs).

Nevertheless, it was not the aim of this research to study on the impact of this phenomenon to the Earth critically, although a general conclusion regarding the effect of the space weather will make.

1. 5. SIGNIFICANCE OF STUDY

Solar radio bursts potentially provides possibilities of important phenomena in solar physics. It is an ideal indicator on investigating acceleration processes which are responsible for higher excited velocities. Besides, it also can be used as natural plasma probes traversing the corona and the interplanetary space, thus providing various space plasma parameters due to the various wave-particle and wave-wave interactions.

This study aims to demonstrate at least, a portion of type II and III radio bursts observed in the corona occur in the presence of CMEs by understanding the scenario of both solar radio bursts. A possible mechanism is discussed for the origin of such an emission associated with a solar flares evolving in the leading edge of the CMEs frontal structure.

1. 6. SUMMARY

The material in this thesis is therefore structured from the current development of the new concept of observing method of application by using e-CALLISTO (Compound Astronomical Low-frequency, Low-cost Instrument for Spectroscopy in Transportable Observatories) network data, which is under the International Space Weather Initiative (ISWI) project covering the full processing path from raw data and detector responses to concrete physical parameter results of solar radio burst type II and III. This work provided an overview of study including its background, rationale and significance.

THE SUN, SOLAR FLARE AND CORONA MASS EJECTIONS

2. 1. INTRODUCTION

The Sun is considered as one of the strongest radio sources and observation in radio region can provide evidence on structures throughout the solar atmosphere. It is a unique and the closest star shines by converting protons into alpha particles. It has been classified as a main sequence star with spectral classification G2V. The transportation of energy from the central regions of the Sun is primarily through photon radiation, although electron conduction contributes in the innermost region and convection dominates near the surface. However, the dynamical behaviour of the Sun exhibits a variety of physical phenomena, some of which are still not at all or only barely understood due to the complexity of the structure of the Sun. Along the process, many research works have done to fulfil the objectives of this study.

Solar astronomy can be regarded as a mature field of roughly 150 years of age. To put this into perspective, our Sun is about 4.6 billion years old and is approximately half way through its lifetime. The visible solar disc has a diameter of 1.4×10^9 m when viewed from Earth the Sun subtends an angle of about 0.5^o. Its mass is 1.989×10^{30} kg and its luminosity is 3.85×10^{26} W [18]. The structure of the Sun is determined by the conditions of mass conservation, momentum conservation, energy conservation and the mode of energy transport. Sun can be practically studied at all radio frequencies, from the ionosphere cut-off of order 10 MHz (λ = 30 M) till sub-millimeter domain above 300 GHz ($\lambda \leq$ 1mm). This region lies in Rayleigh – Jean limit $hv \ll kT$ and therefore the radio flux is proportional to the brightness temperature. The Sun's energy is generated by nuclear fusion of hydrogen by the proton- proton chain in the core, which extends out to around 0.2 R$\odot$. This core has a temperature and electron density of around 15 MK and 10^{34} cm^{-3}. In principle, the energy generated and travels outwards through the Sun's interior. Initially, the temperature gradient and opacity are low enough for the energy to be transported by radiation. However, at roughly 0.7 R$\odot$ the temperature has cooled to 1MK and a steep temperature gradient causes the Schwarzschild criterion to be broken. This instability leads to the onset of convection. In the convection zone, hot material rises upwards to the visible solar surface, or photosphere. The effects of this can be realized on the photosphere as granulation cells which are around 1,000 km in diameter. The centres' of these cells are bright where hot material rises. Larger scale convection effects can be seen as supergranulation cells which have diameters of around 30,000 km.

2. 2. ATMOSPHERE OF THE SUN

In general, the atmosphere of the Sun is divided into three regions with different physical properties. The photosphere is generally considered to be the surface of the Sun with 200 km thickness where the sun's energy is transfer by radiation form. It is one of the coolest layers of the sun with a temperature of 6000 K, and it has a density of about 10^{-6} kgm^{-3}. It is comprised of about 73.5 % hydrogen and 25 % helium, with the other 1.5 % primarily consisting of oxygen and carbon. The photosphere shines about 398,000 times. At this region, the diameter of the Sun is 1.39 $x10^6$ km. There is a large magnetic disturbances sometimes break through the photosphere and cause sunspots known as a darker regions [19].

Above this layer, lies the rarer and more transparent known as the chromosphere. In this region, hydrogen is almost wholly ionized in the upper chromosphere. Chromospheres roughly 2,500 km thick dominated by the super granular structure. These granular exhibits as a convective cell that tends to sweep relatively weak magnetic fields to the edges. The temperature of the chromosphere rises monotonically [20]. One still unresolved puzzle about the chromospheres is why at some frequencies (at least 10 −100) GHz the polar coronal holes appear brighter than the rest of the quiet Sun due to corresponds to an elevated temperature in the upper chromosphere in coronal holes relative to normal quiet Sun. The phenomenon is especially well suited to study via radio emission due to the unique sensitivity of radio waves to this height range in the chromosphere. There is some evidence that all coronal holes, even those not at the poles, are brighter. This means that the temperature of the lower chromospheres is greater at an equivalent optical depth. When viewed in Hα these features appear dark and are known as filaments, or appear bright (when viewed over the limb) and are known as prominences. The filament, or prominence, disruption is often observed in the pre-flare phase of a solar flare and CMEs.

Meanwhile, the corona extends from the top of a narrow transition region to Earth and beyond has a temperature millions of degrees which is still consider as a mysteries properties. It composed by protons, electrons an uncertain amount of helium nuclei and a small portion of highly ionized heavier atoms. It can be observed clearly during eclipse and where the solar wind originates. The overall shape of the corona varies with the solar cycle; near sunspot maximum. The Figure 1 below shows the structure and atmosphere of the Sun.

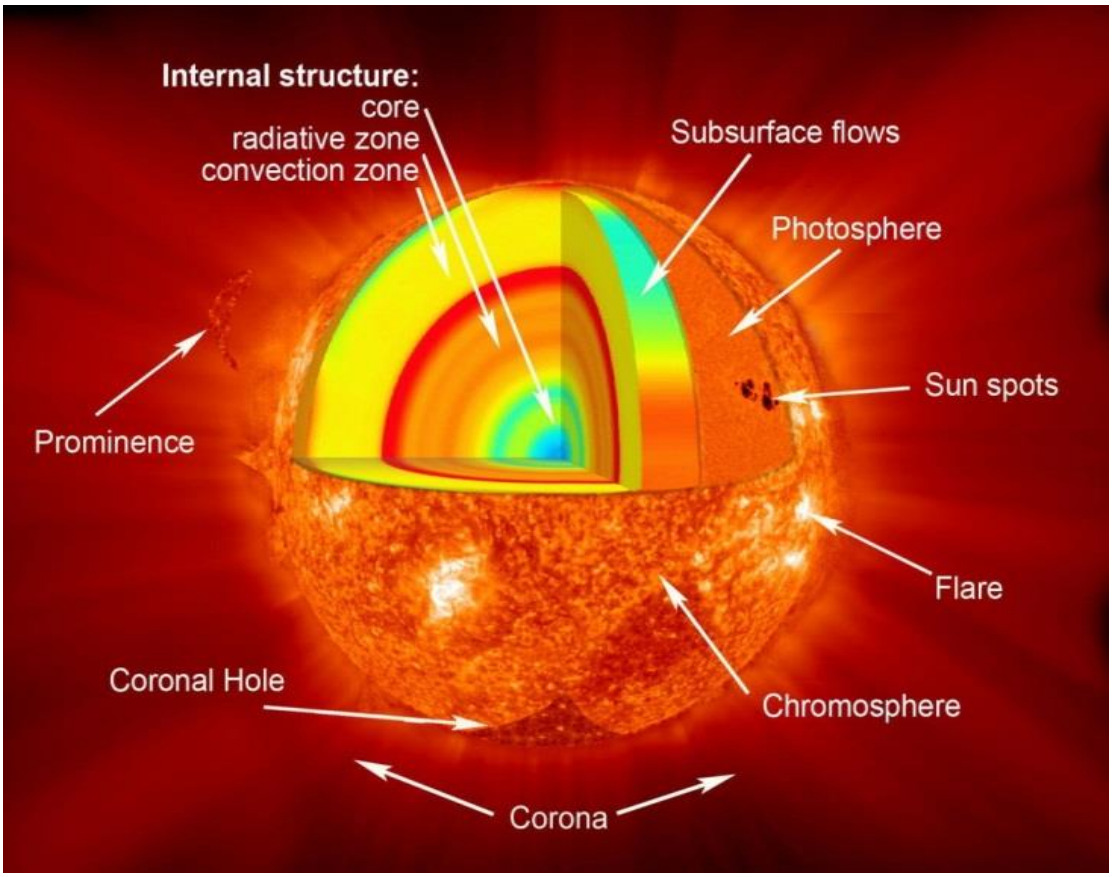

Figure 1. The structure and atmosphere of the Sun.

Each region of the Sun also has its own characteristics and the behaviour of physical properties of each layer also is different. Figure 2 illustrates the schematic diagram of temperature and gas mass density in the solar photosphere, chromosphere and lower corona, including the transition region.

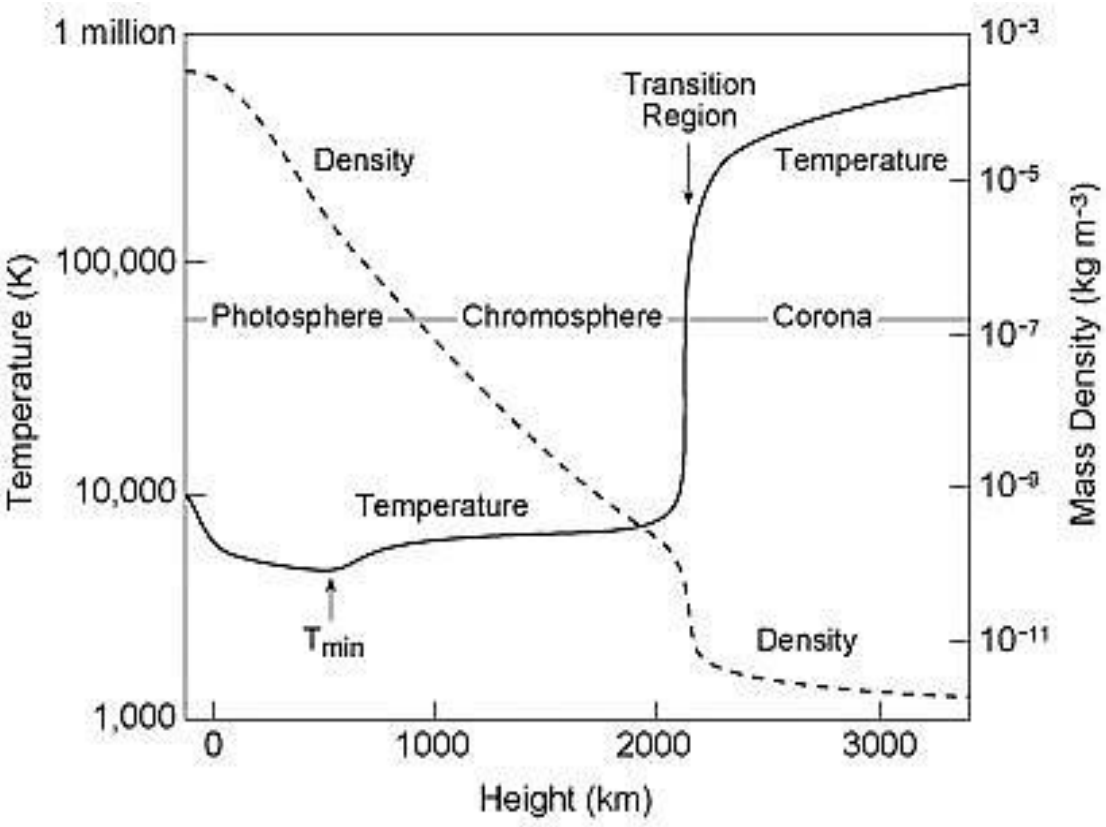

Figure 2. Schematic diagram of temperature and gas mass density in the solar photosphere, chromosphere and lower corona, including the transition region.

Monitoring the solar activity based on solar events from photosphere till interplanetary medium is generally for space weather condition. Considering that matter, radio index F10.7 index, is often used as a proxy for the Sun's influence on parameters measured on the earth such as the temperature in a given atmospheric layer.

Although Coronal Mass Ejections (CMEs) and solar flares are two different events, it could not be denied that CMEs occur during large solar flares. Energy partition of both events at the same time also has been studied [21]. CMEs are thought to explode just before the eruption of solar flares. Both events are associated with high energy particles and depend on the magnetic of the Sun.

The solar flares and CMEs can stimulate plasma oscillations which can release radiation at metric and decametric wavelengths. Metric radio burst is normally a non-thermal particles accelerated and trapped during those events [22]. In the presence of flares, strong radio bursts are observed over a broad frequency range. Whereas it is well established that flares do not drive CMEs, both of them correspond to different aspects of the same magnetic energy release.

2. 3. SOLAR FLARE

Solar flare is considered as a high energetic and complicated phenomenon in which mass eruptions occur, energetic particles are generated and highly energy radiations are emitted. During a flares, large quantities of energy are transferred between the corona and chromosphere through thermal conduction, non-thermal particle beams, radiation transport and mass motions. This event is triggered by fast drift of individual sunspot proper motion within complex magnetic configuration due to instabilities of equilibrium of coronal magnetic field [23]. Since the magnetic force is much stronger than other forces in the corona, any coronal structure is mainly controlled by magnetic field. Flares are classified according to their brightness in the X-rays. There are commonly three (3) types of radiation that are associated together with the solar flares. There are (i) thermal radiation (radiation that is associated with the temperature), (ii) non thermal radiation (radiation that is not associated with temperature), and (iii) the Terahertz radiation (THz) that is emitted as part of the black body radiation from anything with temperatures greater than about 10 Kelvin in which the radiation can be examine in the frequency that ranging in between 100 to 10^{12} Hz. Previously, there are many studies have been lead concerning the solar activities which include solar flares.

Based on intensive study, some flares exhibit as 'explosive phase' during the maximum cycle which is associated with hydrodynamic effects. In this scenario, an optical continuum reaches a peak increase of several per cent, which is in solar white-light flares based on the radiative hydrodynamic s models [24]. The previous data showed two different kind of spike event; (i) spike clusters which originating in post-flare phase [25] and (ii) originates from the main flare phase and well originate with non-thermal flare emission [9]. It is widely accepted that the solar flare is related with the relatively strongest magnetic field [26] found that the variability under magnetic condition in electron density, N_e, ion temperature T_i and electron temperature T_e, respectively changed with local time and height due to day to day flares monitoring.

It is undeniable that solar flare plays an important role in the Sun-Earth connection due to sudden changes of strong magnetic fields in the Sun's corona. Within short time intervals of about $10^2 \sim 10^3$ s, large quantities of energy of $10^{22} \sim 10^{26}$ J are emancipated. The changing magnetic field converts magnetic potential energy into kinetic energy by accelerating plasmas in the corona. The plasma is channelled by the magnetic field up and away from the Sun. It is also accelerated back down along the magnetic field into the chromosphere. In the chromosphere, the plasma crashes into denser gas and releases its kinetic energy into thermal energy, sound, and light energy.

Meanwhile, an observation of solar radio burst by low spectral and spatial resolution instruments can provide us only the light curve and a crude spectrum of the whole flare which may consist of many distinct sources with different characteristics. In the radio range, these phenomena are usually explained by two distinct processes: (i) radiation at longer metric-decimetric wavelengths exhibit flux densities decreasing with frequency (usually narrowband), and (ii) attributed to excited plasma emissions higher in the solar corona [2].

It could not be denied that the analysis and interpretation of observations in different wavelengths are required to discover out which the flare are triggering mechanisms. While this process has become generally accepted as the trigger, it is still controversial how it converts a considerable fraction of the energy into non-thermal particles [7]. It was observed that the interaction between coronal structures can generate the circumstances for

reconnection and the consequent energy release. This interaction can be forced either by flux emergence or by rapid motions of photosphere structures [27].

As it gives also access to the highest energy particles accelerated during flares, since high frequency radio diagnostics are more sensitive to these particles than are hard X-rays produced by non-thermal bremsstrahlung. During this stage, the Sun's radio emission can increase up to a million times the normal intensity just a few seconds. Based on the SOHO /LASCO data from 2004-2009 there were nine events which is about 14 % of the type II solar radio burst after the X-ray flares event not followed CME in the region of 20-70 MHz [28].

A number of reviews due to radio emission from flares has been addressed in these volumes previously: in the classic review by [29], in reviews by [30,31], and to some extent by [32-34]. There are also numbers of distinct emission mechanisms produce radiation at radio wavelengths, both incoherent and coherent mechanisms, from both thermal and non-thermal electron distributions.

Over the past twenty years, there are many theories and proposals for the particle acceleration processes involved in flares. However, the most popular classes of mechanisms for electrons are accelerated by an electric field parallel to the magnetic field by shocks and stochastic acceleration by waves [35]. There is also a complete scenario that can explain flare electron acceleration by a self-consistent chain of sub-processes.

In general, there are three types of acceleration commonly quoted in solar flares. (i) Direct electric field acceleration [36,37] can boost a particle to high energies simply via the Coulomb force from the electric field and may drive in the current sheet or in the reconnection site, but it is hard to maintain a large-scale coherent direct current, DC electric field. (ii) Shock or first-order Fermi acceleration can energize particles by making them repeatedly pass through the shock front back and forth and this mechanism may be present in the fast shock produced by the super-magnetosonic outflow jet from the reconnection region. However, it would be difficult to reflect the particles in the upstream region and (iii) Stochastic (second- order Fermi) acceleration by turbulence or plasma waves is the most likely mechanism [38,39] for solar flares, compared with the shortcomings of the other two mechanisms.

Still, it is not fully understood how the energy is released and converted into thermal heat and into non-thermal particle acceleration energy. There are many complex models which propose how this occurs, yet most models at some point invoke magnetic reconnection. There are also other models which do not feature magnetic reconnection as the main cause of energy release. One particular model suggests electrons are accelerated in the corona to energies of up to $10 - 100$'s of keV. These electrons then propagate down the newly connected field lines. Upon reaching the loop foot points the electrons encounter an increased plasma density where they undergo Coulomb collisions and emit the hard X-ray emission.

The understanding of why solar flares occur has come from the study of many H alpha and magnetic observations of active regions; the critical circumstance is how they react. A successful long series of synoptic high-resolution observations of flares, with accompanying magnetograms, has made it possible to evaluate the circumstances under which they occur. Although the researcher can confidently predict the flare occurrence in certain regions in the near future (even several days ahead). Still, it is not easy to state precisely when they will occur, and except for the occasional rising filament just before the flare, the vast majority of flares occur without identifiable precursors. It is hoped that further study will cover the new possibilities for solar flare prediction. A schematic profile of the flare intensity at several wavelengths due to the different phase is sketched in Figure 3.

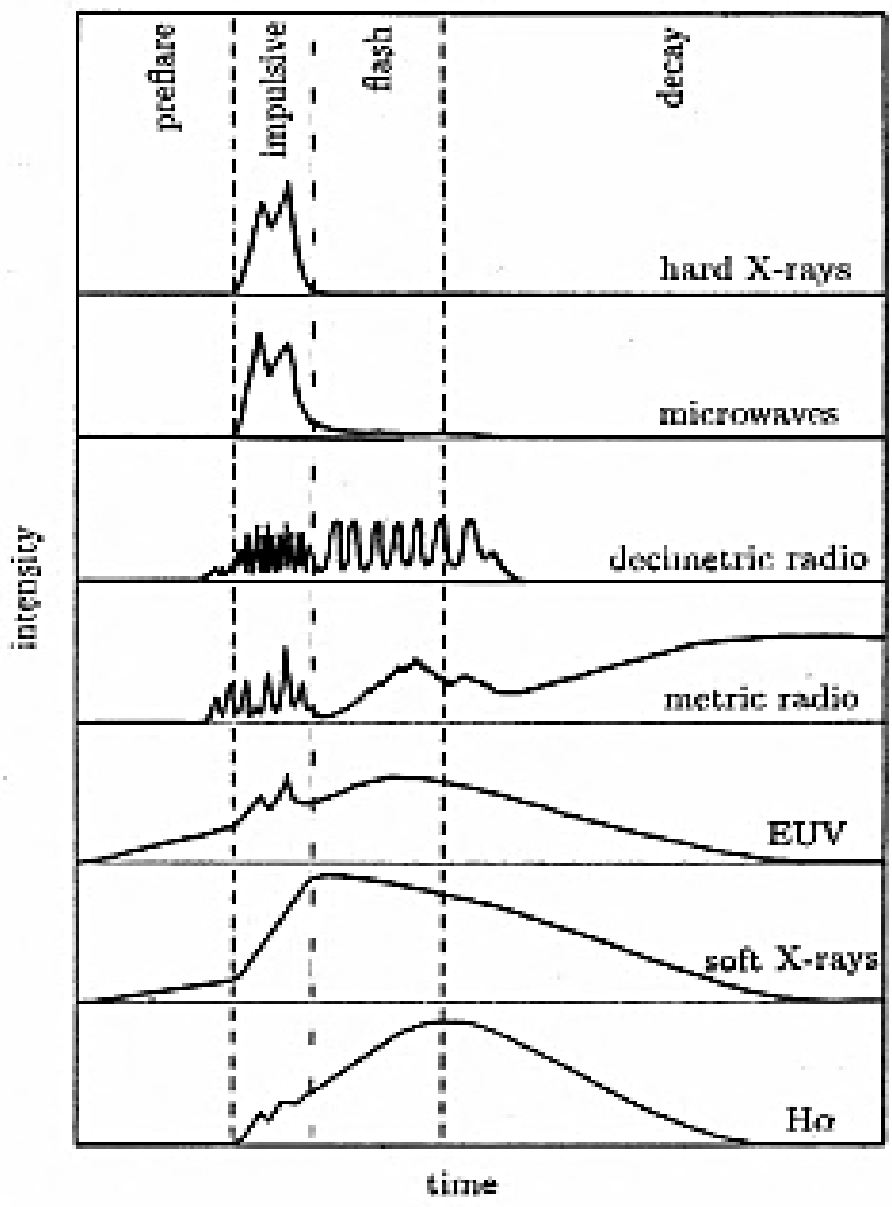

Figure 3. Schematic profile of the flare intensity at several wavelengths due to the different phase [25].

The various phases indicated at the top vary greatly in duration. In a large event, the pre-flare phase typically lasts a few minutes, the impulsive phase from 3 – 10 minutes, the flash phase 5 – 20 minutes, and the decay one to several hours [40]. In this case, the energy then propagates from the corona into the dense chromosphere along a magnetic loop by thermal conduction or free-streaming non-thermal particles, depending on the flare and the flare phase. Meanwhile, radio and X-ray observations gave evidence for two basic types of flare processes: an impulsive phased followed by a long-duration or gradual phase. It was found that flares were often preceded by filament activations, and growing loop prominence systems were recognized as the limb counterpart of two-ribbon disk flares. With regards to

understanding instruments, the thrust of this work is to cross-calibrate the X-ray solar monitor instruments with concurrent events in an actual use situation in space.

Though, time profiles at various radio wavelengths and X-ray ranges are not always well correlated. For examples, the time profiles with delays of several seconds at short microwaves and hard X-rays (> 30 keV) were found [41-44].

2. 4. CORONAL MASS EJECTIONS (CMEs)

CMEs have been studied extensively since 1970s. The CMEs phenomenon was discovered only in 1972 [45], but has become the most important form of solar activity because it is the most energetic phenomena on the Sun with a wide-range influence throughout the heliosphere that affected the space weather. This phenomenon can generate major disturbances in the interplanetary medium and trigger severe magnetic storms when they collide with the Earth's magnetosphere. It associated with a whole host of radio bursts caused by non-thermal electrons accelerated during the eruption process. As the largest scale eruptive phenomenon in the solar atmosphere, it can be observed as observed as enhanced brightness propagating out from coronal-loop-sized scale (10^4 km), expand to cover a significant part of the solar surface which is responsible for the most extreme space weather effects at Earth [46]. Moreover, CMEs may frequently interact with the Earth (and other planets), producing a series of impacts on the terrestrial environment and the human high-tech activities [47,48]. Further observations indicate that CMEs can also be observed in other wavelengths, such as soft X-rays [49,50] , an extreme ultra-violet (EUV, [51,52], radio [53] and so on (H. S. Hudson & Cliver, 2001) .

Previous study shown that CMEs associated with solar flares have a higher median speed than those associated with eruptive filaments and that the median speed of CMEs associated with strong flares is higher than that of weak-flare-associated CMEs [54]. However, the speed of CMEs may not more than 3000 kms^{-1} [55]. Majority of CMEs faster than 400 kms^{-1} decelerate, whereas slower ones generally accelerate in the case of between 2 – 30 solar radii [56]. Moreover, the magnetic properties of CMEs that close to the Sun is not easy to be understood [57] .

CME also can be define as a different plasma physical process and may even lead to the conditions for reconnection, causing a flares. There are two classes of CMEs, namely flare-related CME events and CMEs associated with filament eruption are well reflected in the evolution of active regions, flare related CMEs mainly occur in young active regions containing sunspots and as the magnetic flux of the active region is getting dispersed, the filament eruption related CMEs will become dominant [58]. This is confirmed by statistical analyses. Based on previous two events that has been analysed critically, the coronal mass ejection has the dominant component of the released energy, and covers an extensive fraction (30 %) of the existing magnetic energy [59]. It should be noted that a CME is not simply the explosive result of a flare, but has its own magnetic driver. Strong shock waves are expected to develop from fast CMEs [60].

Interestingly, in some cases, the flare may be only a minor part of a much larger destabilization of the corona, when the magnetic confinement of a considerable part of the corona is broken up. It expands and is expelled by magnetic forces in CMEs. The front speeds could exceed up to 3000 kms^{-1} [61-63]. This phenomenon can exhibit a variety of forms, some having the classical "three-part" structure [64]. Typically, it can be interpreted as

compressed plasma ahead of a flux rope followed by a cavity surrounded by a bright filament/prominence. The second structure is more complex geometry.

Meanwhile, several CMEs appear as narrow jets, some arise from pre-existing coronal streamers while others appear as wide almost global eruptions. This phenomenon also can be divided into two categories [65] .

The CMEs are the most important transient constitute a form of intermittent massive expansion of mass from the solar corona. It is believed that the formation and eruption of prominences is one of the central issues of CME initiation [66]. It is responsible for non-recurrent disturbances in the interplanetary medium and their interactions with Earth's magnetosphere cause severe geo-effective storms. They may appear with a frequency of one event per every few days during solar minimum to several events per day during solar maximum. The CMEs carry typically 10^{12} kg of coronal material; originate from active and filament / prominence regions where the magnetic field is closed and result from the catastrophic disruption of large scale coronal magnetic structures, such as coronal streamers. There is also an evidence for interaction between CMEs in the interplanetary medium from the long-wavelength radio and white-light observations [67].

It is believed that closed magnetic field lines are stretched up to the interplanetary space, as confirmed by the counter streaming electron flux from the explosions [68]. It occurs from closed magnetic field regions, where magnetic free energy is stored and released during eruptions. The erupting magnetic structure that develops the CME must have access to a mechanism providing vast amounts of energy over a relatively short time scale. The speed distributions for accelerating and decelerating events are nearly identical and to a worthy estimation they can be fitted with a single log-normal distribution [69]. However, to compute the acceleration is not an easy way because it depends on the projection effects and acceleration distance [70].

As the cycle of the Sun is towards to the phase of solar maximum, the eruption mechanism of Coronal Mass Ejections is currently an extremely active area of research. While there is a consensus that CMEs are the drivers of interplanetary shocks [71]. Therefore, the origin of coronal shock waves is not completely understood. Not only that, investigations on them and their relations with all other accompanied phenomena, such as solar flares, filament eruptions, radio bursts and particle accelerations are also involved. Previous study also focused on the properties of CMEs such as occurrence rates, kinetic energy, the locations relative to the solar disk, angular widths, speeds and accelerations, masses, and energies [32,50,72-78]. There have been many studies on the statistical properties of CMEs by [63,71,73,77,79-82] which based on the SOHO / LASCO observations.

The probable conservation of the magnetic support of the former prominence is the physical key factor for the later identification of in-situ observed magnetic clouds in the solar wind with the preexisting CMEs and before existing prominences on the disc. Previous work also has shown that the CMEs and prominences eruptions seem to occur roughly at the same time [83]. The CMEs of course cannot be observed directly with the flare effects, since they are defined in terms of the corona graphic observations. Solar flares, on the other hand, are observed in the low corona and below, so the observing domains are almost always disjoint. The previous study also showed the other "non-corona graphic" views of the CMEs, many of which allow the CME development – within model restrictions – to be tracked back to the lower atmosphere [84].

The frequency of occurrence of CMEs observed in white light tends to follow the solar cycle in both phase and amplitude, which varies by an order of magnitude over the cycle [85]. It is found that its kinetic energy correlates strongly with the peak GOES flux [76,86].

A previous study by [87] found that the field strength in prominences has been measured about ~ 3 – 30 G in quiescent prominences and 20 – 70 G in active prominences, occasionally exceeding 100 G. the density estimates from white light [88], the radio region (N. Gopalswamy & and Kundu, 1992; N. Gopalswamy & Kundu, 1993) and the ultraviolet region [89] observations are consistent with such densities. Unfortunately, the magnetic field of the CMEs near the Sun is unknown. Moreover, timing arguments is another aspect that produces a different impression of the energetics [32,90].

CMEs can exhibit a variety of forms, some having the classical "three-part" structure which is (i) a bright front (ii) a dark cavity and (iii) a bright core [64] usually interpreted as compressed plasma ahead of a flux rope followed by a cavity surrounded by a bright filament or prominence. It tends to cluster about the equator around solar minimum but broadens over all latitudes near solar maximum [91]. There are several CME-related models have been developed to describe their pre-eruption structures or progenitors, their initiations, and their eruptions [92-97].

Although the study of CMEs is more than four decades, to understand the mechanism for producing fast CMEs is not easy. This is because a region of strong magnetic non-potentiality narrowly collimated around a *Polarity Inversion Line* (PIL) plays the critical role here, but the exact topology remains controversial [98,99]. It should be noted that the role of CMEs in flare energetics is complicated. Most flares, even including some of the GOES X-class level [100] do not have associated CMEs. Yet this happens, they have not associated CMEs can rival that of the flare emission itself [101]. The CMEs energy usually is broken down into kinetic energy, enthalpy, gravitational potential energy and magnetic energy [88]. Since the restructuring of the solar flare generally thought to drive the CMEs, its magnetic energy must therefore be taken as negative, rather than positive.

The CME interaction has significant effects for space weather prediction based on halo CMEs: some of the false alarms could be accounted for by CME relations [102]. They tend to locally adapt to the ambient solar wind. They are also responsible on a major cause of the geomagnetic storm and primary factors determining the geo-effectiveness. However, it also depends on the distribution of the solar properties [103].

Still, the ideal models require the presence of a twisted flux rope or a sheared arcade still relevant to be implemented [92]. Detailed summarize on statistical, morphological and physical properties on CMEs of 23rd cycle.

SOLAR RADIO BURST TYPE II AND TYPE III

3. 1. INTRODUCTION

This section is devoted to the literature review of solar radio burst type II and III as the main focus in this study. Concerning the importance of historical of solar radio burst, the first part describes the evolution of solar radio burst and findings.

3. 1. 1. Solar radio emission

Solar radio emission is a rich source of information about electrons accelerated during a solar flare. Generally, this radio emission can be divided into two categories, (i) a thermal emission and (ii) non thermal emission [104].

A schematic diagram of types of emission mechanism that will dominate at different frequencies in the solar atmosphere is illustrated in the Figure 4.

.

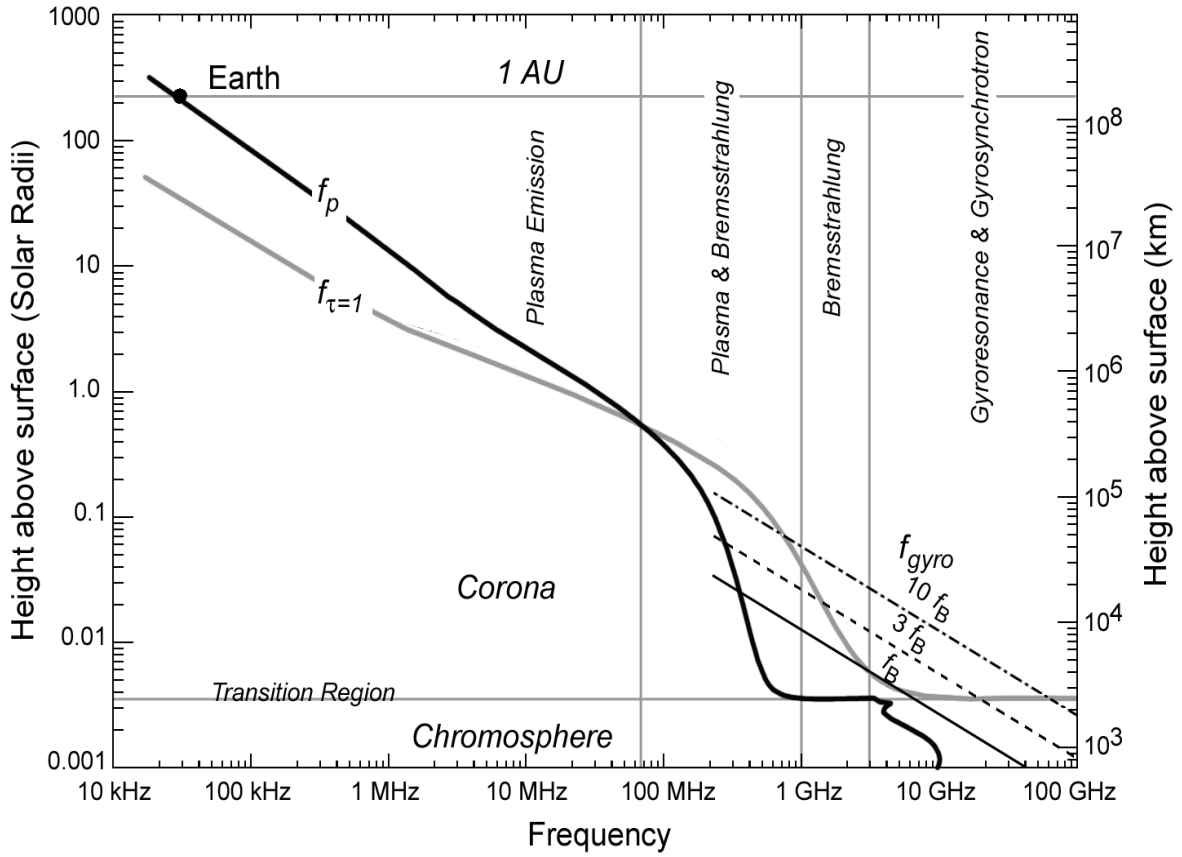

Figure 4. The highest curve in this plot specifies the type of emission mechanism that will dominate at different frequencies in the solar atmosphere [105].

The curves in Figure 4 are based on the dependence of different emission mechanisms on the plasma parameters of temperature, density and magnetic field strength. Generally, radio waves at the meter and decimeter waves can be used as a diagnostics of the solar processes [25,106]. At this frequency, the energy is $hv << kBT$ (the Rayleigh-Jeans regime). In this case, the Sun is produced incoherently by continuum processes or coherently by nonlinear resonant processes involving the electron plasma frequency, the electron gyro frequency, or the harmonics thereof [107].

In general, emission from the Sun at the centimeter wavelength is due primarily to coronal plasma trapped in the magnetic fields overlying active regions. There are two mechanisms can contribute to the radio emission from non-flaring coronal plasma which are a thermal bremsstrahlung (free-free) and thermal gyroemission [108,109]. Thermal bremsstrahlung is the minimum possible radio intensity emitted by the plasma. The emission originates from thermal electrons spiralling along coronal magnetic field lines, and its intensity depends on the coronal density, temperature, magnetic field strength, and angle between the magnetic field and the line of sight [36,110-114].

The strong radio emission over sunspots and sunspot groups has stimulated a large amount of theoretical and observational work over a long period of time, particularly after the first high resolution observations by [115] and the first detailed modelling by [116]. Recent works on gyro-resonance emission are reviewed by [117,118]. Meanwhile, thermal gyro-resonance emission occurs where the radio observing frequency is a low harmonic of the electron gyro-frequency in the radio source [119].

3. 2. SOLAR RADIO BURST

Solar events might trigger shock waves at propagate in the solar corona or in the interplanetary medium. These shocks are detected primarily through their specific signatures (type II solar bursts) in the metric range (corona) until kilometre range (interplanetary medium). With a minimal assumption of the electron density profile along the trajectory of the propagating disturbance, it is possible to estimate its velocity in the corona or in the interplanetary medium. On the other hand, bursts from the solar atmosphere and solar wind display a characteristic fall in frequency with an increasing distance from the Sun. However, normally the parameters did not occur simultaneously that refers to complexity of their sources and interactions along interplanetary medium [120]. This arises from the decreasing density of the solar plasma at a greater distance as the shock in the plasma moves outward from the Sun and into the interplanetary medium [121].

A solar radio bursts are a radio emission of solar flares and CMEs that emphasizes its brief energetic and explosive characteristics. A power law electron energy distribution with exponent -3 to -5 is found satisfactory to account for the time profile of the radio burst. In general, bursts are considered to be a significant characteristic of solar activity because they are generally attributed to a sudden acceleration of particles from the Sun [108,122]. The first observations and radio burst classification in decimetric region was done by (Young, Spencer, Moreton, & and Roberts, 1961).

On few decades on, solar burst had been recognized over wide range from millimeters to decimetre using ground based instruments. Their radio observations provide important information concerning physical conditions in the solar corona. In the solar corona, there are many particle acceleration phenomena that are caused by the interaction between coronal

magnetic field and plasma. The non-thermal electrons accelerated in the solar corona emit radio waves in the metric range resulting in many types of observed solar radio burst [106].

Literature about radio bursts is rather extended and appeared [2,29,105,108,123]. One of the main reason detecting solar burst is because this is the important tool for specifying magnetic, thermal and density structures at the time. Indirectly, it provides evidence for electron acceleration that rely high speeds, approaching that of light, as well as powerful shock waves. The burst emission which is always associated with solar active regions starts at the time of a flare. Burst emission, always associated with solar active regions, starts at the time of a flare and often abruptly and simultaneously over a wide range of wavelengths.

The concepts of solar radio burst are characterizations by complex variability patterns including both non-stationarities and non-linearities [124]. This is due to non-linear injection processes and the properties of the complex ambient coronal structures [125]. Meanwhile, solar radio bursts in decimetric is the key in understanding not only the mechanism of acceleration and the location of the energy release but also on propagation, escape or trapping of energetic particles. This solar burst does not occur simultaneously but instead of different drift to lower frequencies at later times. Next figure shows the schematic diagram of correlation between the solar flare phenomena and different types of burst.

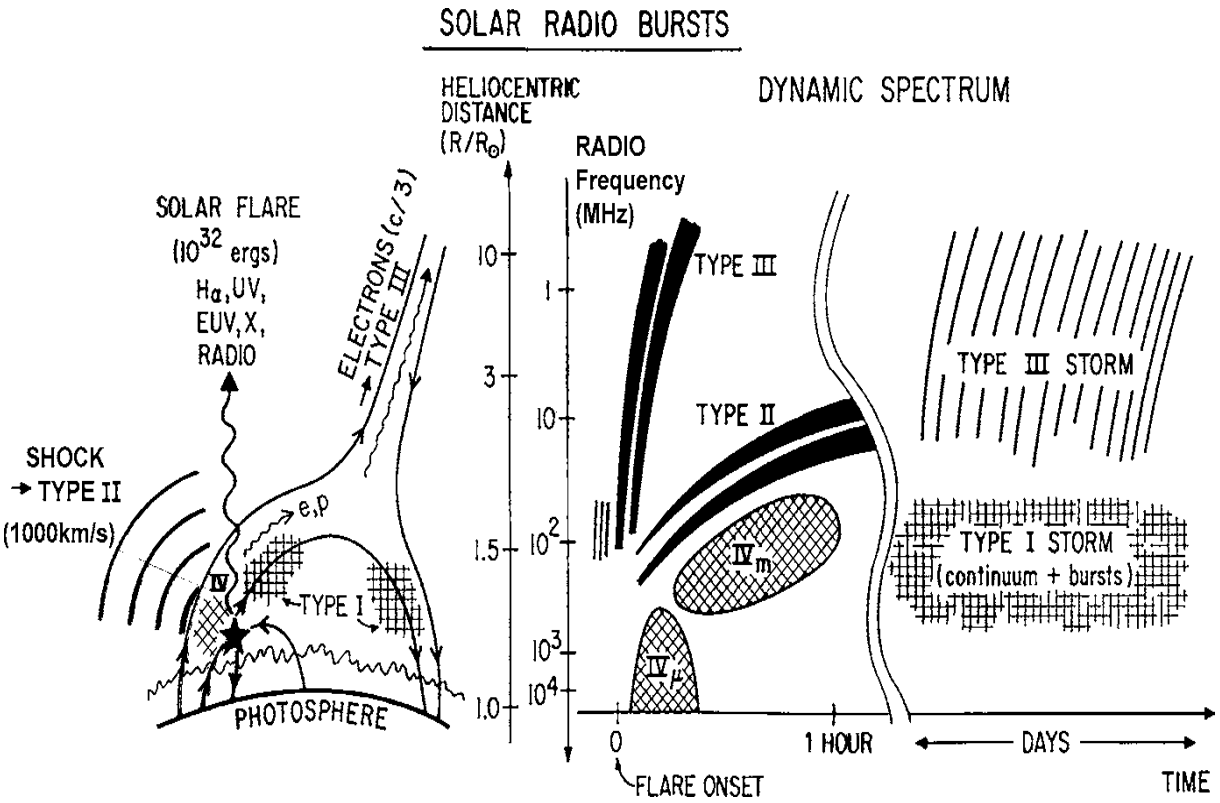

Figure 5. Schematic diagram of correlation between the solar flare phenomena and different types of burst [108].

The relationship between the plasma frequency, ν_p, and the electron density, N_e, can be described by Equation (3.1) where the plasma frequency is given in Hz:

$$v_p = \sqrt{\frac{e^2 N_e}{4\pi\epsilon_0 m_e}}\ Hz = \sqrt{81 N_e}\ Hz \qquad (3.1)$$

here, N_e is the electron number density in m^{-3}; ε_0 is the permittivity of free space = 8.854×10^{-12} Fm^{-1}; e is the electronic charge of the electron = -1.602×10^{-19} C; and m_e is the mass of the electron = $9.10^9 \times 10^{-31}$ kg.

A common practice to characterize solar radio burst signals is to record the dynamical radio burst profile. Classification of the burst is based on bandwidth, frequency drift rate and duration of the emission. The first detections of solar radio bursts (at much lower frequencies) were made inadvertently in 1942 through the radar system during World War II. However, the first spectral observations of solar bursts at meter wavelength was made by [126] . During a burst, the energy received may be as high as 100,000 SFU, with the energy also depending upon the frequency measured. Bursts of energy from the Sun of microwave radio frequencies can disrupt wireless cell communications several times a year.

During a burst, the intensity increases by factors up to 10^3.This burst often accompanied by solar flares and CMEs especially during a maximum period through a wide range of frequency from MHz till GHz. Normally, in a view of the space weather implication, excess radio noise produced by a strong solar radio burst has impacts on geosynchronous satellite transmission, wireless cell sites, *Global Positioning Satellite* (GPS) signals and radars [127,128].

There have been many attempts to analyse the statistics of solar bursts. The initial statistical studies of solar bursts were inadequate to single-frequency observations, [108,129-132] using data recorded during Solar Cycle 20. Some of the first statistical studies of this kind analyzed by [133,134] using radio data recorded at up to five frequencies. There is also a study on a frequency agile observation from Bern, although over a restricted frequency range ($6 - 8$ GHz) (Bruggmann, Benz, Magun, & Stehling, 1990). Previous study on the distribution of number of bursts versus the frequency range of the spectral peak, and in some respects with intensity level has been reported by [135] and [136] using data recorded at Sagamore Hill from 1968 to 1971. Meanwhile, a study of large flares was presented by [137]. More recently, the study of the peak flux distribution in different frequency ranges of more than 150,000 solar radio bursts has been recorded at fixed frequencies detected by the Owens Valley Solar Array (OVSA) [138]. There is also an analysis that statistically focused on the connection between solar flare with geomagnetic storms [139-141]. From the solar cycle point of view, the peculiar solar minimum that followed the 23rd solar cycle and the delayed onset of cycle 24 have received extensive attention [142]. This leads to the extension of the solar cycle 24 starting point which expected to be in maximum in the early of 2014.

3. 3. SOLAR RADIO BURST TYPE II (SRBT II)

In general, formation of SRBT II is due to electrons accelerated at an outward propagating coronal shock front. One main significance of this type is that it is the earliest indicators of CME-driven shocks. The onset time of this type precludes the possibility of the CME driven shock causing it [143]. The motion of the shock through the radial plasma

density profile can be observed based on the decreasing of the signal in frequency. One can deduce the propagation speed of the driving shock wave from eruption region. SRBT II were first identified by [144] and also discovered by [145] and classified as a broadband lasting from 20 minutes to a few hours. Thus the CME kinetic energy is the indcator of the life time of the type II bursts [146]. This burst usually distinguishes from the fast-drifting type III bursts and could be produced by synchrotron radiation by electrons spiraling in a magnetic field. It exhibits considerable individual variation discovered in the dynamic spectra as slowly drifting bands, often in pairs differing in frequency by a factor ≈ 2 [147]. They were quickly interpreted in terms of a coronal shock wave accelerating electrons, driving Langmuir waves near the electron plasma frequency fp, and producing radio emission near fp and $2f_p$ [147,148].

The shocks basically formed when the seed of the driver exceeds the wave propagation speed in the ambient medium called *Alfven* in which is governed by both the magnetic field and plasma density. This origin of metric SRBT II is still under debate. Magnetic splitting in some cases require unacceptably high speeds relative to the ions in a laminar shock model. M. Khotyaintsev has proposed two alternative models: emission from different parts in the shock front, or emission from in front and behind the shock front. In bandwidth of meter - SRBT II vary from 50 − 300 MHz and the bandwidth of m-type II occurs mostly at 50 MHz. It should be noted that if the emission is at the fundamental of the plasma frequency,

$$f[MHz] = f_p = 9 \times 10^{-3}\sqrt{n(r)} \qquad (3.2)$$

The electron density n(r) as ~ 2500 cm^{-3} at a heliocentric distance *r*. From that, the slope of the type II burst (*df/dt*) can be convert to the shock speed if when the density scale height $H = [n^{-1}dn/dr]^{-1}$ in the ambient medium [149] is known.

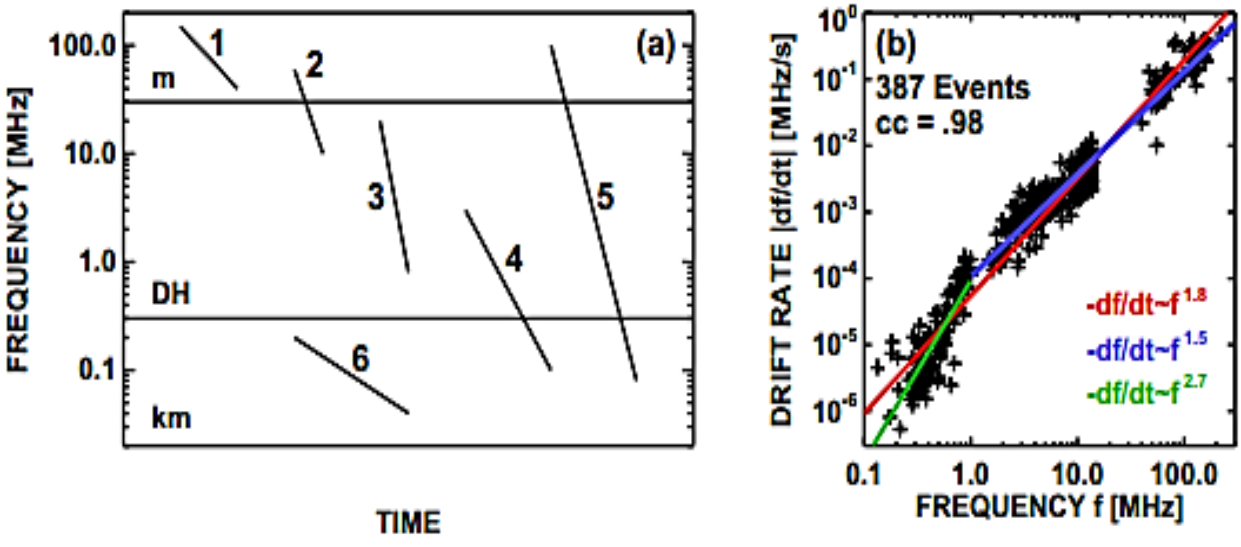

Figure 6. A schematic dynamic spectrum illustrating the variants of type II bursts: 1. Purely m, 2. m - DH, 3. DH, 4. DH - km, 5. m - km, and 6. Purely km. (b) the drift rate (df/dt) dependence on the emission frequency (f) in the m, DH, and km domains using data from various sources: m from Potsdam data, DH and km from Wind/WAVES RAD1 and RAD2 data as well as data from ISEE-3 [146].

This type also has a high-frequency cutoff at ~ 150 MHz, attributed to the fact that the Alfven speed is very high in the core of the active regions and falls off rapidly as one goes away from the active region radially as well as laterally [150]. Roughly, 60 % of the fast CMEs were not associated with DH type II bursts, and is expected to be radio-rich [151]. In addition, almost 93 % of the metric type II bursts did not have IP signatures based on data from November 1994 to June 1998 [152].

There have been many studies of the possible association of SRBT II with either flares or CMEs [153-162]. SRBT II has extensively studied to understand their sources and in connection with CMEs and Solar Energetic Particles (SEP) events [50,163] based on signatures of the shock-associated plasma oscillate signatures of type II bursts occurred near off after the maximum of chromosphere flare. The preceding theory of this type always related with larger and faster of CMEs and (higher *U* and *Rc*) shocks. It is also known as individual variation. This type is associated with the electron beam accelerated by the interplanetary shock or outstanding events associated with large flares. Based on their dynamic spectrum, the properties of the shocks are usually inferred by assuming a plasma emission mechanism. This mechanism is really important diagnostic of the electron number density in and near the flaring source.

Meanwhile, drift rate (*df/dt*) measured over different wavelength domains [164-166] can be written as

$$\frac{df}{dt} \propto f^{\varepsilon} \tag{3.3}$$

where ε ~ 2. It has been showed that ε = 1.8 for frequencies from 0.1 to 250 MHz (valid over six orders of magnitude in *df/dt*). The f − df/dt relationship is referred to as the universal drift-rate spectrum [167], which suggests that there must be something common for the type II bursts at different wavelength regimes: the CME driven shock. The exponent ε can be readily derived assuming that the emission occurs at the local plasma frequency (f_p) [168].

On the other hand, coronal SRBT II conventionally classified as a second phase phenomenon which may have nothing to do with the CMEs but instead may be the result of a blast wave initiated in the first phase by an associated flare [169,170]. A portion of SRBT II may occur in the absence of CME-excited shocks. It is found that most SRBT II that lack a clear CME association occur with flares within 30° of central meridian where CMEs are difficult to observe [153].

Until now, traditional argument in favour of a flare origin of coronal shocks is based on the back extrapolation of the SRBT II lanes, which usually relates to the interval between the onset and the peak energy release of the flare [168,171,172]. Though, the flare impulsive phase is often closely associated with the acceleration phase of the flare-related CMEs [173-175].

Statistical studies reveal that most, if not all, metric SRBT II occur during events where both flares and CMEs are observed. The appearance of metric type II bursts without CMEs is exceptionally rare. On the other hand, whenever a metric SRBT II without a flare is observed, the flare probably occurred behind the limb. It was found that a large fraction (34 %) of them to be radio-quiet (lacked type II emission) [176].

3. 4. SOLAR RADIO BURST TYPE III (SRBT III)

The theoretical basis for the plasma hypothesis of Solar Radio Burst Type III (SRBT III) was first introduced by [29] in the frequency range 500 MHz to 10 MHz. SRBT III is also known as a fast drift burst which is the most common of the metre wavelength bursts. It can be considered as a pre-flare stage that could be a signature of electron acceleration. It is well known that an isolated solar radio burst type III can exhibit a wide range of forms (T. Takakura, 1960). During the near maximum cycle, the average rate of occurrence growing up to 3 detections per hour with duration of individual times about 10 seconds. This type is associated with solar flares and usually occurs before optical events. Further evidence showed that type III are generated in a weak-field region comes from the absence or low degree of circular polarization of the bursts [177]. However, [178] against the theory and strongly agree that type III burst require a very strong field to produce a fundamental and second harmonic of gyro frequency. The subject of nonlinear wave-wave interaction which involving interaction of electrostatic electron plasma that called as Langmuir waves active region radio emissions also have been studied [109,110,179-182] and the most recent and comprehensive ones can be found in a recent book dedicated to solar and space weather radiophysics [183].

An extensive study of SRBT III associated with solar flare event was carried out actively since 1958 [184]. During the explosion, these active regions relatively have strong magnetic fields with denser and hotter compared with their surroundings and enhanced radio burst typically from $10-100$ minutes. SRBT III has been studied since the analysis of Clark Lake in 1962 [185] are thought to be produced by electron beams propagating along open magnetic field lines via the plasma emission mechanism. This type is one of the most studied solar coherent bursts, and generally occurs at the beginning of the impulsive phase of a solar flare. There are two steps process in which electrostatic oscillations are (i) first produced by the ejected solar flare via beam-plasma instability and (ii) then converted to electrostatic oscillations, usually called Langmuir waves are excited at frequencies near the local produced at both the fundamental f_p and harmonic $2f_p$. It has been studied since the analysis of Clark Lake in 1962 [185] are thought to be produced by electron beams propagating along open magnetic field lines via the plasma emission mechanism. This type is one of the most studied solar coherent bursts, and generally occurs at the beginning of the impulsive phase of solar flares.

There are many mechanisms have been proposed to explain SRBT III properties. So far, however, there is still a lack of knowledge about the corona structure and the apparent randomness of the phenomenon. Literature review of this study will concentrates on the development of SRBT III and implementation in the low frequency radio region. The present work is aimed to understand the formation of SRBT III by looking at several parameters that will evolve this burst however, still have a lack of understanding due to the data is focused on the selected event and there is not much event during the phase.

The eruption mechanism of solar flares and type III are currently an extremely active area of research especially during the solar cycle is towards maximum In this case, the total energy of solar burst type III is of the order of 10^{15} ergs. It occurs in the impulsive phase, which is more intense at meter wavelengths and may have a continuum attached to it [186]. This burst usually associated with a single flare or flare-like events that excited through the lower solar corona in a bunch of electrons which emit *l*-waves (electron plasma waves) incoherently [187]. The electron is thought to be accelerated within a second or so [188]. In between of the process, the instability is formed and sustained through velocity dispersion, whereby the high energy electron fluxes race ahead of the low energy electron fluxes creating

a transient bump-on-tail instability in the reduced, one-dimensional distribution (f_r / v > 0). In specific range, the event starts with a group of metric type III bursts at 200 – 400 MHz [189]. As the beam excites plasma waves at the local plasma frequency, the frequency changes with density can be represented as

$$\omega_p = \sqrt{\frac{4\pi e^2 n_e}{m_e}} = \pi 90 \sqrt{\frac{n_e}{10^8 cm^{-3}}}\ [MHz] \qquad (3.4)$$

where *e* is the element charge, m_e is the electron mass and n_e the electron density.

In general there are two classes of generation mechanisms of SRBT III: (i) nonlinear wave-wave coupling processes [190] the coalescence of two Langmuir waves, first proposed by [184] and (ii) the highly nonlinear process proposed by Yoon [191,192] and direct emission mode conversion due to density inhomogeneity [109,193,194]. A standard homogeneous quasi-linear theory argues that the back-reaction to wave growth should plateau the beam, remove its free energy, and cease the production of Langmuir-like waves and radiation within much less than 100 km of the source of the beam [195]. Yet, one possible clue is that nonlinear wave processes limit the wave growth by removing wave energy from the linearly unstable region of phase space [196,197].

The SRBT III consequences from the ejection of plasma oscillations localized disturbance due to excited in the plasma frequency incoherent radiations such as gyro synchrotron and free-free emissions appear in the radio wavelengths plays a dominant role at the meter and decimetre wavelengths, which may be associated with the flare primary energy-releasing sites [198]. There are three low-frequency variants of type III burst that originate in the interplanetary (IP) medium [63]: (i) isolated type III bursts from flare -scale energy releases, (ii) complex type III bursts during CMEs, and (iii) type III storms. Determination of solar burst type III could be interpreted as a very fast outward movement of the disturbance through the solar corona with could exceed from 3 x 10^4 to 10^5 km/sec. This velocity represents one-third velocity of light. The electrons in this type are accelerated to energies of at least 10^4 to $l0^5$ eV. Previous study also shown that this type of burst extends out to 1 AU [199] with more than 20 keV electrons [200]. Therefore, this type is used as tracers of magnetic field structures. At very low frequencies (~ 1 MHz), several thousand of bursts can be emitted from an active region during one complete solar rotation [201].

SRBT III is the most frequent bursts observed which a drift type burst that similar in form to cluster into groups of 10 or so. The frequency of maximum intensity drifts rapidly from high to low frequencies. The rate of drift increases with increasing frequency. The exciting agency for SRBT III is a beam of energetic electrons with speed 0.1 c ≤ v ≤ 0.6c, propagating outward from the Sun through the corona. These beams provide energy for the plasma emission mechanism.

However, it may be that in such complex events other phenomena such as type II and IV radiation are involved. It can be said that this type is rich in variety. At one extreme are the uncomplicated bursts with a sharply defined leading edge, narrow bandwidth and a short duration which increases with decreasing frequency. Statistical studies by various authors (Maville, 1962; Swarup.G.et.al, 1960) have shown that the correlation of isolated type III bursts with flare is quite high.

An important question concerning the origin of SRBT III is how they correlate with the mildly relativistic electrons and Langmuir waves produced from the electrons. It should be noted that observations show that Langmuir waves associated with solar type III radio bursts

are highly localized [202,203]. One fundamental theory, it is believed is that Landau resonance with the unstable electron beam is responsible generates Langmuir waves, which are thought to undergo nonlinear wave-wave interactions that produce electromagnetic emissions at the local electron plasma frequency (f_{pe}) and its second harmonic ($2f_{pe}$) [190,194,204-207].

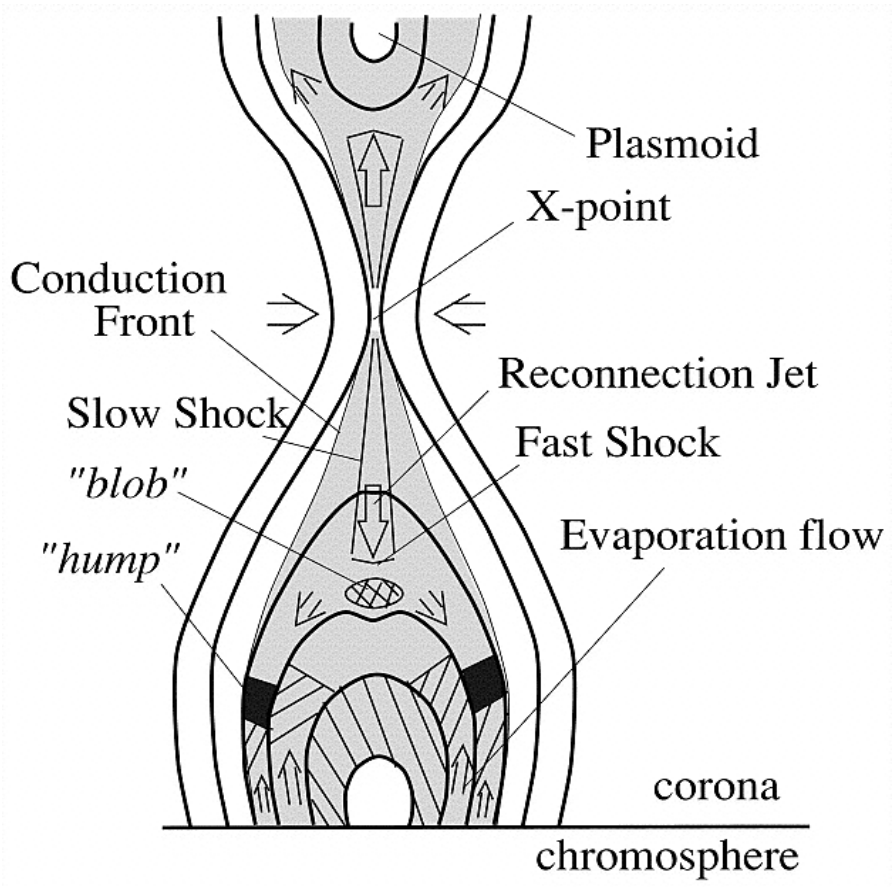

Figure 7. Schematic diagram of the magnetic reconnection of the burst (credited to Yokoyama & Shibata, 1997).

The second question concerning the origin of type III burst is how the generated Langmuir waves can convert to electromagnetic waves either the fundamental or the second harmonic of the electron plasma frequency associated with the observed bursts. In general, a Langmuir wave spectrum can be classified into two components: (i) the ‘‘forward’’ spectrum [beam-generated Langmuir waves] and (ii) the ‘‘backward’’ spectrum of Langmuir waves [backscattered Langmuir waves] [208]. Nevertheless, there is an initiative to explain in detail by a stochastic - growth theory which is developed to explain the nonlinear saturation level of Langmuir waves in comparison (P. A. Robinson, 1992; P. A. Robinson, Cairns, & Gurnett, 1993). This theory addresses the development of fluctuations in the waves and unstable distribution due to their self-consistent interaction in the pre-existing inhomogeneous background plasma (I.H. Cairns & al., 2000; I.H. Cairns & Grubits, 2001; I.H. Cairns &

Menietti, 2001; I.H. Cairns & Robinson, 1997, 1999; P.A. Robinson, 1995). It is believed that situation in which the time-integrated growth rate of the waves is a stochastic variable because of repeated interactions between a free-energy source, waves, and the background plasma that cause the energy source to attain a state close to time- and volume-averaged marginal stability with stochastic fluctuations about that state that affect the wave gain. Until now, the mechanism of the conversion is still not fully to be understood, but still is an issue which needs to be considered.

In solar flares perspective, a theoretical scaling law (Yokoyama & Shibata, 1998) for the flare temperature *T* as:

$$T = \left(\frac{B^3 L}{2\pi\kappa_0\sqrt{4\pi\rho}}\right)^{\frac{2}{7}} \propto B^{\frac{6}{7}} \ (Reconnection) \qquad (3.5)$$

where *T*, *B*, and κ_0 are the temperature at the flare loop top, coronal magnetic field strength, coronal density, and heat conduction coefficient, respectively. It should be noted that the magnetic reconnection should be considered which is a highly conducting that rearranged and magnetic energy is converted to kinetic energy, thermal energy, and particle acceleration. Figure 7 shows a schematic illustration of the reconnection model of a solar flare based on the simulation results (Yokoyama & Shibata, 1997).

3. 5. COMBINATION OF SRBT II AND SRBT III

One of the most important uncertainty in climate models is the role of Sun activities. It is believed that solar activities such as Coronal Mass Ejections (CMEs) and solar flares have a very close connection and significant impact of the climate changes and Earth's environment. Therefore, it is important to study the phenomena in details. Both phenomena can be also detected in the radio region in terms of solar burst perspective. Solar flare is related to SRBT III while CMEs can be identified by SRBT II characteristic. Generally, the explosion of CMEs will occur during a large solar flare from an active region of the Sun. However, it depends on the distribution of the explosion of the charge particles from the Sun.

One similarity of both types is that it originates from the solar corona, most strongly from the sunspot active regions. During the explosion, these active regions relatively have strong magnetic fields with denser and hotter compared with their surroundings and enhanced radio burst typically from $10-100$ minutes. Imaging studies of type III solar bursts will provide information about the magnetic field topology, by tracing the motion of the burst location [209]. Due to the propagation effect such as scattering and ducting, these observations can also provide information on small scale properties of the coronal medium. Being sensitive to low level magnetic reconnection activity [210], these observations will help to discover the possibility of using activity seen in radio for identifying precursors of significant events [211]. Low radio frequency radio observations are hence destined to play an important role in developing our understanding of solar coronal physics.

There are many mechanisms have been proposed to explain SRBT II and III properties. So far, there is still a lack of knowledge about the corona structure and the apparent randomness of the phenomenon [212]. In this study, the complex SRBT III seems it associated with metric SRBT II is the subject of interest. The results indicate that the onset of SRBT II depends on the local Alfvén speed, which is governed by both the magnetic field and

the plasma density. This determines that the SRBT II cannot appear at any altitude. It has been known for decades that about 50 % of SRBT II are preceded by a group of SRBT III by several minutes [108]. Recently, it has been shown that the overall frequency envelope of the precursor type III bursts drifts at a rate close to that of the associated type II bursts [213]. This SRBT III usually take place in the impulsive phase of the flare and are located between the site of the impulsive energy release and the associated SRBT II [213]. This makes sense if a reconnecting current sheet is located between the solar flare and the associated CME: the SRBT II is invoked by the CME-driven shock, and the beam of energetic particles accelerated by the electric field in the current sheet is responsible for the SRBT III.

On the basis of the above arguments, it seems, at least to us, that the CME-driven shock plays a much more important role in exciting the type II radio bursts than any flare-related blast wave. A CME has to take off from a stationary configuration. Therefore, a CME-driven shock cannot be produced by the CME velocity exceeds the local magnetoacoustic speed [50].

Literature review of this work concentrates on the development of both bursts and implementation in the low frequency radio region. The total energy of SRBT III is containing of 10^{35} electrons per explosive [214]. It is well known that each burst of this type is due to the passage through the corona bunch of a fast electrons that ejected in the explosive phase during a flare event. It can occur in groups as higher as 10 bursts per group but sometimes can appear as an individual one with a large densities of electrons. Interpretation of this burst also has been discussed by [29] where there is an evidence that showed this burst is proportional with X-ray emission during a flash flare in a second of time. In this case, the electrons are believed to be accelerated due to the development of the instability stage [188]. However, because this ejection is very fast and short time of the explosion, there is an argument that said there must be an exciting agent which initiate the particles to be a fast ions rather than a rest electrons. This exciting agent has a streaming velocities with less than 0.2 *c* [108].

Overall, it can be said that all literature that has been SRBT III. The quantitative theory still needs to be developed for understanding the properties of SRBT III in the lower solar corona and planetary space (D.B.Melrose, 1986). There is also no detailed theory currently exists that is capable of explaining a type III burst from the deep corona to 1 AU and beyond (Iver.H.Cairns & Robinson, 1998). In order to improve the model of solar burst type III, one should consider are the solar flare models depend on certain properties such as sunspot area, McIntosh classifications, Mount Wilson classifications, and various measures of the magnetic field (Huang, Zhang, Wang, & Li, 2013). Moreover, it should be noticed that the pattern also depends the solar cycle model. It is important to consider all parameter, mechanisms ,previous of theory and model to understand in detail the behavior of the formation of this event. Thus to understand and predict the behavior of the Sun is not an easy way. Therefore, the dynamisms of the Sun itself should not be neglected.

The low frequency radio emission of solar is informative because this range can tell us the behavior of the Sun within $0.1\ R\odot - 0.3\ R\odot$. In other words, they originate in the same layers of the solar atmosphere in which geo-effective disturbances probably originate: the layers where energy is released in solar flares, where energetic particles are accelerated, and where CMEs are launched.Therefore, this region is very important to study. This range is very rich with a single and group of solar burst type III that associated with solar flares. It is meant that it can be considered that there is a large number of solar flares with a tendency to form CMEs. One big challenge of this range is the population of different interference source that might affect the solar burst data. Yet it is still can be eliminated during the analysis process.It is hoped that a latest data might answered the mechanism of type III burst based on solar flares and CMEs events.

DESIGNING LOG PERIODIC DIPOLE ANTENNA (LPDA) AND EXPERIMENTAL METHOD

4. 1. INTRODUCTION

To date, various methods have been developed to study the solar activities in radio region. E-CALLISTO network is one of the systems that possible to monitor the Sun within 24 hours. Construction of a good antenna is very important for us to solve several issues that relate to solar radio bursts such as (i) to identify a different types of solar burst (ii) to find out their nature and emission mechanisms, and (iii) to relate their properties with parameters in solar flare and CMEs events.

4. 2. LOG PERIODIC DIPOLE ANTENNA (LPDA)

For the broadband application, the log-periodic dipole principle was selected. In principle, antenna can be used to transmit or receive electromagnetic waves. The properties in both cases are the same due to the principle of reciprocity. Among the types of antennas, LPDA have attracted much attention lately due to the broadband frequencies [215]. During recent years, logarithmically periodic antennas have been widely used due to their frequency response characteristics, simplicity of design and directivity [216]. This study is one of the International Space Weather Initiative (ISWI) project in order to monitor the solar activity 24 hours per day coverage of solar observations in state of support develop countries participate internationally with a latest technology of instrument [40].

Up to date, the LPDA plays an important role in the modern communication and radar system [217]. Development of LPDA has started since 1961 initiated by Isbell [218]. Later, Carrel analyzed the LPDA mathematically and computed its radiation pattern, input impedance, etc., using a digital computer [219]. It must be sensitive to a broad frequency range and angular distribution of the incident radio pulse. On the other hand, it plays an important role in handling the noise issue and thus is essential to detect preferably pure signals. One main criteria that make LPDA become more relevant is due to it sensitivity that possible to detect signal of the Sun. Moreover, it also economical and practical to be implements.

This antenna potentially produces a wider bandwidth and can have gains as high as 10 dB [220]. The prerequisite for the antenna is increased nowadays since it plays a vital role in monitoring the Sun. The linearly polarized LPDA is the most practical transmitting antennas provide general broadband transmission and reception in wide range frequency. One of the advantages of LPDA is that they are mainly frequency-independent of base impedance and radiation pattern. In combination with a test receiver, the antenna is ideal for field-strength measurements. In this case, the longest element is active on the antenna's lowest usable frequency where it acts as a half wave dipole. The dipoles are mounted on two boom structures which in essence are transmission lines since the dipoles are mounted on them un-insulated. As a consequence, the booms have to be isolated from each other by using dielectric spacers [221].

Figure 8. The elements of the antenna at different sizes.

In order to obtain more gain than with a single log-periodic array, two arrays may be stacked. For very wide bandwidths, the log periodic array must be correspondingly longer [222]. Since it is dealing with transverse waves, all aerials are polarized. In principle, this means that only half of a randomly polarized wave can be received. Still, the mechanism of modification of improving the quality of the LPDA is needed to be done. The antenna is a horizontal orientation and static. One of the suggestions is that by putting a tracking sensor so that the antenna can track as the Sun is rotating from the East to the West. Another solution is by doing interferometry technique and start by two antennas at the same site.

This can provide a better resolution of the image of the burst. This is very important, especially to understand the dynamical structure of solar flares and Coronal Mass Ejections (CMEs) associated with different types of solar bursts. For this period, we are focused on the short term variability of solar flare and CMEs events.

Figure 9. Logarithmic Periodic Dipole Antenna at the National Space Centre, Banting Selangor, Malaysia.

The data is then can be compared with an X-ray region data. We also successfully analyze a solar radio burst type II due to the CMEs event. There are also other types such as type U, V and IV that have been analyzed in detailed. Since our first antenna is operating without a balun, we can start to design a balun of the antenna for the next project. The impact of solar activities indirectly affected the conditions of earth's climate and space weather. It is suggested to design a better cover of the feed point seems the wind in the particular area to be strong. The preparation of construction of the antenna is presented in Figure 9.

Figure 10. Preparation of construction of LPDA.

4. 3. LPDA ANALYSIS

We have examined the antenna by evaluating the temperature of solar radio burst type III. According to the results, it was found that the background sky temperature of the receiver of the antenna is 300.15 K. This makes sense because the temperature during that time is 27 degrees Celsius. Our observation also showed that the burst still can be detected if the temperature of the local site is minimum or less than 30 degrees Celsius. At the feed point at the antenna, the temperature of the burst only is 32 K [223]. Since the temperature of the solar

burst at the end of the point of the system should be decreased because of the noise of the cable and other factors, the results of the temperature of solar burst that detected by the CALLISTO system is reduced to 28.75 K. Detailed results of solar burst parameters are illustrated in Figure 11.

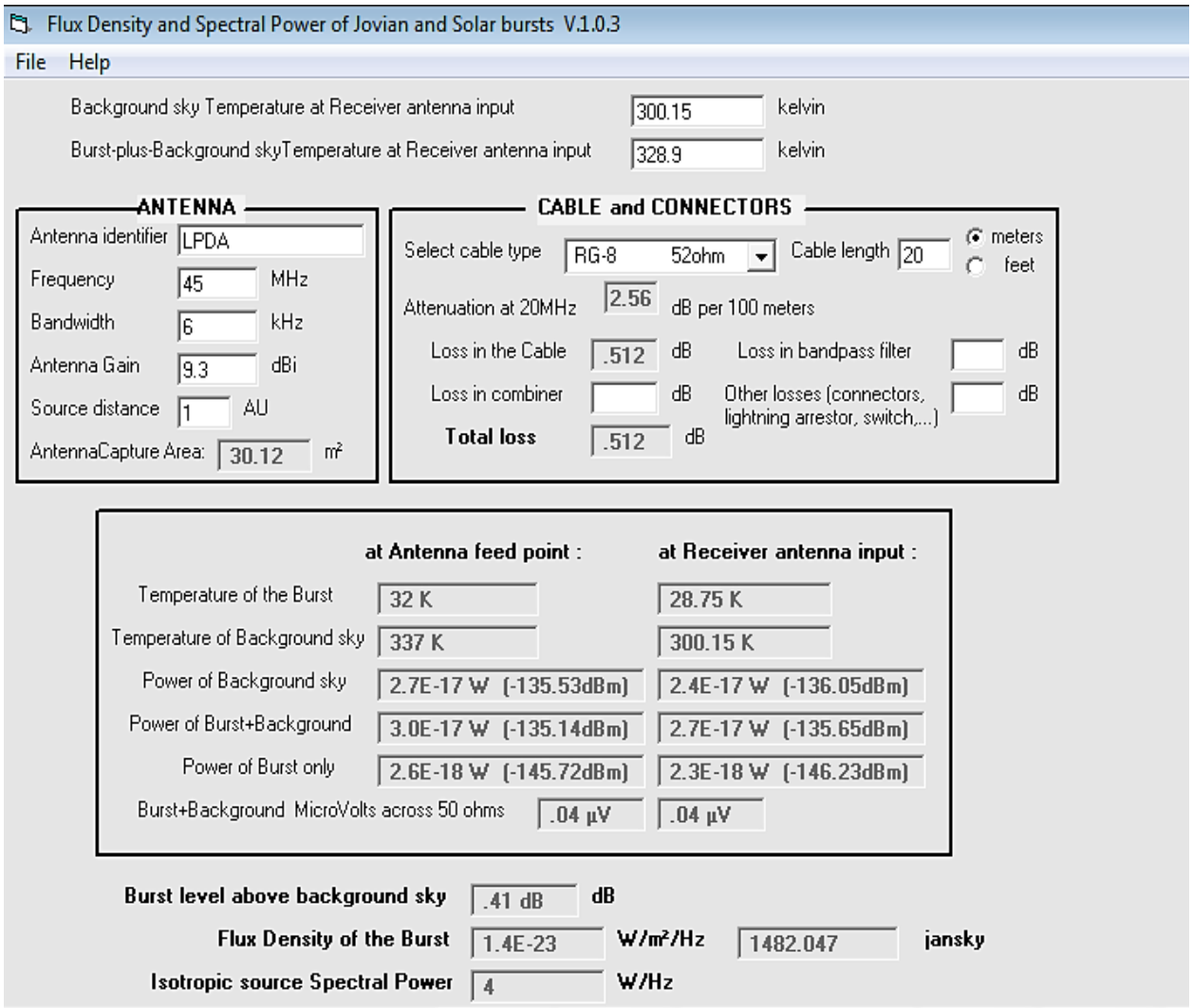

Figure 11. The temperature of solar radio burst at the (i) feed point of antenna and (ii) CALLISTO receiver.

Through the study and research, we found that this antenna potentially captures a signal that covers about 0.08 m^2 area of the Sun. Although the size is considered small, it is still relevant because we are focused on the burst which is generated from the eruption of particles such as electrons, proton and plasma. In this case, the gain of the antenna is 9.3 dB. Although in theory the value is 10 dB, the actual signal might be less because of the length of the cable. It should be noted that, in terms of length, there is approximately 2.56 dB of attenuation for every 20 meters. It means that the signal will lose about 0.512 dB per 100 meters. These results show a better understanding of how the system operates in terms of the process of

analysis of the temperature of solar radio burst. But of course, the improvement of the modification of the antenna still needed to be done. Our next task will focus on the other parameters such as the radiation pattern, polarization, operation of the frequency band, gain, input impedance and efficiency of an antenna which indicates the power or field strength radiated in any direction relative to that in the direction of maximum radiation which is also should be considered.

4. 4. OPERATION AND CONSTRUCTION

Log Periodic Dipole Antenna (LPDA) consists of a system of driven element, but not all elements in the system are active on a single frequency of operation. An aluminium rods where chosen for the LPDA as it does not rust. A different lengths and different relative spacing allowed the signal changes in frequency to be made without greatly affected the electrical operation. The diameter of these rods and tubes were chosen so as to incorporate the compactness as well as the ease of assembly for the antenna elements. The dipoles are connected to the source using a twin transmission line in such a way that the phase is reversed at each connection relative to the adjacent elements. The feed point for the array is seen to increase smoothly in dimension, being greater for each element than the previous element in the array. Output from the transmitter is converted into electromagnetic energy by the antenna and radiated into space. At the receiving antenna, the electromagnetic energy is collected and converted into electrical energy and fed to the receiver. Only a tiny fraction of power is reflected back to the spectrum analyzer indicating that most of the power has been radiated by the antenna [224].

In this framework, the variability of solar radio emission beginning from February 2012 conducted. While the main goal of wide-band imaging is to obtain a high dynamic-range continuum solar burst profile, the reconstructed spectral structure can also be a useful astrophysical measurement. Our concern is to investigate time variations of solar burst types II and III.

The antenna has been successfully constructed with the value of gain is more than 5dBb [225,226]. The elements of two booms is alternate each other with the same size with 180° (π radians) of phase shift from one another. This can be done by connecting individual elements to alternating wires of a balanced transmission line. Routine observations will start from 7.00 am till 7.00 pm, 12 hours every day [227].

The antenna has a boom length 5.45 m and covers the range from 45 MHz till 870 MHz with gain 7 dBi. Due to the principal of LPDA, the length, width and spacing of the 19 elements of a LPDA increases logarithmically and decreases smoothly, as one move away from the feed point. The sizes of elements are as high as 3.96 meters and as low as 0.071 meters. We also need to make sure that the low frequency-dependence of radiation pattern and input impedance. This can be done by making sure that all metallic parts are electrically connected to the mast flange and thus offer the highest protection against electrostatic charges. By using two boom lengths, it is hope that the elements are balanced enough since the length is quite long which need a good front-to-back ratio of the antenna patterns of signal direction. However, the axial length should be extended up to 6 meters for a handling the antenna purpose.

In order to make a portable LPDA, the size of boom length becomes an issue. The boom has been divided into three of sizes, 2 meters respectively. Therefore, a hole for the screw to join it again is needed. This antenna is directly connected via a low loss coaxial cable to the

measuring instrument. It mounted horizontally on a steerable azimuth/elevation tower, and controlled by the computer to automatically point the Sun during the day time.

Overall, the studies in the present work are based on the main objective to monitor solar burst in the lower region of frequencies. By constructing and understanding the principle of log dipole periodic antenna and then connect it to the CALLISTO spectrometer as receiver, some solar activities observations such as solar flares and Coronal Mass Ejections (CMEs) can be done.

4. 5. EVALUATION OF SIGNAL TO NOSE RATIO (SNR) OF LOG PERIODIC DIPOLE ANTENNA (LPDA)

In this section, some theoretical aspect and parameter that need to be considered for evaluation will be highlighted. We began with a relationship between element factors (τ) with the size of the element represented as equation below:

$$f_2 = \frac{f_1}{\tau} \tag{4.1}$$

$$f_3 = \frac{f_1}{\tau} \quad and\ f_n = \frac{f_1}{\tau^{n-1}} \tag{4.2}$$

where *f* = frequency of each element and element factor can be represented with this equation:

$$\tau = \frac{L_n}{L_{n-1}} \tag{4.3}$$

Meanwhile, the spacing *d* of each element can be represented by:

$$d_{2-3} = \tau d_{1-2}\ , d_{3-4} = \tau d_{2-3} \ldots d_{(n-1)-n} = \tau d_{(n-2)-(n-1)} \tag{4.4}$$

On the other hand, we can measure a noise ratio or Excess Noise Ratio (ENR) is a term to describe the output of the noise source used as an input stimulus. In this case, the lower noise level must be equal to the noise generated by a (theoretical) resistor at the standard reference temperature of T_{ref} = 290 K [228].

$$Excess\ Noise\ Ratio\ (ENR) = \log\left(\frac{P_H}{P_0} - 1\right) \tag{4.5}$$

Without going into great detail regarding derivation, the noise can be related to input stimulus and Y-factor as follows or in the case where T_1 (representing the "cold" condition of the noise source) equals the standard reference temperature, T_0 = (290 K):

$$NF_{dB} = 10\log\left(\frac{T_2}{T_0} - 1\right) - 10\log(Y - 1) \tag{4.6}$$

Consequently, this equation can be simplify with:

$$NF_{dB} = ENR_{dB} - 10\log(Y-1) \quad (4.7)$$

In terms of equipment accuracies, there are two major factors to consider (i) the noise source output and (ii) the ability to ascertain the Y-factor [229]. These two sets a minimum uncertainty for any noise figure measurement.

Calculation Y-factor of the Sun (Y-Sun) is also called hot-cold measurement method [230]. The Y-Sun can be estimated by using the Java FITS Viewer. The Java FITS Viewer uses in terms of the analog–digital converter (ADC) 10-bit resolution. The power value in terms of 10-bit AC output has been reduced to 8 bits by dividing it by 4.

$$Y_{Sun} = \frac{Digithot - Digitcold}{Digitrange} \times \frac{Voltrange}{g} = 3.46dB \quad (4.8)$$

In order to calculate the SNR, the Power Flux Density (PFD) will be measured. However, it is necessary to calculate the effective area of the antenna, A_{eff} at the first stage. In this case, the symbol *G* represents gain and *G (*dB) is a gain in dB units. Since the solar burst data is at frequency, *f* = 240 MHz, this value will be selected and *c* is the speed of light in m/s. From the analysis, the gain is equal to 5dB and the wavelength, is 1.25 meter.

Therefore,

$$A_{eff} = \frac{\lambda^2}{4\pi} = 0.6217m^2 \quad (4.9)$$

The viewer is set to automatic background subtraction so it determines the average background noise level for the entire spectrum and subtracts it when the spectrum is displayed. The background also can be subtracted manually by selecting a region that having the noise level.

From the calculation, the power flux density (PFD) of the burst can be calculated by using the value of the antenna effective area, A_{eff}

$$PFD_{burst} = \frac{S.A_{eff}}{2} = 4.53841 \times \frac{10^{-21}W}{m^2Hz} \quad (4.10)$$

With the temperature of the Sun and the CALLISTO system is:

$$T_{Sun} = \frac{S_{Sun}A_{eff}}{2k} = 328.9K \quad (4.11)$$

and

$$T_{Sys} = \left(\frac{T_{Sun}}{Y_{Sun}-1}\right) \quad (4.12)$$

Based on the analysis, the value of solar flux density, S = 146 sfu taken from the NOAA list at spaceweather.com on 9th March 2012 [231]. From that the system noise temperature, T_{sys} can be measured. In this equation, *k*, and *T* is a Boltzmann constant and

antenna temperature of the Sun respectively. The power flux density due to the system noise temperature, PFD_{sys} is also calculated [232].

$$PFD_{SYST} = kT_{Sys} = 1.85 \times \frac{10^{-2}W}{Hz} \quad (4.13)$$

Therefore,

$$SNR = PFD_{burst} - PFD_{syst} = (-17.43) - -177.33) = 3.9dB \quad (4.14)$$

This LPDA was modeled with a low loss coaxial cable, RG 58, 5.5 meter long. Therefore the cable attenuation at 50, 450 and 900 MHz is 0.7, 2.1 and 3.0 dB respectively. When the transmission line is soldered to the antenna, the side of the antenna effectively has less inductance and a higher velocity factor. Finally, the signal noise ratio is getting from the difference between the power flux density of receiving solar flux PFD_{burst} and the power flux density of system noise the calculation, 3.9 dB indicates that the power level of the solar burst is higher than the receiver system noise [233].

4. 6. CALLISTO SPECTROMETER

It is planned to carry out co-ordinated radio spectral observations of the solar corona from various locations around the world during the International Heliophysical Year (IHY) 2007 [234]. A new generation of broad-band radio spectrometer is currently designed and built to provide high-dynamic-range imaging capabilities superior to that of existing instruments.

The Compound Astronomical Low-cost Low-frequency Instrument for Spectroscopy and Transportable Observatory (CALLISTO) has been described in detail by [189]. With these solar instruments in radio wavelength, a more accurate determination of the specific frequency of energy become feasible due to high time resolution [235]. CALLISTO was considered as a global network of spectrometer system with the purpose to observe the Sun's activities located in different regions of the Earth [236]. ETH Zurich has developed a number of solar radio spectrometers since 1980s [237,238]. It will convert the high-frequency electromagnetic signals into a form convenient for detecting and measuring the incoming radio emission. With large instantaneous bandwidths and high spectral resolutions, these instruments will provide increased imaging sensitivity and enable detailed measurements of the dynamic solar burst.

This spectrometer e-C07 having a detector sensitivity of 25 mV/dB including control cables and radio frequency adapters was supplied by ETH Zurich. It consist a channel with 62.5 kHz resolution, while the radiometric bandwidth is about 300 kHz. For each sample, it will take exactly 1.25 msec per frequency-pixel while the integration time is about 1msec. The frequency in the output data is expressed in MHz and the detector output is expressed in millivolts. Both are stored in a simple ASCII which can be analysed with any spread sheet like IDL, Math-CAD or EXCEL. At this system, an additional measurement was taken when applying a 50 Ω resistor to the antenna terminal as a reference level to evaluate the power level in dB above this broadband load.

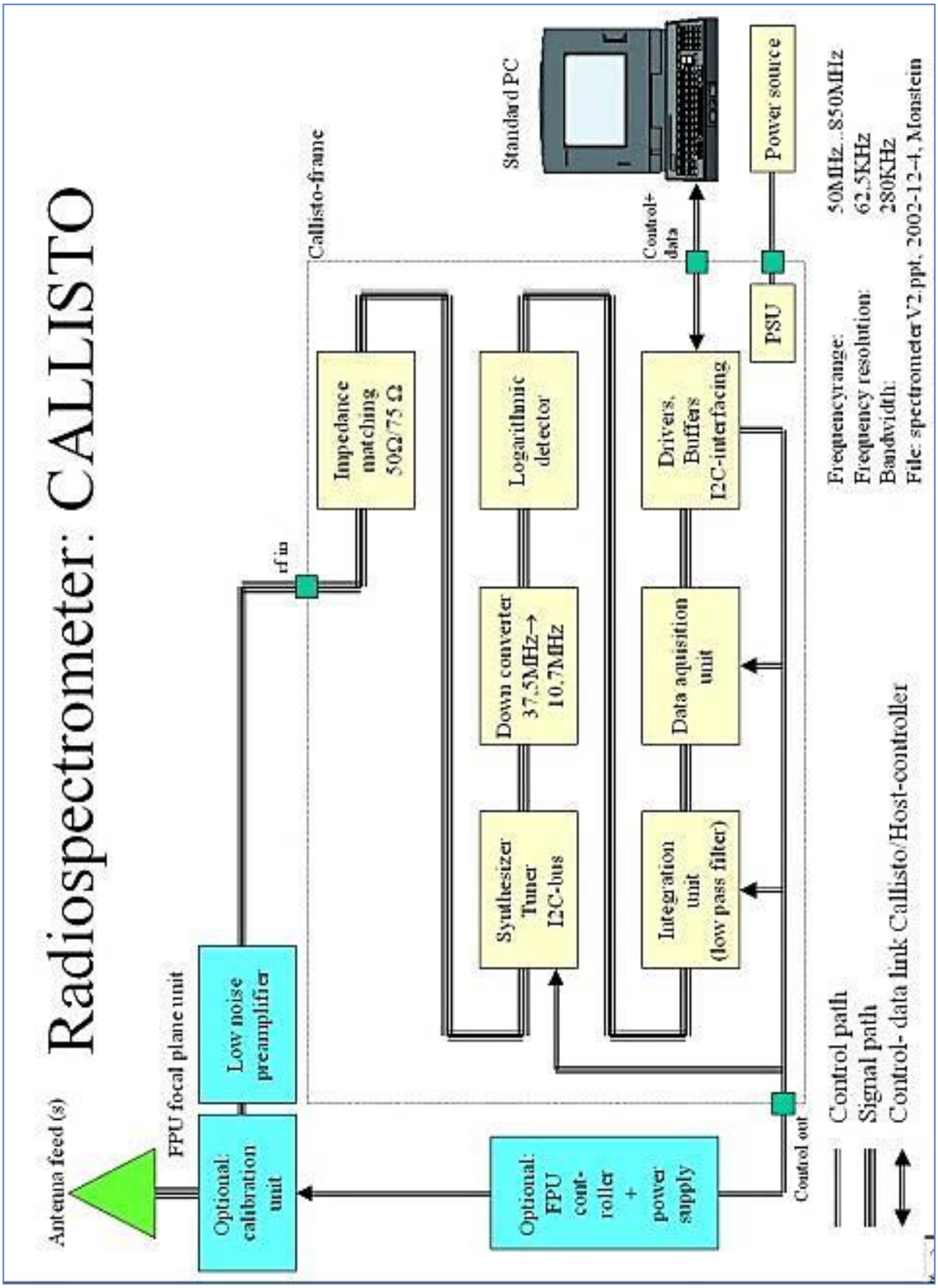

Figure 12. The CALLISTO system.

Meanwhile, Figure 12 showed the main configurations of the system developed by Christian Monstein which consists of a LPDA antenna, CALLISTO spectrometer and Windows computer connected to the internet. For standardized the time, GPS clock is used to control the sampling time of the spectrometer and a tracking controller control the antenna direction. We used the antenna directly control via low loss coaxial cable to the CALLISTO spectrometer.

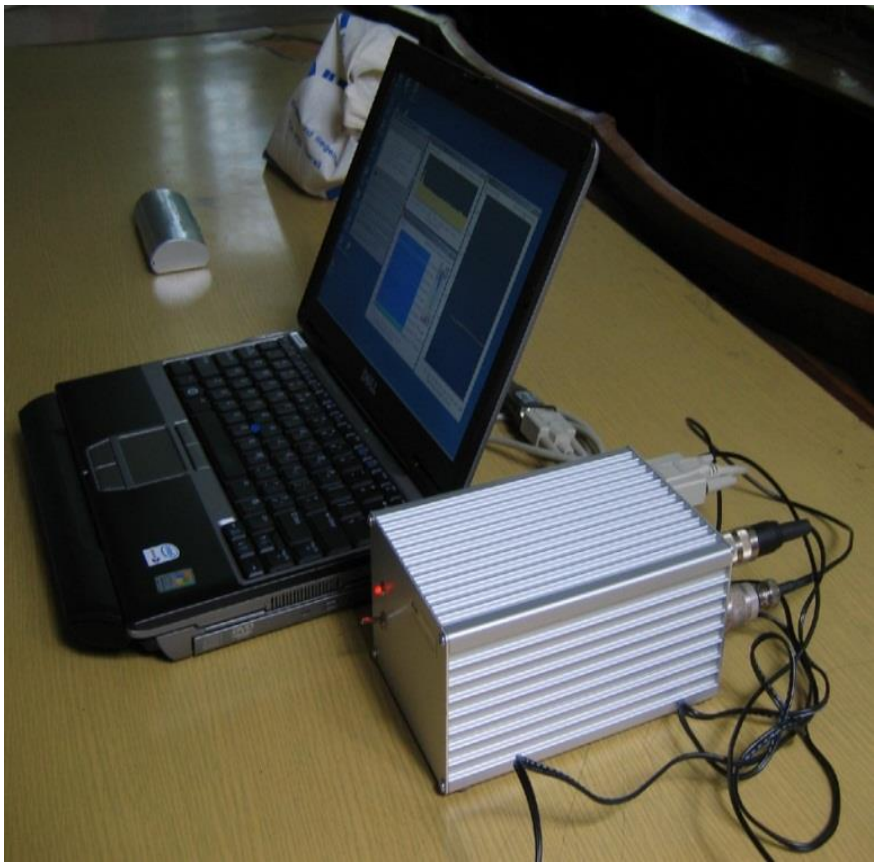

Figure 13. The CALLISTO spectrometer that connected to the notebook for acquisition data.

This LPDA directly control via low loss coaxial cable to the CALLISTO spectrometer. Up to now, the wide-band frequency techniques have focused on optimizing the accuracy and dynamic range achievable in the continuum burst by divided it into 15 minutes for each image to gain high resolution of frequency.

4. 7. SYSTEM CONFIGURATION

The main observations system consists of LPDA, low noise amplifier (LNA), CALLISTO spectrometer and Windows computer connected to the internet. For standardized the time, GPS clock is using to control the sampling time of the spectrometer and a tracking controller controls the antenna direction. The observations will start from 7.00 am till 7.00 pm, 12 hours every day.

The CALLISTO solar spectrometer hardware consists of the main board for data acquisition and interface with a RISC processor ATmega16 and of two synchronous receivers. The dynamic range is about 50 dB with a noise figure less than 10 dB. It can accumulate 800 samples /second with 500 channels and 200 frequencies per sweep. Within 1 second a total of 1000 measurements can be made. Basically, there is no need for a permanent operator. Once the system is powered and configured it runs automatically, controlled by an internal scheduler of the computer. This scheduler allows automatic starting and stopping of observations as well as controlling of an optional focal plane unit with up to 64 different configurations. It is recognized by a 6-bit digital output connected to a standard SUB-D25 connector. This option is needed for automatic calibration or antenna switching.

4. 8. LOW NOISE AMPLIFIER (LNA)

In order to gain the higher sensitivity of signal, special low noise amplifier (LNA) which is mainly known as RF (Radio Frequency) amplifier is used that acting as negative resistor. In general practices, LNA is an electronic amplifier used to amplify possibly very weak signals by an antenna. It is regularly located very close to the detection device to reduce losses in the feed line. By using an LNA, the effect of noise from subsequent stages of the receive chain is reduced by the gain of the LNA, while the noise of the LNA itself is injected directly into the received signal.

Figure 14. Low Noise Amplifier (LNA).

Thus, it is necessary for an LNA to boost the desired signal power while adding as little noise and distortion as possible, so that the retrieval of this signal is possible in the later stages in the system. A high quality LNA has a low NF (for example G ~ 1 dB), a large enough gain

(for example G ~ 20 dB) and should have large enough intermodulation and compression point. Further criteria are operating bandwidth, gain flatness, stability and input and output Voltage Standing Wave Ratio (VSWR). For low noise, the amplifier needs to have a high amplification in its first stage. Figure 14 shown the LNA that been used in the system. It has to be mounted as close to the antenna as possible to improve the overall sensitivity of the instrument. It compensates for cable loss between the antenna and CALLISTO spectrometer. The gain of the LNA is in the order of 20 dB and the noise figure of it is less than 2 dB. RF-input and output that we used are N-connectors of female type.

4. 9. CALLISTO APPLICATION SOFTWARE

The CALLISTO measurement time and frequency are controlled using a scheduler file and a frequency file. The number of frequency channels is set to the typical value of 200, so that the time cadence per channel is 0.25 second. In order to avoid strong RFI from unwanted signal, the range of frequencies of were selected between 150 MHz and 450 MHz. The detector output is read in analogue - to - digital converter (ADC) digits, where 256 ADC digits correspond to 2500 mV and stored in Flexible Image Transport System (FITS) file every 15 minutes. Data are stored with a scale factor and an offset applied so that the measured ADC digits range fits into the byte data range $(0 - 255)$.

4. 10. SITE

The National Space Agency, Banting, Selangor is an ideal and a main site for a broadband solar observation because the minimum of RFI for the CALLISTO system in Malaysia [239]. Table 1 below showed a geographical coordinates of the site.

Table 1. Geographical coordinates of the National Space Centre, Banting.

Parameter	Value
Latitude	2.912932 N
Longitude	101.684335 E
Altitude above sea level (meter)	63
Local time	Every day from 7.30 am till 7.30 pm

One of the apparent disadvantages of the spectral expansion and limited averaging procedure is that this data can be only automatically saved in a daily basis only. Another difficulty in the interpretation is due to the fact that the observations suggest a few non-axisymmetric harmonics.

COVERAGE OF SOLAR RADIO SPECTRUM IN MALAYSIA AND SPECTRAL OVSERVIEW OF RADIO FREQUENCY INTERFERENCE (RFI) BY USING CALLISTO SPECTROMETER

5. 1. CALLISTO CONFIGURATION AND MALAYSIA SOLAR SPECTRUM COVERAGE

Recent years have witnessed considerable developments in new area in solar bursts. The study of radio emission specifically in solar radio bursts of low frequency becomes extensively serious by the development of the CALLISTO network since 2002 [25]. This study is focused on low frequency from 45 MHz till 870 MHz with 28 sites all over the world to obtain 24 hours solar monitoring [240]. Up to date, the coverage of solar activities has been reached more than 95 %. In Malaysia, solar radio research has just started since Jun 2011 and joining the e- CALLISTO network is a good opportunities to start the solar radio astronomy research [241]. At the preliminary stage, the construction of LPDA and installation of CALLISTO system has successfully done by 22nd February 2012 [242].

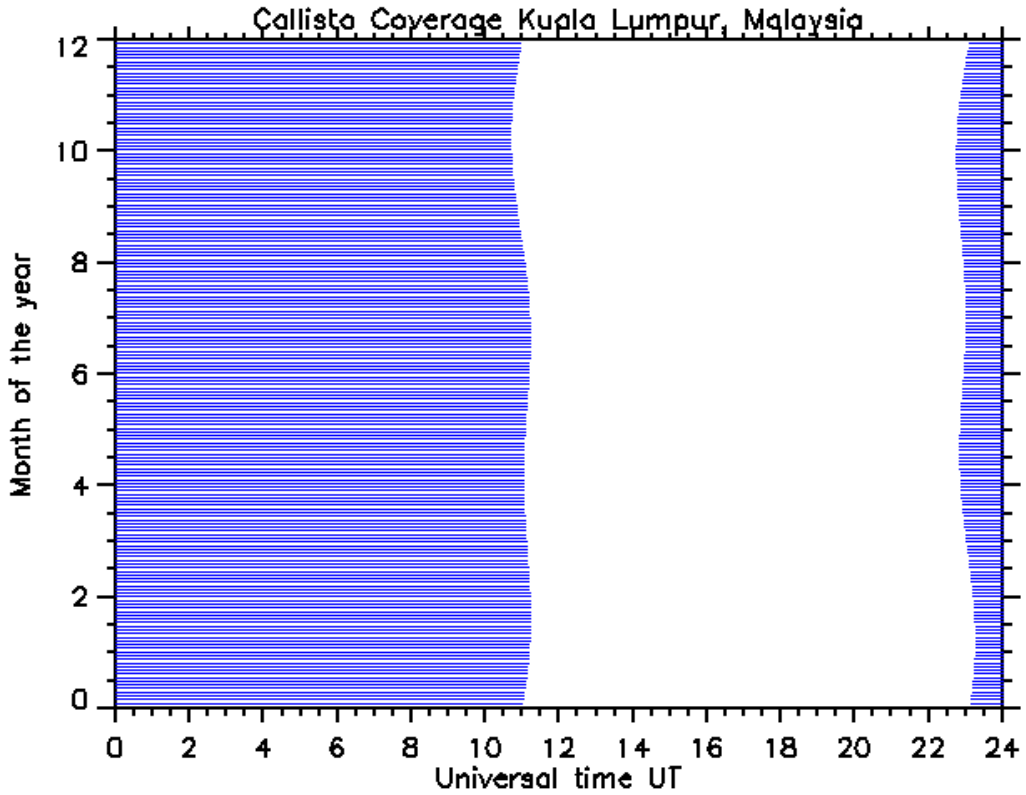

(a)

Figure 15. Current status of CALLISTO coverage of Kuala Lumpur Malaysia (**a**) and worldwide (**b**).

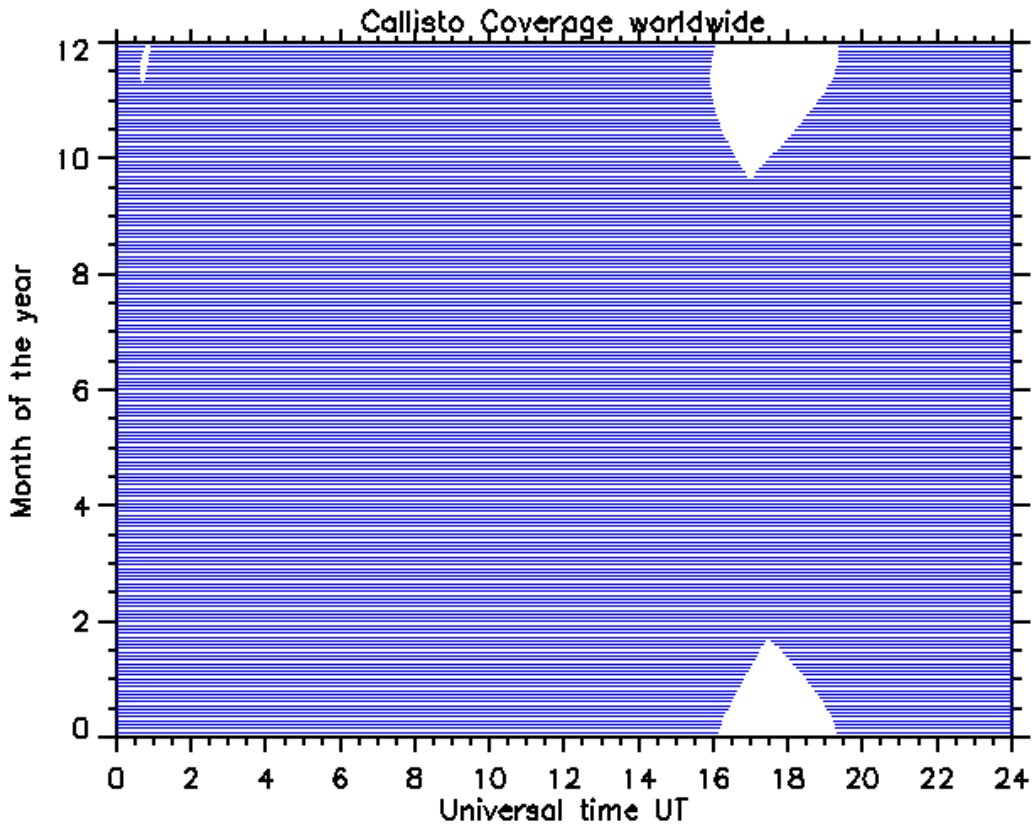

(b)

Figure 15 (continue). Current status of CALLISTO coverage of Kuala Lumpur Malaysia (**a**) and worldwide (**b**).

The e-CALLISTO network has had its first success in December 2006, when the last large flares of the present cycle occurred [243]. Meanwhile, the CALLISTO system was successfully installed at the National Space Centre, Banting Selangor located at (3°5′00″N 101°32′00″E). This is one of the candidate sites for radio astronomical purpose in Malaysia with a very minimum population density and far away from city [244]. Figure 15 shows the current status of CALLISTO coverage in Malaysia compared with worldwide coverage in Universal Time (UT) and month of the year parameters [245].

Here, the objective to monitor Sun's activities within 12 hours throughout a year is possible. Daily observing period is starting from 11:30 to 23:30 UT. Due to 12 hours monitoring, Malaysia site almost covered fifty per cent of the CALLISTO coverage [246]. It could not be denied that modern society is strongly dependent on complicated electronic systems, spacecraft and other application which are vulnerable to extraterrestrial influences [247]. The radio wave propagating towards the Sun will, in general, suffer deviation from its original direction together with absorption attenuation. Therefore, the increasing use of wireless systems as a mode of communication requires a study of the possible effects of solar activity in the radio frequency ranges that are used and projected for use in technology systems [248].

5. 2. RADIO FREQUENCY INTERFERENCE (RFI) TESTING

In this case, an RFI survey has been done in a day starting from 9.00 am till 17.00 pm on 21st of February 2011 [249]. The direct measurement direct to the Sun is called ON-source while the measurement away from the Sun is called the OFF - source. The continuous signal of frequency responses from the CALLISTO spectrometer is identified [250]. The data will be transferred to a computer for further analysis. This measurement involves technical basis to decide how to continue the concerning spectroscopic measurements below 870 MHz. Occasionally, the Sun was very quiet in a few days after installation and configuration [251]. Detailed analysis also revealed the interference sources that caused an interruption of solar signal. In order to achieve a good signal of the Sun, it is necessary to recognize the range of minimum interference [252].

It must be emphasized that there is an interference level which are rather high with up to 50 Db [253]. Apparently, it is revealed that in the UHF-band a few signal can be recognized (besides a lot of analog-TV), two DVB-T channels between 650 MHz and 700 MHz. Furthermore, there is a high level interference is received from FM-band (80 – 108) MHz, from VHF-band (30 − 300) MHz and from UHF-band (300 MHz − 3000) MHz. It is interesting to note that from the analysis, the mobile phone transmission and a strong signal from TETRA (Terrestrial Trunked Radio) can be detected respectively at 850 MHz and around 390 MHz. An interesting feature can be observed between 240 MHz and 280 MHz [254]. It shows downlinks from US military satellites with about 10 dB above the noise level. In addition, the range from (250 − 270) MHz is categorized as a minimum interference of range [246]. All reserved frequencies are still free from the interference [255].

Unfortunately, most of the strong and fluctuate interferences are home made by local electronic devices and local oscillators and clearly been seen from (85 − 150) MHz [256]. However, it would be difficult or impossible to eliminate it completely. Due to these results, there are three frequency ranges can be identified for useful astronomical observations: (i) between 45 MHz and 80 MHz (ii) between 240 MHz and 380 MHz and (iii) between 780 MHz and 850 MHz. From the analysis, it is found that the signal to noise ratio is 3.9 dB [257].

In short, more work is required to analyze the nature of solar radio bursts, although preliminary indications are promising. The increasing of RFI sources is hardly to prevent, but, by subtracting the background data in the analysis process. One of the best ways to ensure the safety of radio astronomical measurements is by choosing the protected frequency bands for the measurements. Finally, the observation of RFI would give a clear picture to select a good data. In short, the National Space Centre, Sg. Lang, Selangor Malaysia is one of the strategic countries to monitor the Sun due to consistent 12 hours per day throughout the year. When a module of subtraction of RFI automatically implemented for each datum, one can study the evolution of solar bursts and further predict the behaviour of solar flares and other solar activity phenomena [258].

5. 3. CONCLUSION

Thus, with the implementation of the CALLISTO system and development of solar burst monitoring network, a new wavelength regime is becoming available for solar radio astronomy. It could be possible to improve the system and actively contribute the solar radio burst data to be used all over the world [259].

RESULTS OF SELECTED EVENTS AND DISCUSSION

One of the main reasons to study more about the dynamics of solar radio bursts is because solar these bursts can interfere with GPS and communications systems. More importantly, these bursts are a key to understand the space weather condition. Recent work on the interpretation of the low frequency region of a main solar burst is discussed. Continuum radio bursts are often related to the solar activities such as an indication of the formation of sunspot, impulsive phase of solar flares and Coronal Mass Ejections (CMEs) and their frequencies correspond to the densities supposed to exist in the primary energy release volume [260]. Specifically, solar burst in low frequency play an important role in interpretation of Sun activities [261].

In this section, the question on what changes occur when a solar radio burst goes from the impulsive phase to the main phase will be focus, specifically on what causes this change, and how [262].

To answer this question, a particularly well-observed solar radio burst on was selected, which shows the obvious shear change via the evolution of the burst [263]. However, the researcher would like to know what these observations mean vis-a-vis other factors and events associated with the events. It is important to fully understand the process of CMEs by knowing the background environment especially in the active region. Normally, it will take several days for a sun to rotate with slow solar disks sources and varying radiation in the active region. Apart from reporting the experimental results, the primary goal of this chapter is also to discuss and analyze several the data and come out with reasonable interpretation.

To provide an analytical description of each type of the burst, we listed the parameter that might influence the formations and the evolution of the burst such as sunspot number, radio flux and the active region that trigger the burst. We also focused on the specific range of frequency in order to observe the potential location that might need to be highlighted. This is very important because when there is expected any event of solar activities we are already targeting the range of frequencies [264].

6. 1. SELECTED RESULTS: A CASE STUDY OF SRBT III

6. 1. 1. Observations on 9th March 2012

Observations of low frequency solar radio burst type III associated with the ejection of plasma oscillations localized disturbance is due to excitement in the plasma frequency [265]. Here, the results of the dynamic structure of solar flare type III occurred on 9th March 2012 at National Space Centre, Sg Lang, Selangor, Malaysia is reported by using the CALLISTO system [266]. These bursts are associated with solar flare type M6.3 solar flare which suddenly ejected from the active region AR 1429 starting at 03:32 UT and ending at 05:00 UT with the peak at 04:12 UT. During a solar flare, large quantities of energy are transferred between corona and chromosphere through thermal conduction, non-thermal particle beam, radiation transport and mass motions [267]. From the observation, it showed that an initial strong burst occurred due to strong signal at the beginning of the phase. It was also found that both solar burst and flares tend to be a numerous on the same days and the probability of chance coincidence is high. It showed an impulsive lace burst detected at 4:24 UT and it is

more plausible that the energies are confined to the top of the loop when compared with the X-ray results. Associated with this event was type II with velocities 1285 km/s and type IV radio sweeping along with a full halo Coronal Mass Ejections (CMEs) first seen in SOHO/LASCO C2 imagery at 09/0426Z [268].

The type III solar radio bursts, which are generated when high-energy electrons are ejected from the Sun, are characterized by a rapid drift in frequency from hundreds of megahertz to tens of kHz. It is believed that the process of producing type III solar radio bursts is associated with the excitation of Langmuir waves, which are oscillations in the electron density in a plasma, followed by the conversion of these waves into radio emissions. During solar flares there may be large increases (bursts) in radio emission lasting anywhere from a few seconds to several hours [269].

In order to understand the possible mechanism of the dynamic structure of the burst, relationships and time integrations of the bursts with soft/hard as well as solar flares would have to be investigated. Chronology of solar burst type III is being shown in light curves and spectral profile as shown in Figure 16 in order to understand the phase of each burst take their own place during this solar event. In general, each figure showed systematic variations of solar radio burst type III with frequency. During this time, the solar flare generates radiation across the electromagnetic spectrum at various wavelengths. Both solar burst and flares tend to be numerous on the same days and the probability of chance coincidence is high [270].

The short duration of individual burst suggests local acceleration of electrons to a few times the thermal energy. This is the only type of burst which is not been specifically associated with solar flares. It is generally accepted that type III bursts must be some form of fundamental frequency plasma emission and signifies by non-thermal in origin. This hypothesis explains important observed characteristics of type I storms, notably the high brightness temperature and strong O mode polarization. The long life of a storm points to continue local energy release in the source region, which is probably related to the magnetic field recombination after new flux intrudes into existing fields.

For this event, a time window of approximately 1 and half hour, (88 minutes) covering the phases of impulsive courses (waveforms) and background signals (see Figure 16 and 17) is considered. During 3:42 UT, there is a sign of solar burst has been successfully detected in the region of 250 MHz till 350 MHz is considered. Physically, it showed an initial strong burst will happen due to strong signal at the beginning of the phase. The beginning signal at 3:41 UT is an indicator that strong burst will occur due to the strong signal. In each of the case of the Figure 16(a), a different pattern can be observed with a significant burst at 3:50 UT, with the stripe-like bursts become stronger during this time. It is then followed by a group and complex solar radio burst type III in a few minutes (Figure 16 (b)). Uniquely, an inverted solar burst U can be observed at 385 MHz associated with X-ray solar flare can be observed within one second at 4:12 UT (Figure 16 (c)).

The magnetic island formation and coalescence instability reconnection regime are responsible to the impulsive of different bursts. At this stage, electrons traveling to the top of the loop generate the branch of the U burst with negative frequency drift, whereas those traveling from the top generate the branch with the positive drift. The electron beams travelling through the solar corona excite Langmuir waves near the local electron plasma frequency. Once these Langmuir waves are converted into electromagnetic waves, the radiation can be detected in radio region as bursts with very specific spectral signatures that depend on the magnetic structure which guides the beams.

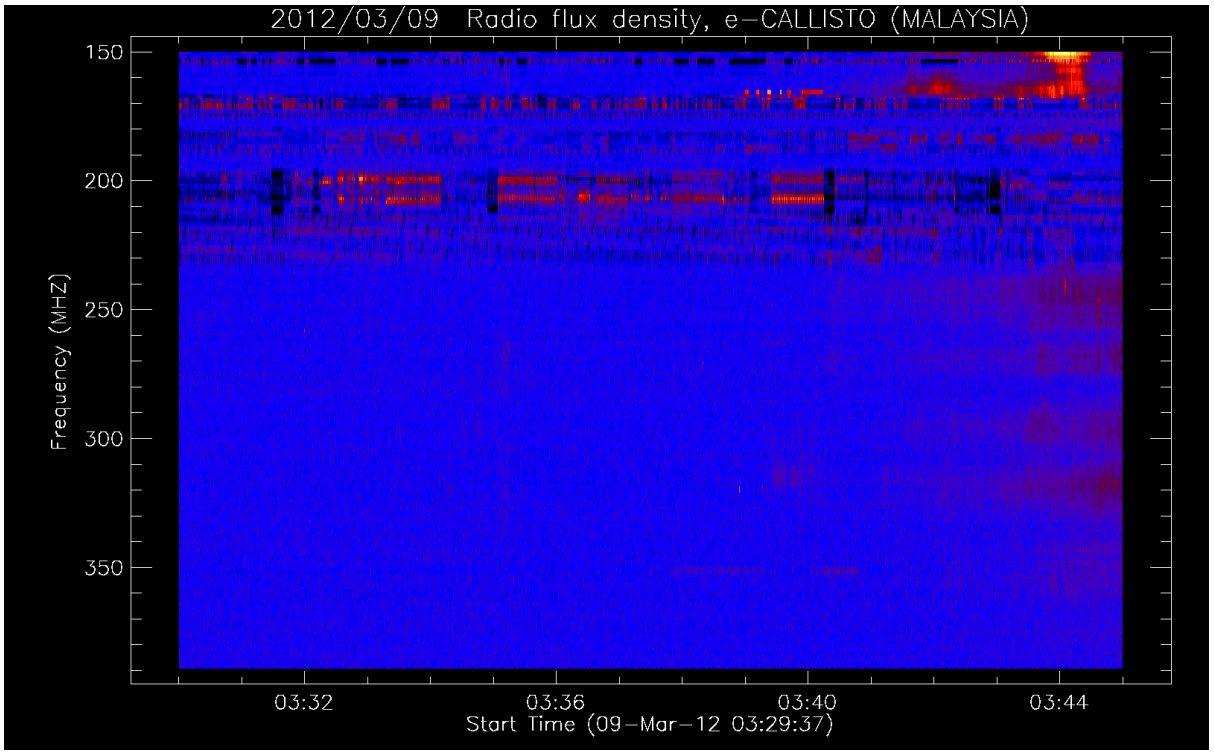
2012/03/09 Radio flux density, e-CALLISTO (MALAYSIA)
150
200
250
300
350
Frequency (MHZ)
03:32
03:36
03:40
03:44
Start Time (09-Mar-12 03:29:37)

(a)

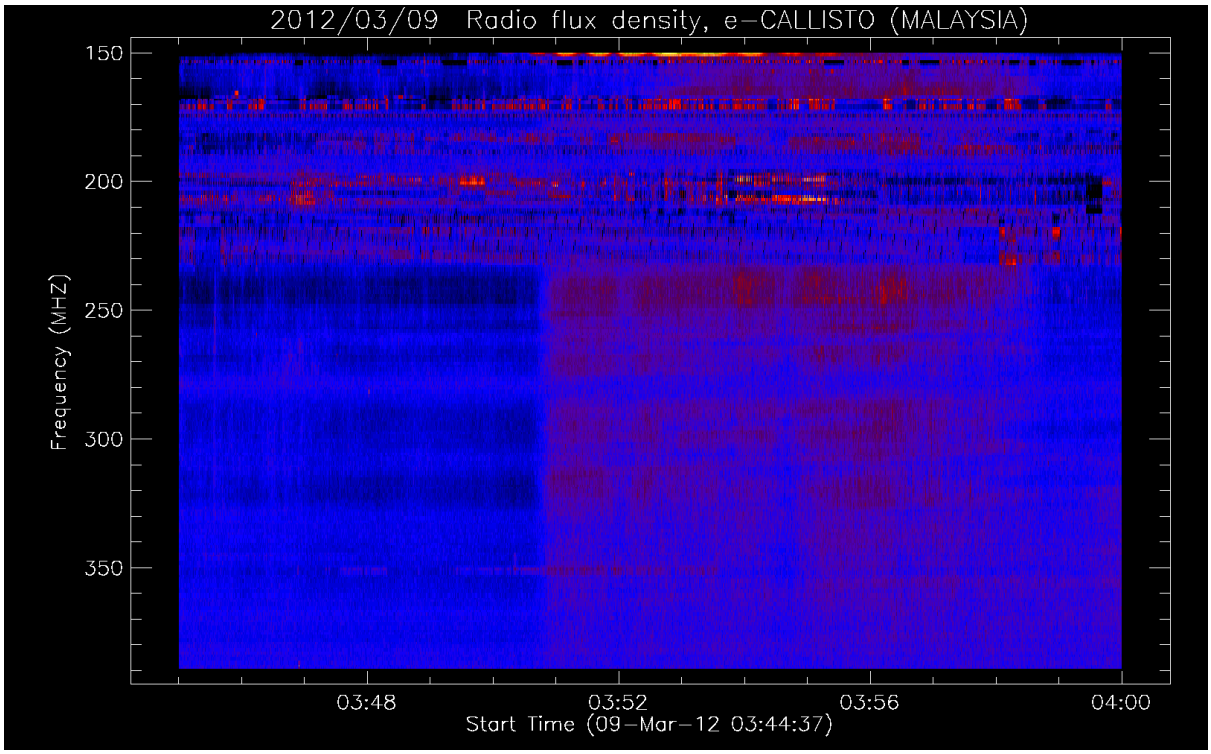
2012/03/09 Radio flux density, e-CALLISTO (MALAYSIA)
150
200
250
300
350
Frequency (MHZ)
03:48
03:52
03:56
04:00
Start Time (09-Mar-12 03:44:37)

(b)

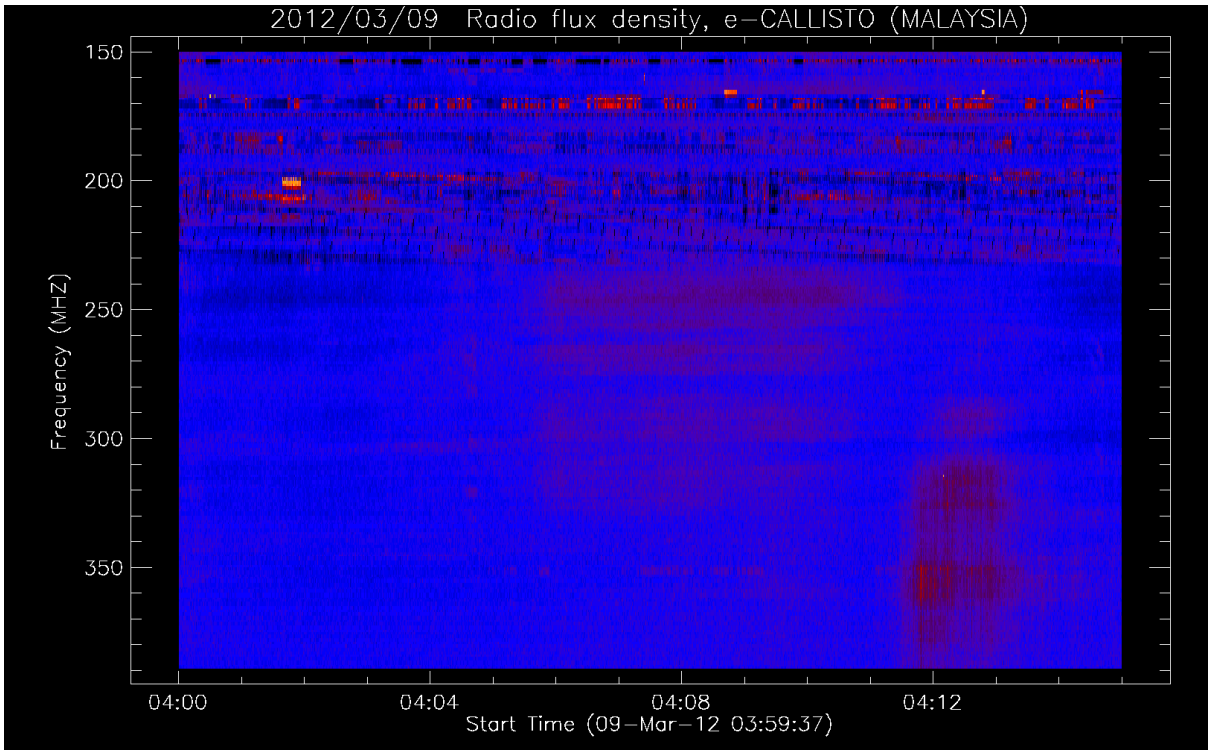

(c)

Figure 16. (**a**) The detection solar burst type III from 3.30-3:45 (**b**) 3:45-4:00 and (**c**) 4:00 to 4.15 UT. A group and complex type III solar burst (iii) an inverted type U solar burst on 9th March 2012.

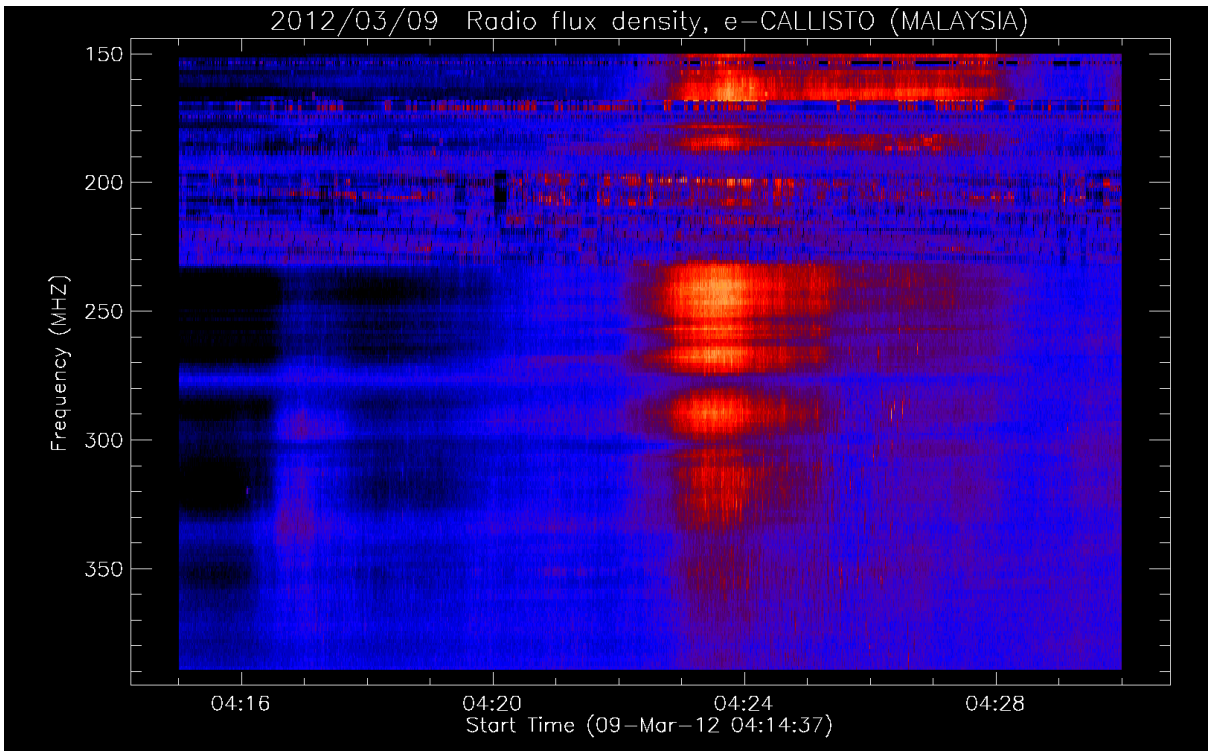

(a)

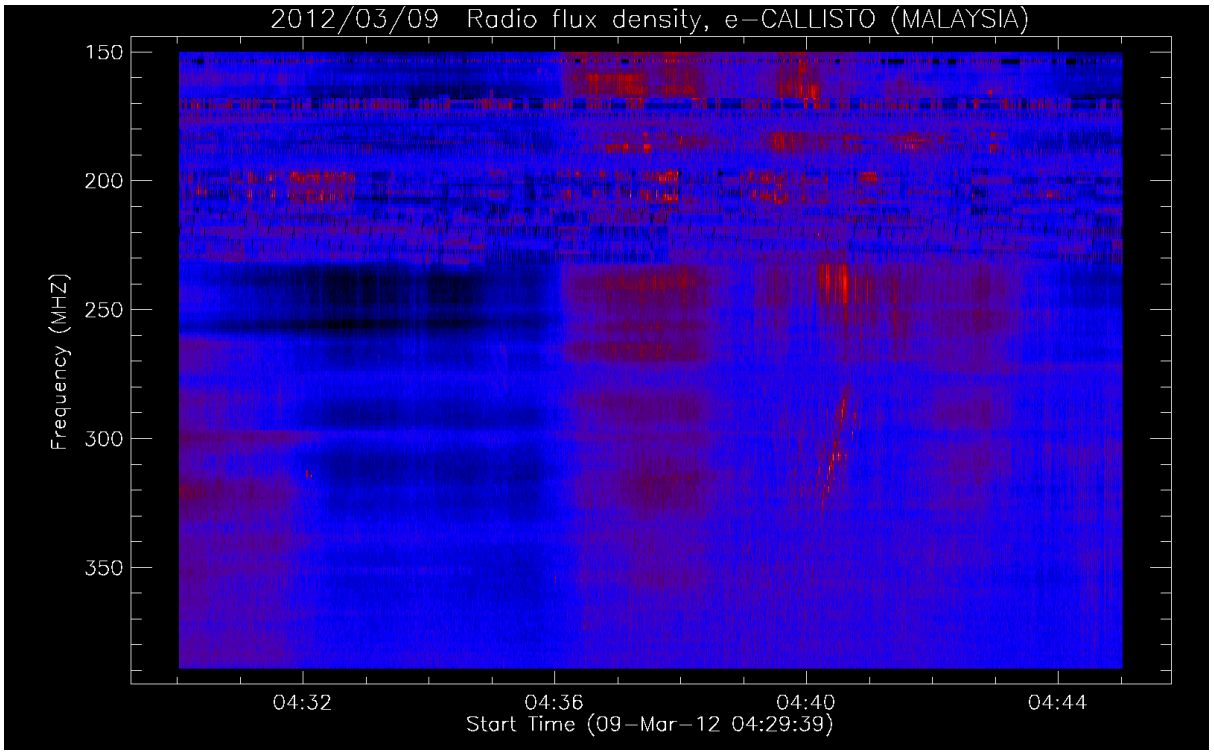

(b)

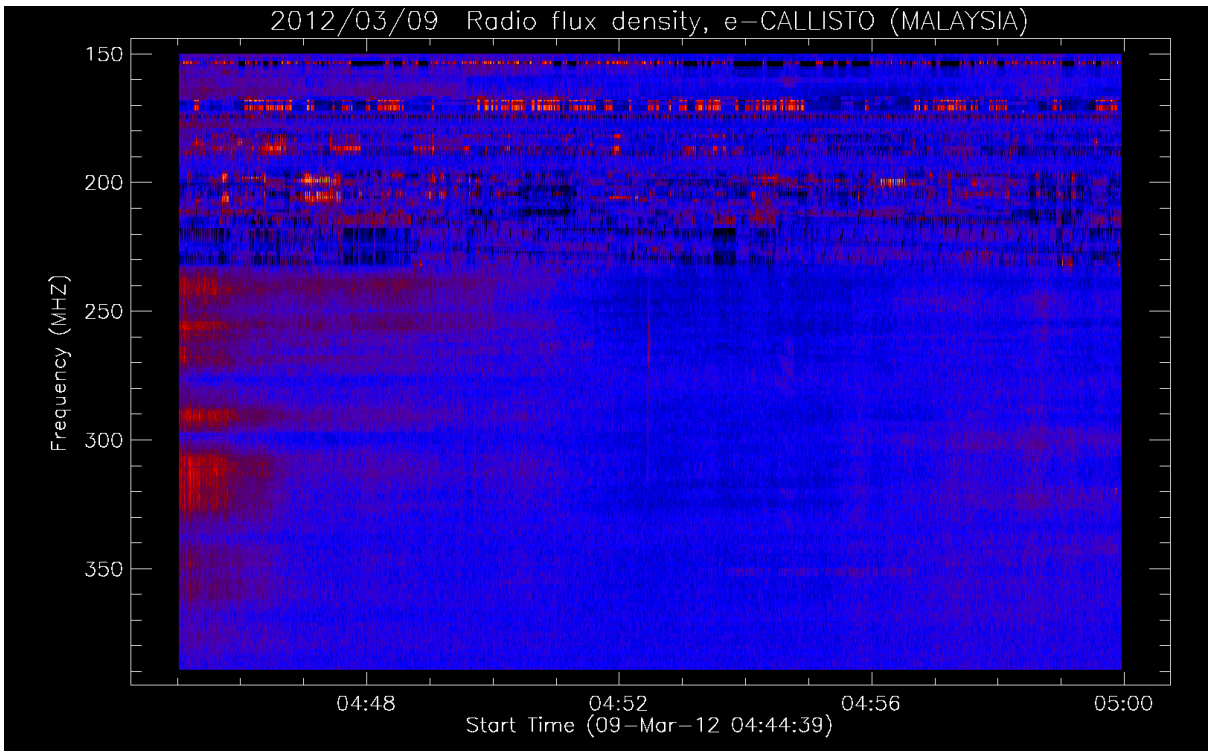

(c)

Figure 17. (**a**) Continuous detection solar burst type III from 4:15-4:30 UT (**b**) 4:30-4:45 UT and (**c**) 4:45-5:00 UT on 9th March 2012.

There is a growing interest in observing solar burst in low frequency of the radio region due to the increasing number of solar activities towards 24th solar cycle. In this article, a comprehensive analysis of variation of solar burst has been presented. There is a growing interest in observing solar burst in low frequency of radio region. It could not be doubted that e-CALLISTO network plays a dominant and important database on the target monitoring solar activities in 24 hours. The results presented in this paper point to the importance of observing Sun activities in radio region. Still our data show hints of possible solar activities that can be detected in this lower region [271].

Our radio observations were carried out simultaneously with the CALLISTO spectrometer is could contribute a good data due to our advantages, which made daily observation for 12 hours throughout the years and the different perspective seems our location as an equatorial site. This factor may be important for observation of burst with long duration. It is hoped that we could possible to gain a better data that can be used as a reference.

It is clearly shows an impulsive lace burst surfacing at 4:24 UT and it is more plausible that the energies are confined to the top of the loop, which is also confined with X-ray results. This fast frequency drift rate (~ 100 MHz s^{-1}) is due to electron beams on open filed lines and bump on tail instability, which is locally in narrowband form which produce from the low corona of the Sun. The burst is now at the end of the phase where it can be observed, and it has now decreased till 4:52 UT [272].

In order to have a clear picture the behavior of the Sun before the event is occur; the scenario of proton flux from the previous days is presented. On a bigger scale, Figure 18 illustrates the pattern of proton flux within four days. Based on the continuous observations, the Sun is active since 7th March 2012 with particles of proton flux growth drastically up to 10^3 cm^{-3}s^{-1}sr^{-1} during 8th March 2012. There is also a halo of Coronal Mass Ejections (CMEs) produced shortly after, and is expected to deliver a glancing blow to earth's magnetic field sometime March 16th. It is believed that the region of the radio-rich emission is associated with the injection of the energetic particles [273].

The distribution of the velocity is in the range of $450 - 800$ kms^{-1}. The solar storm also occurred 10 times stronger than the normal solar wind. Very often, a phenomenon displays a well determined behaviour where observables fluctuate around the average value. However, it is believed that they originate from a region close the disk centre. The average width of halo CMEs is approximately equal to 120º. Further, Figure 6.5 shows distribution of the velocity of CMEs, versus their projected speeds, v (angle from North) on 9th March 2012 [274].

The separation and slight decay within the intermediate area was observed in Region 1429, however it still remained in the large Ekcspot group with a Beta-Gamma-Delta magnetic configuration. There was a new sunspot group rotating onto the North East limb and was numbered Region 1432 (N18E69). This new region is too close to the limb to accurately determine the spot and magnetic classification, however it produced a C9 flare at 09/2025Z. Figure 6.6 illustrates the sunspot 1429 eject X-class solar flare. During this period, M6 solar flare occurred in the active region AR 1429 starting at 03:32 UT and ending at 05:00 UT, with the peak at 04:12 UT [275].

It was found that the geomagnetic field was at active to severe storm conditions due to continued activity from the sheath region associated with the 7th March 2012 CME. Unfortunately, we could not obtain the data during that period because our system is suddenly switched off due to high voltage. Meanwhile, at approximately 09/0049Z, the *Bz* component of the interplanetary magnetic field started to rotate towards a more magnetically connected polarity. The *Bz* component continued to be negative for several hours reaching values near -17 nT with an approximate solar wind speed over 600 kms^{-1}.

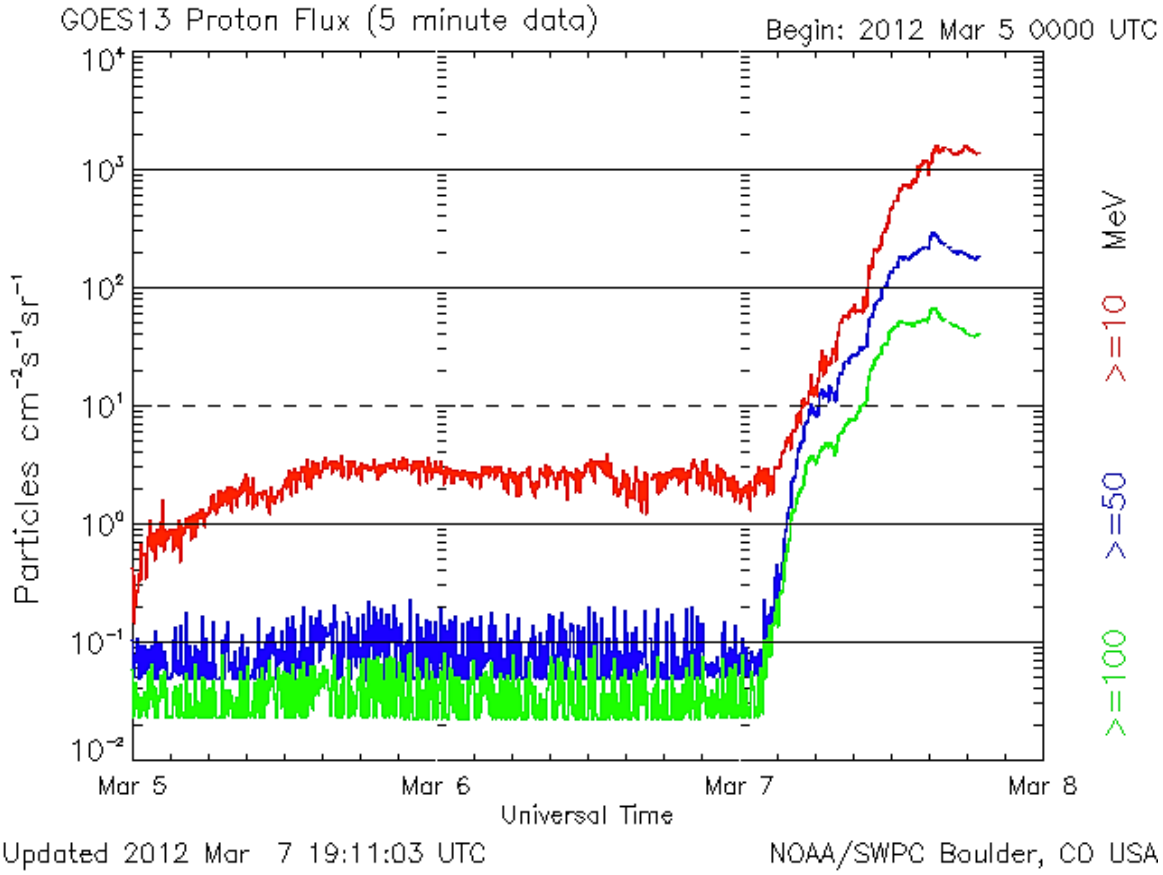

Figure 18. The pattern of proton flux within 4 days.

The geomagnetic field responded with major to severe storm periods during the periods 09/0300 – 1500Z. Greater than 10 MeV proton event that began at 07/0510Z is on-going. Moreover, greater than 100 MeV proton events that began at 07/0405 are on-going.

It was found that the geomagnetic field was at active to severe storm conditions due to continued activity from the sheath region associated with the 7th March 2012 CME. Unfortunately, we could not obtain the data during that period because our system is suddenly switched off due to high voltage. Meanwhile, at approximately 09/0049Z, the *Bz* component of the interplanetary magnetic field started to rotate towards a more magnetically connected polarity. The *Bz* component continued to be negative for several hours reaching values near -17 nT with an approximate solar wind speed over 600 kms^{-1}. The geomagnetic field responded with major to severe storm periods during the periods 09/0300 – 1500Z. Greater than 10 MeV proton event that began at 07/0510Z is on-going. Moreover, greater than 100 MeV proton events that began at 07/0405 are on-going.

It seems these CMEs cause pressures on the Earth's atmosphere when they hit. The CMEs associated with the R2 (Moderate) Radio Blackout that occurred at 0353 UTC March 9 (10:53 p.m. EST March 8) was expected to cause strong geomagnetic storming beginning early on March 11. A little storming has been observed, but there was a weak disturbance starting around 1230 UTC March 11 (7:30 a.m. EDT). This CME by the way was not headed straight for Earth. Therefore, this weak disturbance may have resulted in just the skirting the edge of the CMEs. The CMEs associated with the R2 (Moderate) Radio Blackout event from

1744 UTC March 10 (12:44 p.m. EST March 10) should start to affect Earth late on March 12 to early on March 13 with G2 (Moderate) to isolated G3 (Strong) levels likely. Meanwhile, the solar radiation storm continues its decay and is currently at the S1 (Minor) level. Although region 1429 remains complex, however, it is showing signs of weakening.

The discussion here is confined to those techniques that have been or are being developed for use in solar data and to the inferences about the structure and dynamics of the Sun that have already been made. Although there is no solar radio burst type II formed during this event within this region, this case showed that solar flare with M6 class is dominant with an isolated type III bursts. The conclusion drawn hare relative to the significance of study of solar burst type III lies in the fact that the emission at meter wavelength comes from the magnetic field in the active region, which may provide the key to the energy release mechanism in solar flare and CMEs.

6. 1. 2. Observation during 13th November 2012

It is widely known that a variation of magnetic field lines potentially creates the solar flares. As the Sun rotates around its axis, the magnetic field lines threaded to the Sun also follow the same rotation. However, when there is a difference in the Sun velocity, the magnetic field lines sometimes gets twisted up and become more complicated in their form. When this situation occurs, the magnetic field lines sometimes become too complicated in form as they tend to overlap with each other, and in the end they get twisted up and cut loose from the original lines and set free as solar flares [276].

In this section, a comprehensive analysis of SRBT III observation of short-duration in association with eruptions on the sun and appear like a radio burst type II is presented. This observation allows for the mechanisms of evolution type II and local environment of the burst to be characterized. Yet, the burst is quite unique and interesting to be tackled. The burst is classified as a SRBT III. However, a clear structure of fundamental SRBT II can be observed. This event occurred on 13th November 2012 from 2:00:03 UT till 2:00:06 UT. It peaked with M2.0 solar flare at 2.04 UT [277].

Based on the observation, a fast drift Type III solar burst is formed intermittently within six hours period of observation starting from 00:00 UT TO 3:00 UT. The chronology of the event is very important to understand what factors that caused the solar burst type II broke. This data is taken from our site and there are a few sites that also successfully obtained the data [278]. Figure 19-32 shows the timeline of the solar burst type II and III.

From the earliest prediction, there is a possibility a CME will eject directly to the Earth. This is due to a continuous monitoring within a few days period. Based on the results, it is associated with type M flare from active region AR1613 and AR1614. It was found that the sunspot number is 188 and radio flux exceeds 144 sfu. There are eight sunspots and with density of 9.1 proton/ cm^3. During that event, solar wind also reached up to 369.7 km sec^{-1}. Those parameters provided an alert with sun's activities. The potential of a big explosion of CMEs is considered very high.

Based on observation, the formation of SRBT III is due to multiple radio blackout storms. As can be seen from Figure 22, there is a group of SRBT III (at the background of the intense burst) that formed intermittently with a wide range frequency from 220 MHz till 380 MHz. In conjunction with constraints on the spectrum, it is believed that the burst is drifts in a wide range. This burst actually has been observed intermittently in the last a few hours since 00:22 UT.

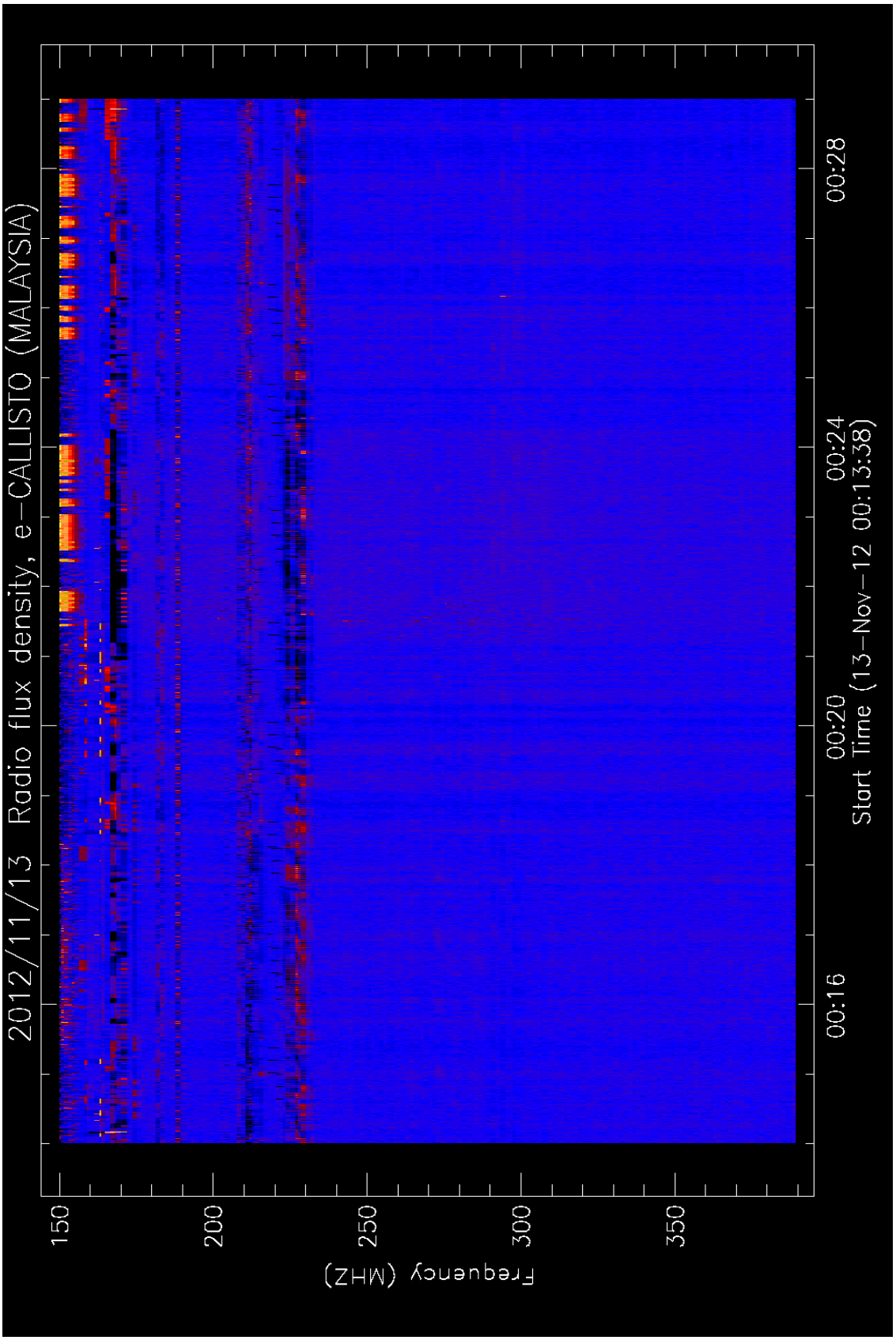

Figure 19. An intermittently and a group of type III burst from 00:00 – 00:30 UT.

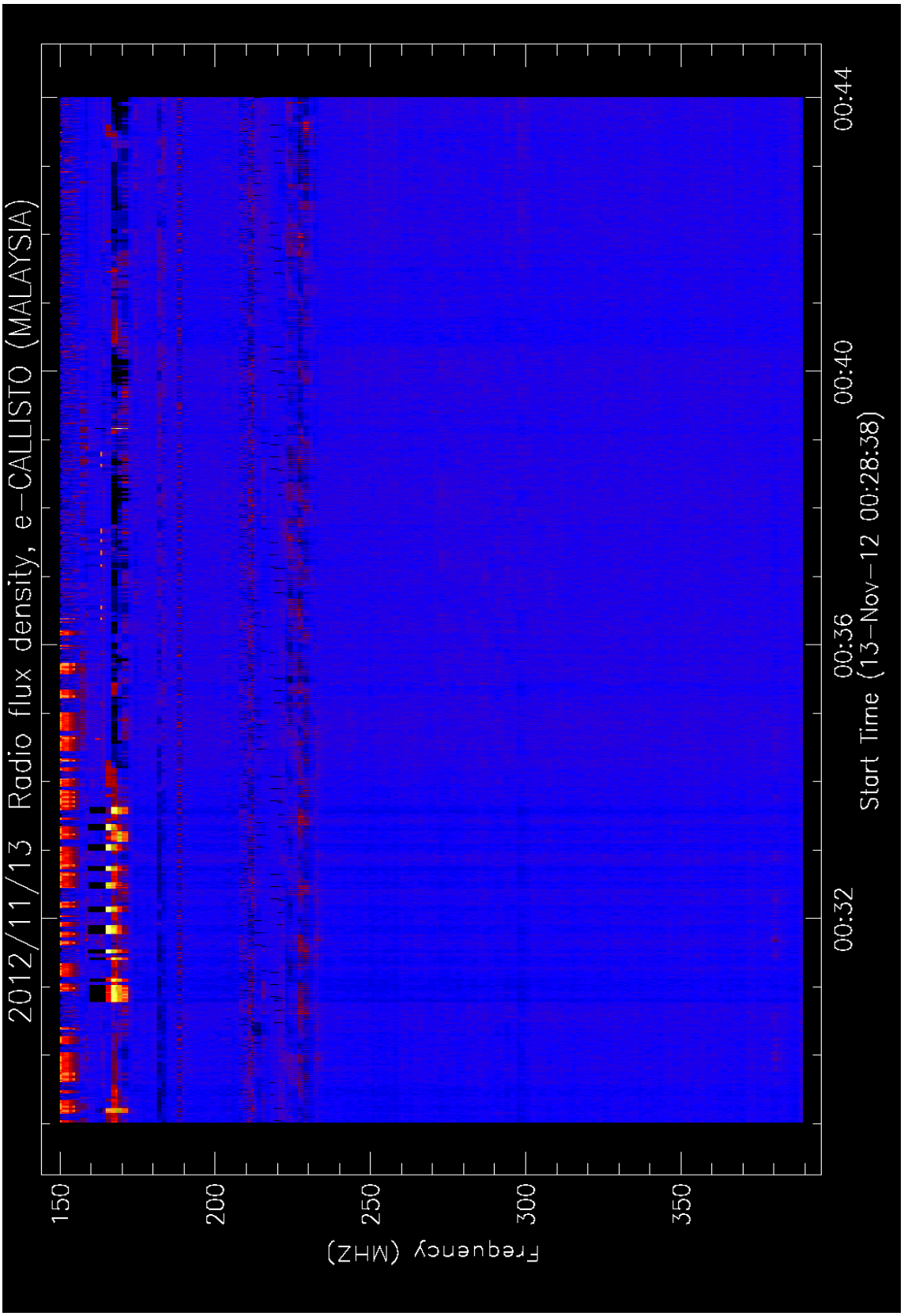

Figure 20. An intermittently and a group of type III burst from 00:30 – 00:45 UT.

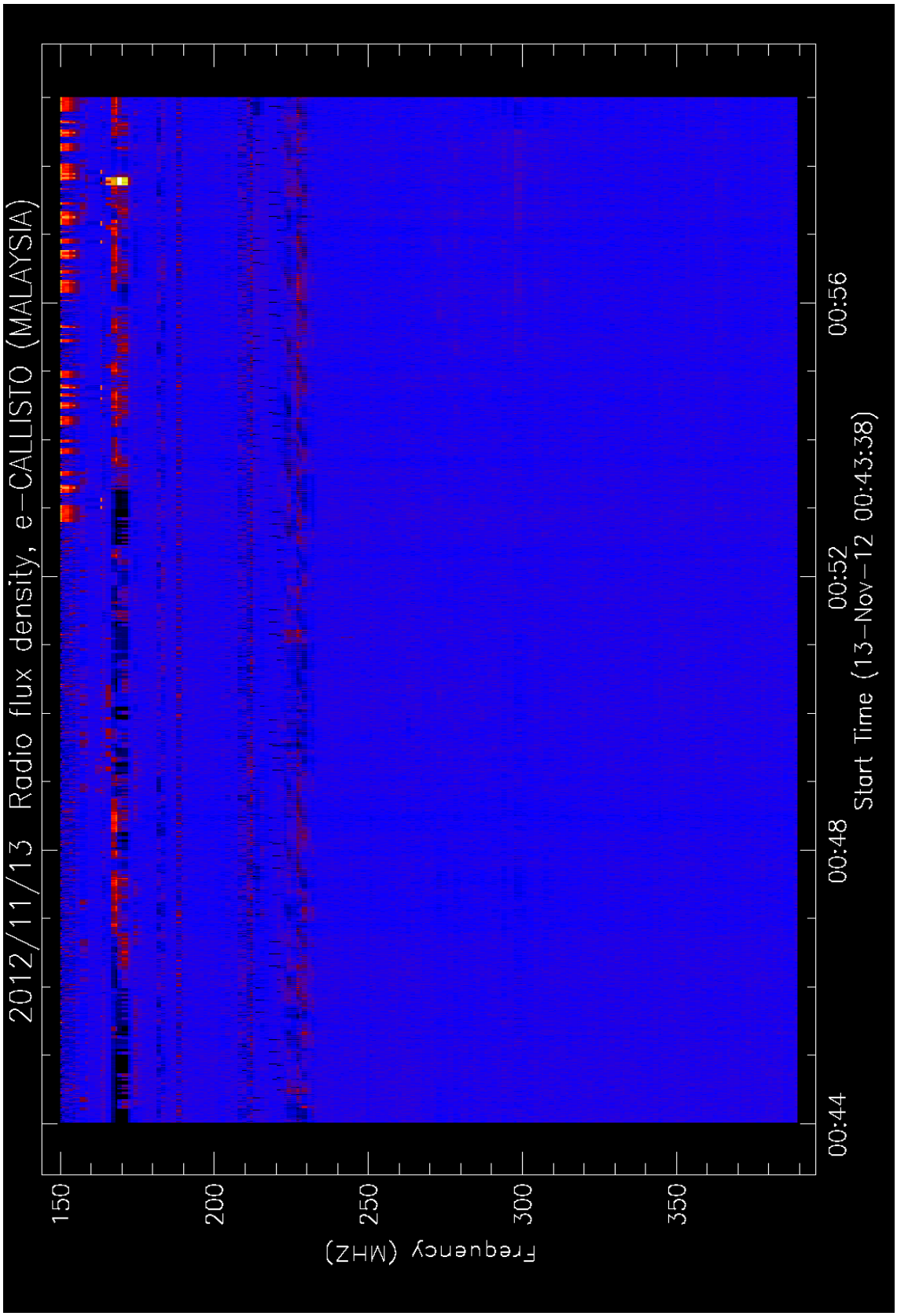

Figure 21. An intermittently and a group of type III burst from 00:45 – 01:00 UT.

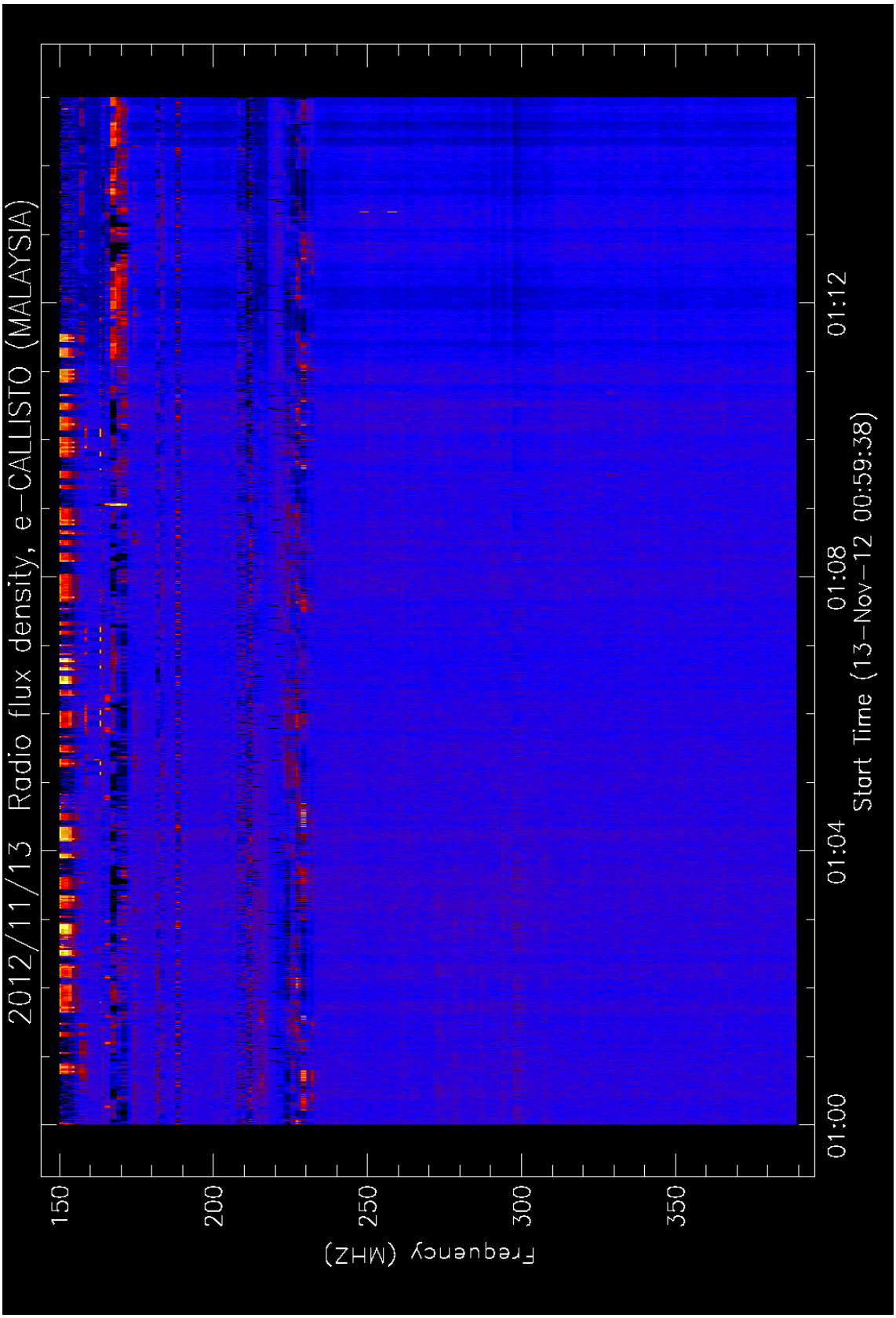

Figure 22. An intermittently and a group of type III burst from 01:00 – 01:15 UT.

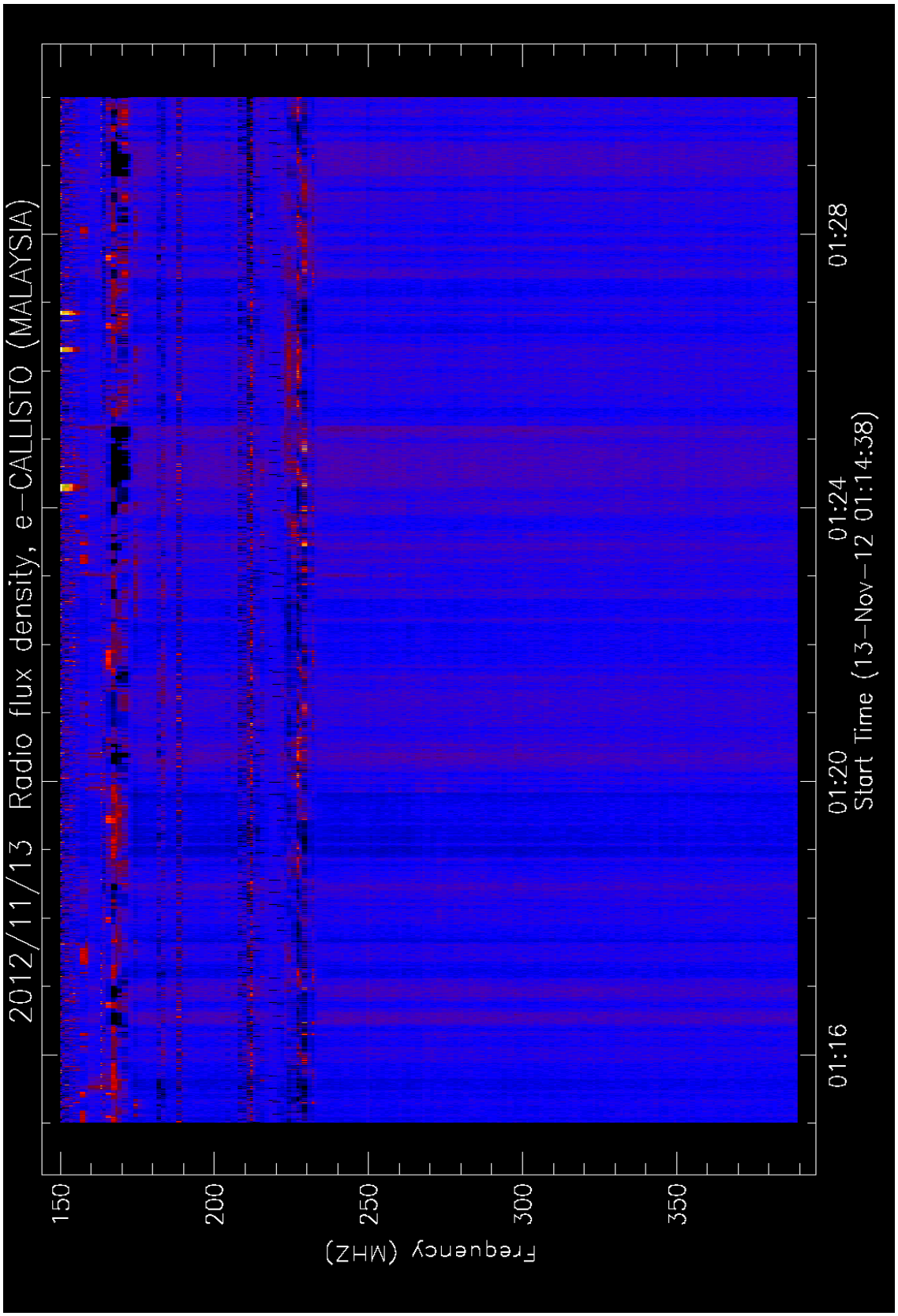

Figure 23. An intermittently and a group of type III burst from 01:15 – 01:30 UT.

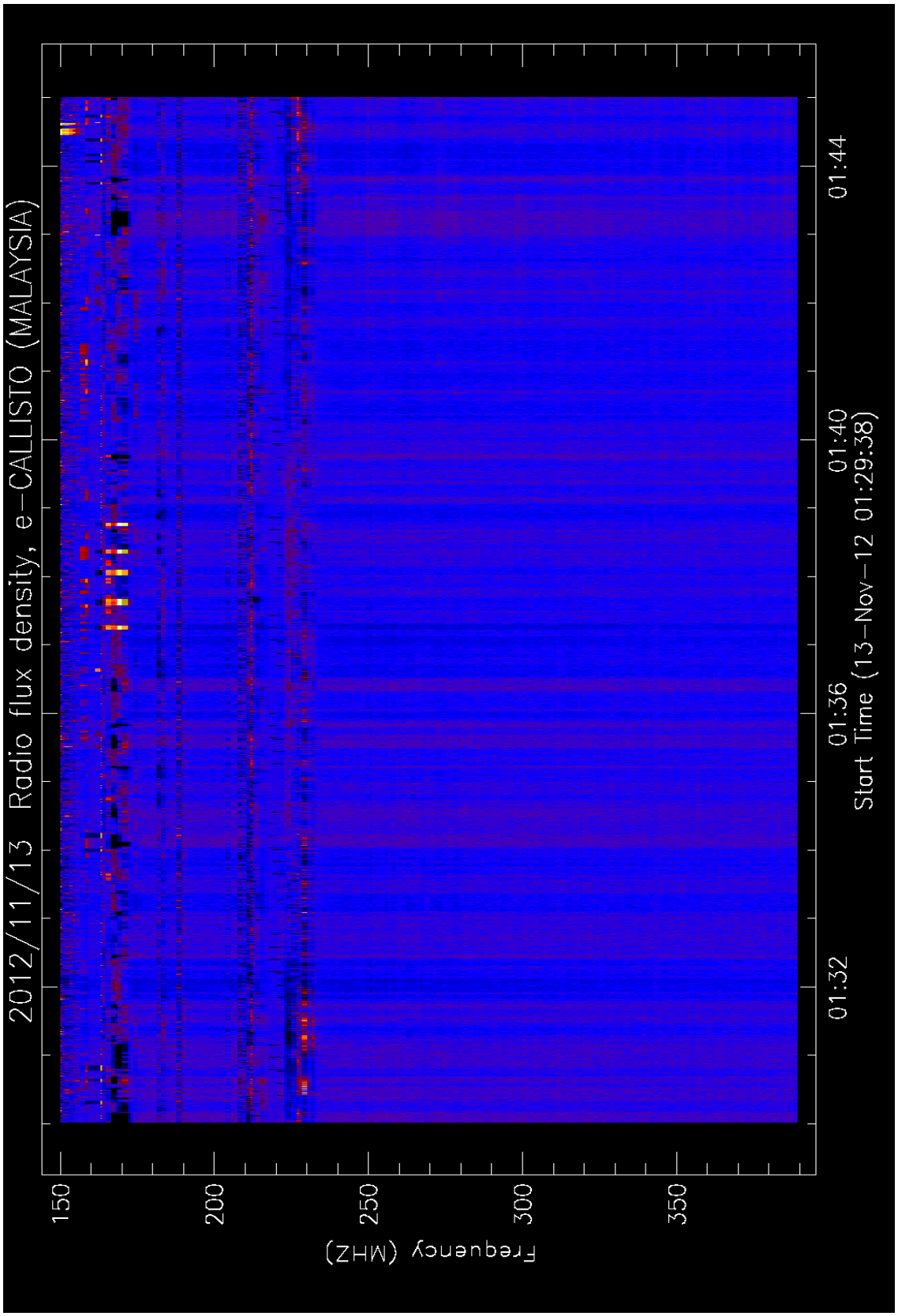

Figure 24. An intermittently and a group of type III burst from 01:30 – 01:45 UT.

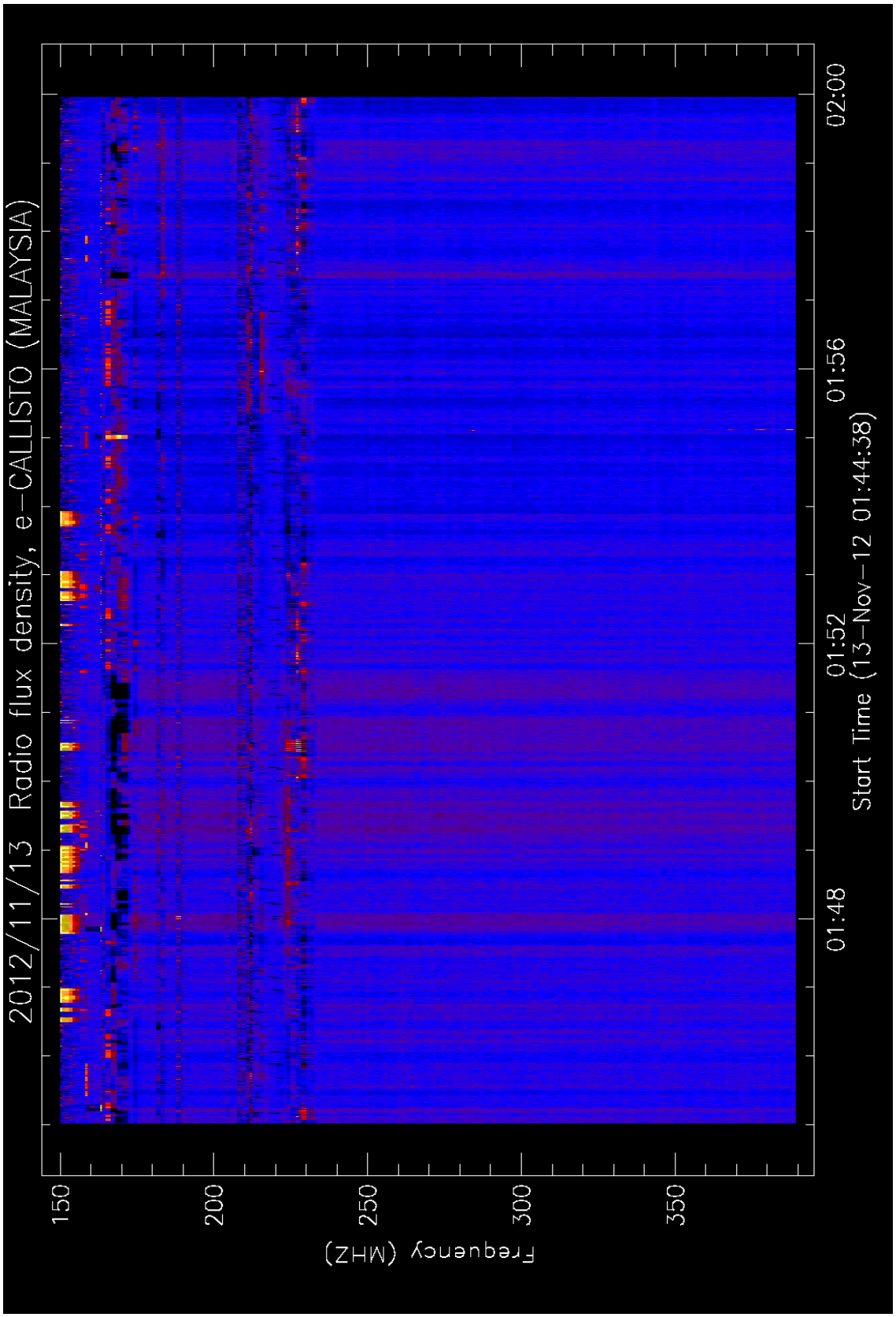

Figure 25. An intermittently and a group of type III burst from 01:45 – 02:00 UT.

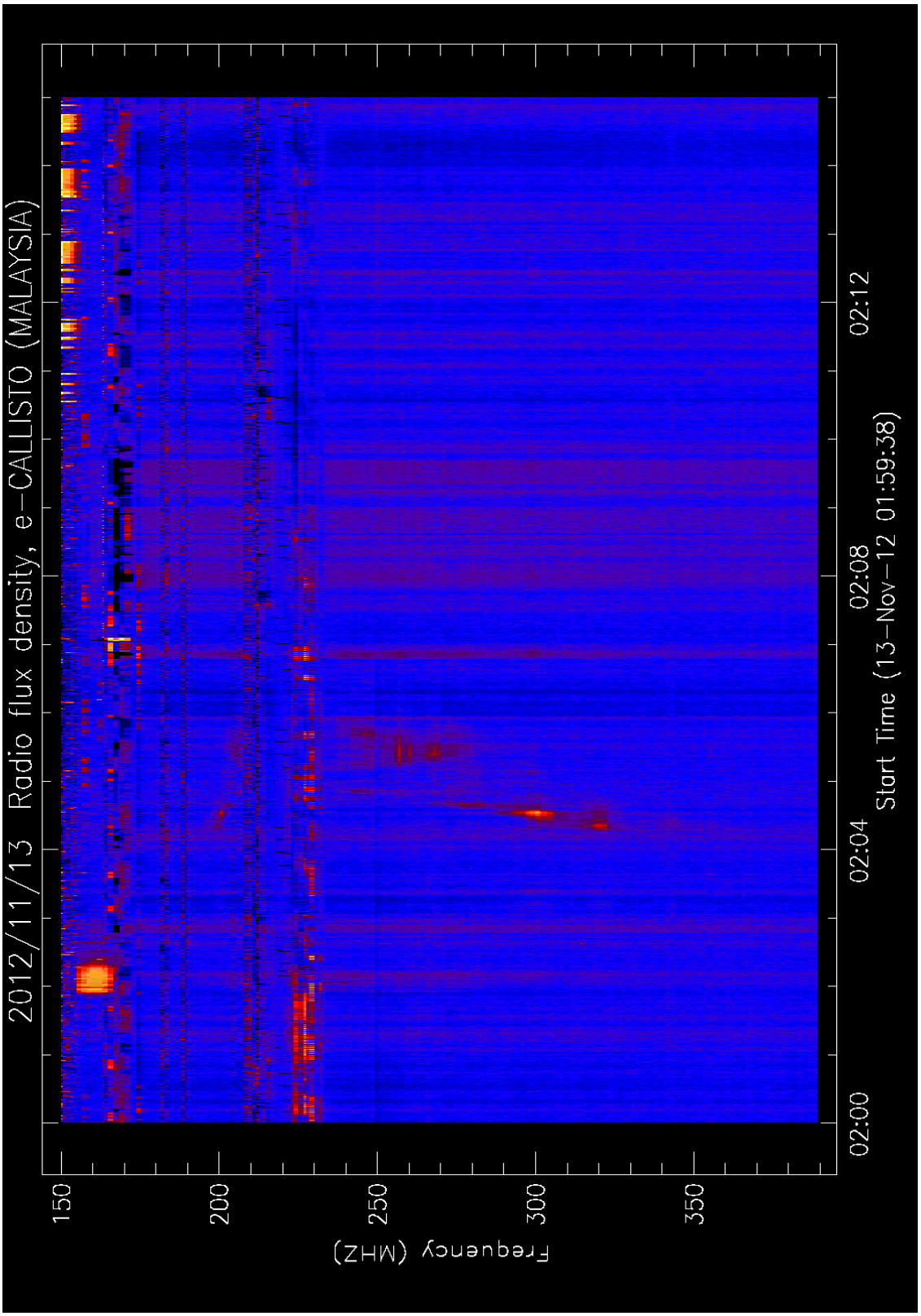

Figure 26. A fast drift type III, a broken type II burst and an intermittently and a group of type III burst from 02:00 – 02:15 UT.

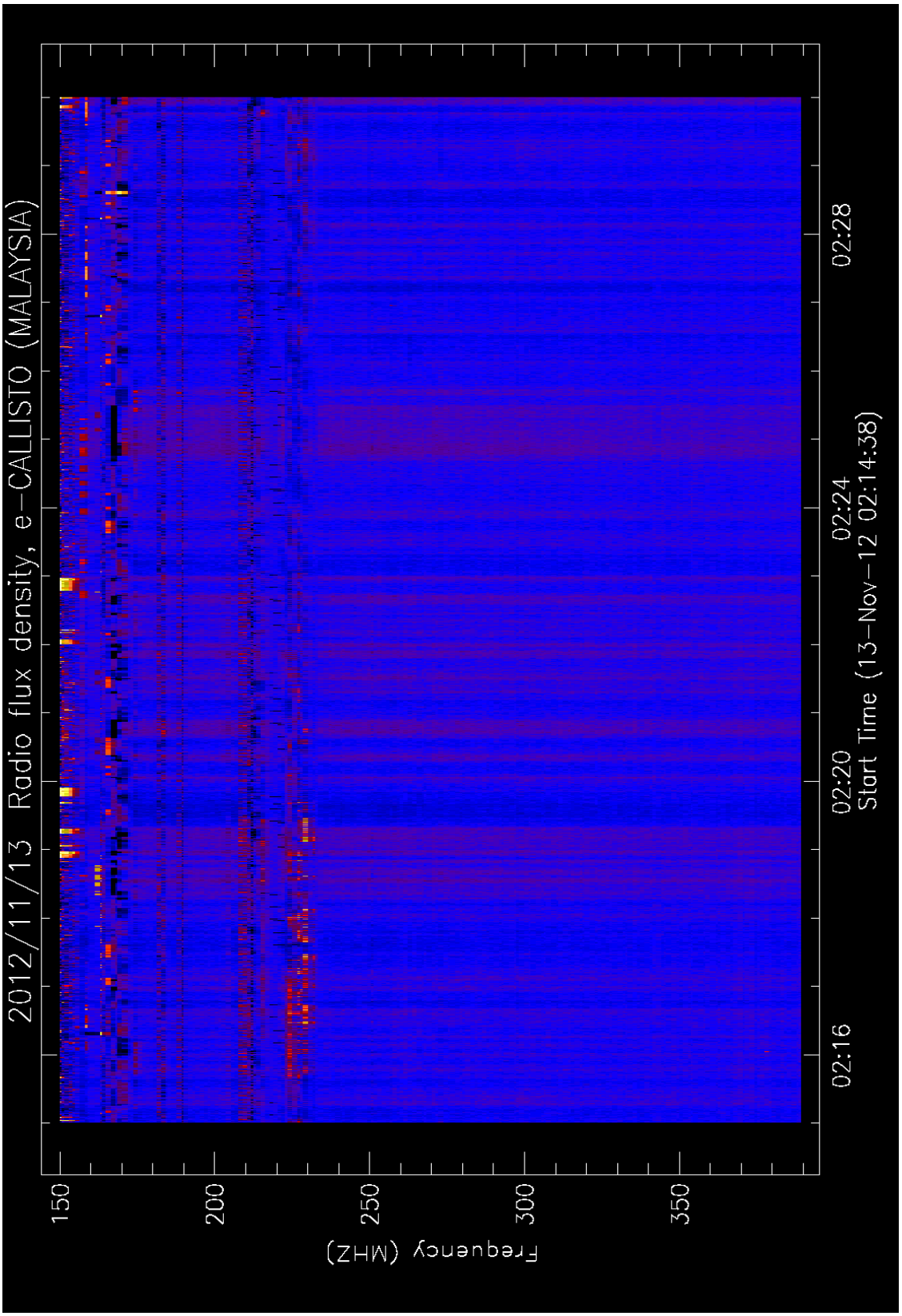

Figure 27. An intermittently and a group of type III burst from 02:15 – 02:30 UT.

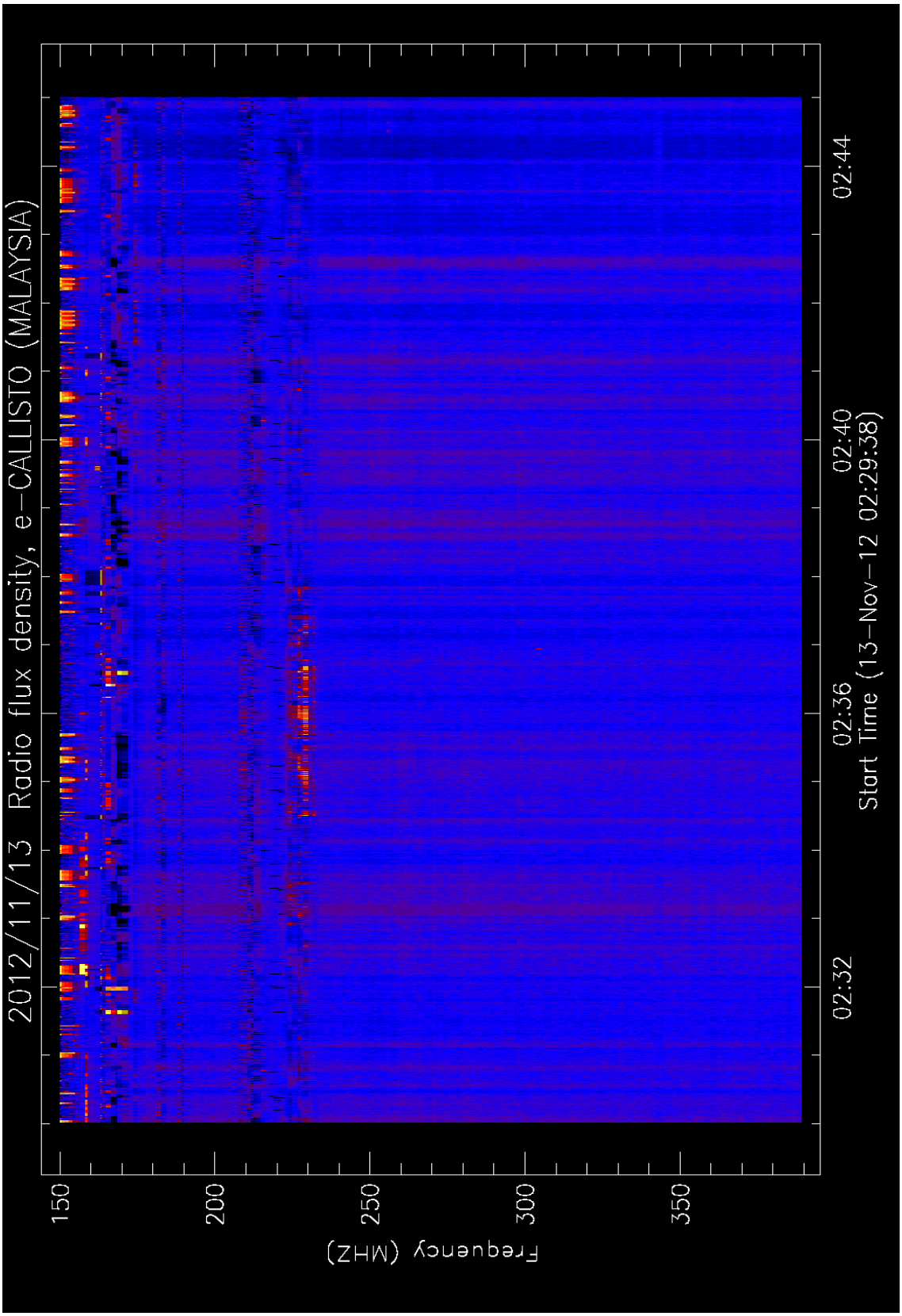

Figure 28. An intermittently and a group of type III burst from 02:30 – 02:45 UT.

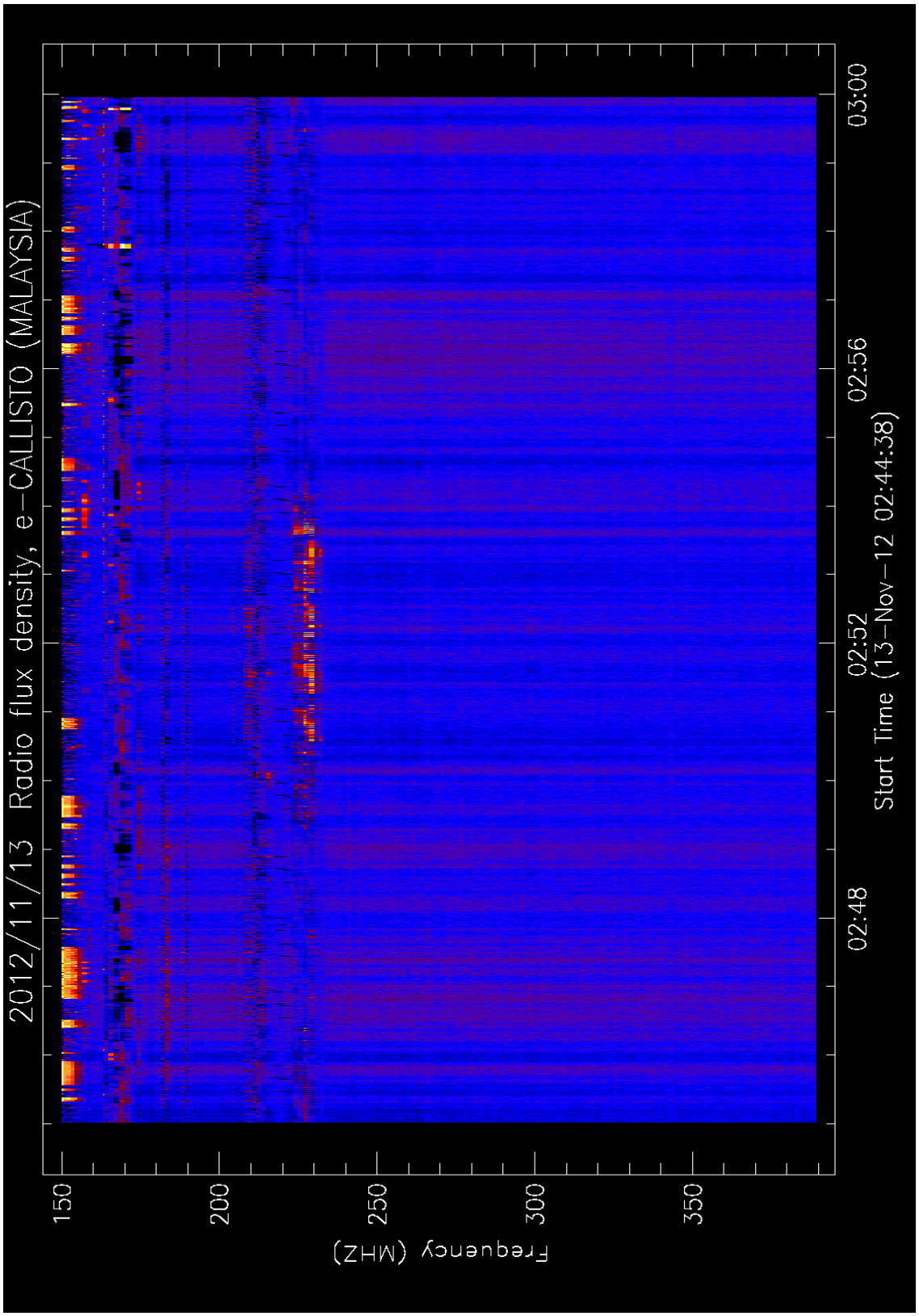

Figure 29. An intermittently and a group of type III burst from 02:45 – 03:00 UT.

The groups of SRBT III until 5:30 UT can still be observed. This proved that a meter solar radio burst will take a long period to decay and AR1613 and AR1614 potentially active for a few days comparison, the dynamic spectra in the X-ray region beginning from 1:00 UT till 7:00 UT.

In particular, an observed random variable may be represented as instability of the magnetic field of the active region. There was a CME event (~ 383 kms^{-1}) that has been detected at 1:28 UT from the LASCO data. As can be seen the x-ray flux is approximately to the 10^{-4} Watts m^{-2} during 2:00 UT. This is the highest point within six hours period of time. The sun remains active with two solar flares type M can be detected.

Overall, the Sun tends to be consistent with multiple storm but not huge CMEs explosion. Based on LASCO observation, the CMEs explosion with a speed of 419 kms^{-1} can be detected at 3:12 UT which means that almost after 1 hour and 10 minutes after the formation of this burst. In conclusion, this event is one fine example of tendencies SRBT III which makes it possible to form SRBT II. The burst is form in between of two events of CMEs in at the same day. It can be observed that solar radio burst type III in a group and individually are continue exploded within the first two hours. Sometimes the signal is so strong and sometimes is not. This shows a dynamic structure of the burst. The burst is origin from active region AR 1613. We can actually observe a fast drift burst from 45 MHz to 870 MHz.

The results of the recent time indicate that the broken solar burst type II is formed within four minutes [279]. Interestingly, in this case, type III solar burst can be observed before the formation type II burst. This is an indicator that the fast drift makes type II burst cannot form the harmonic structure. The long fast-drift type Type III solar burst was recorded before the formation Type II solar burst. It is believed that the event is due to coherent plasma processes, so the frequency of emission is closely related to the plasma frequency (and hence the plasma density) of the medium through which the electrons propagate.

This observation allows for the mechanisms of evolution type II solar burst and local environment of the burst to be characterized. This event occurred from 2:00:03 UT till 2:00:06 UT. It peaked with M2.0 solar flare at 2.04 UT in the range of 240-320 MHz. The burst that was temporally coincident with the X-ray region due to the M6.0 solar flare are clearly seen. The type II burst started about two minutes later when the X-ray flux already declined to the background level. Previously, at 2:04:15 UT, solar radio burst Type III burst can be identified. The type II burst is supposedly to be formed a harmonic structure. However, in this case, we could observe only a fundamental structure. In this case the role of type III shows the tendencies that type II burst could not form a harmonic structure during a very tense of type III burst. Our next analysis will focus in the active region at the surface of the Sun. Figure 6.14 shows the position of Active Region 1613 and other active region that possible to create the solar active due to the eruption process.

The position of Active Region AR 1613 is illustrated in Figure 30. In order to get a clear picture about this unique event, we also make use the data from the Solar Dynamics Observatory (SDO) satellite. This instrument has unprecedented high cadences and sensitivities with 0-1.5 R $\odot$ and 12 seconds. There are a few sunspots that can be observed clearly and the Sun can be classified as an active Sun during this period. Solar activity has been eruptive during the past 24 hours, featuring three C flares and now fresh M-class flare. The active regions 1610, 1611 and 1614 are currently the largest sunspots on the visible solar disk. There is an increasing chance for an isolated M-Class solar flare event. It is also expected that there will be a chance of an M flare, especially from AR 1614 and 1610 [280].

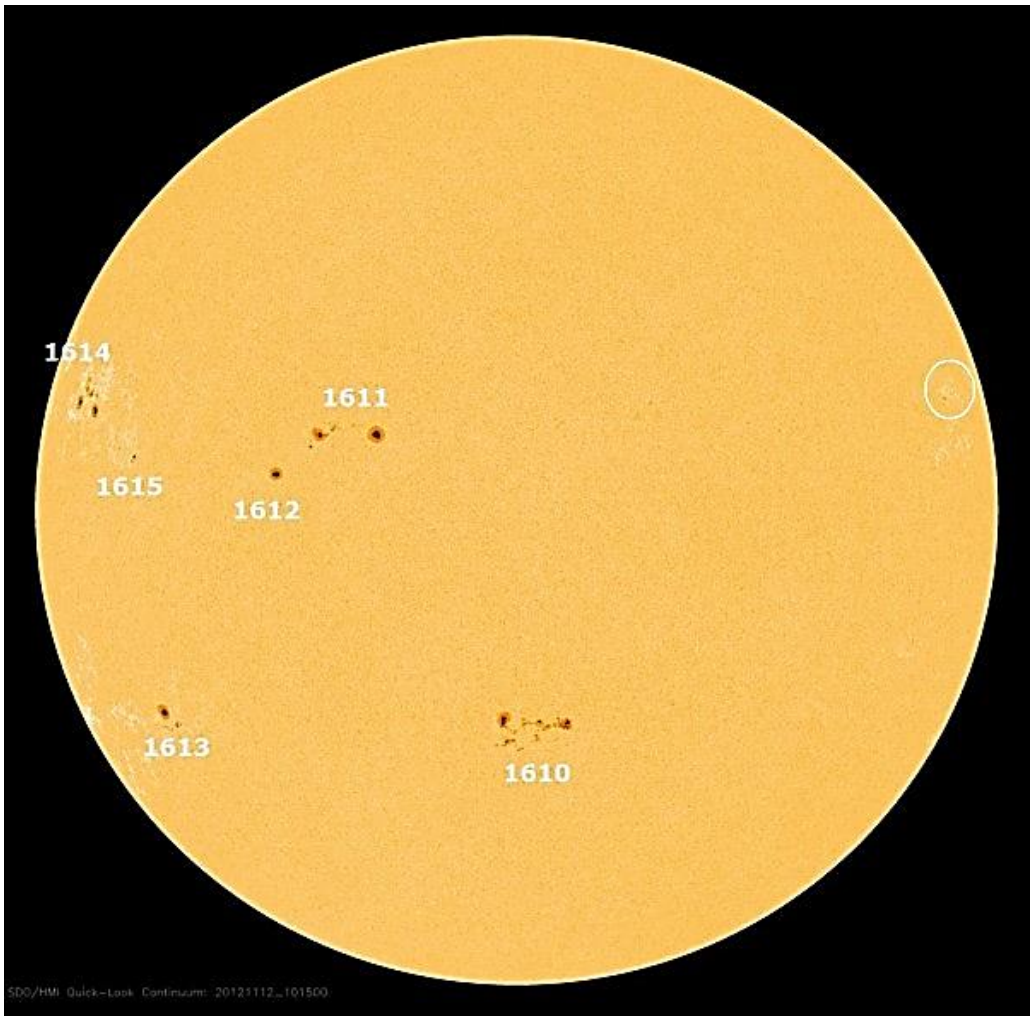

Figure 30. The position of Active Region 1613 (Credited to: Solar Dynamics Observatory (SDO).

Table 2 displays the detailed parameter of each active region that can be observed directly from ground and space observation during 13th November 2012. There are eight active regions and this is the indicator that the Sun is currently active. Some of the active region also remains exploded a huge particle and potentially eject the solar flares. Most the active regions radiate a Beta radiation. The location of the active region can be found in the North region of the Sun. Fortunately, the active region of 1613 is at the S22ºE43º and therefore, the explosion is not directly to the Earth.

Overall, the Sun tends to be consistent with multiple storms, but not huge CMEs explosion. Based on LASCO observation, the wind explosion with a speed of 369.7 kms^{-1}. In conclusion, this event is one fine example of tendencies solar radio burst type III, which makes the harmonic structure of solar radio burst type II fragmented. Although these two observations (radio and X-rays) seem to be dominant on the observational analysis, we could not directly confirmed that this is the only possibility, and we need to consider other processes to explain in detailed the injection, energy loss and the mechanism of the acceleration of the particles. Indirectly, it is believed that the large solar flares with a few numbers of solar storms contribute the distribution of flux energy or the burst.

Table 2. Parameter of each active region during 13th November 2012.

Active Region Number	Location	Lo	Area	Z	LL	NN	Magnitude
1605	N16W82	340	0010	Bxo	07	04	Beta
1609	S14W10	263	0010	Hrx	04	03	Alpha
1610	S22W10	263	0550	Eki	11	51	Beta-Gamma
1611	N15E13	240	0250	Eho	12	12	Beta-Gamma
1612	N09E25	228	0100	Hsx	05	01	Alpha
1613	S22E43	210	0170	Dso	10	10	Beta
1614	N16E58	195	0350	Fho	17	19	Beta
1615	N10E48	205	0160	Cao	10	08	Beta

Table 3. The current condition of the Sun (Credited to Space Weather).

Parameter	Value
Solar wind speed	369.7 km/sec
Density	9.1 protons/cm^3
Sunspot number	188
10.7 cm flux	144 sfu
6-hr max	M2
24-hr	M6

This energy of solar storms comes from the solar magnetic field which is generated from the convection zone. In conclusion, the percentage of energy of solar flare becomes more dominant rather than the acceleration of particles through the Coronal Mass Ejections (CMEs) and that will be the main reason why does the harmonic structure of type II burst is not formed.

6. 2. A CASE STUDY OF A CASE STUDY OF SRBT II

6. 2. 1. Observation during 23rd October 2012

Next to be considered is the event on 23rd October 2012. This occurrence is interesting in many respects. First, this event is one of the nicest solar burst type II that has been successfully observed from the MALAYSIA site. Secondly, it also showed a strong fundamental and harmonic structure [281]. A detailed investigation of solar radio burst type II in meter region and their associated solar flare has been reported. This burst has been observed at National Space Centre, Banting, detected by the CALLISTO system in the 150 MHz till 400 MHz at the low frequency band occurred on 23rd October 2012 between 3:17:45 UT to 3:19:00 UT within 1 minute 15 second. From the dynamic spectra of the CALLISTO, SRBT II burst have been observed with maximum emission near the frequency 350 MHz. In specific, the continuum type III burst will soon structure this burst due to these observations. This burst is ejected and appears at the same point of the Coronal Mass Ejections event. Based on continuous monitoring, there are three solar active regions AR 1591, AR 1593, 1596 and AR 1598 with the number of sunspot exceeding 86 [282].

The development of this burst is often accompanied by a richness which may take the form of multiple independent drifting bands or other forms of fine structure. The main band is split into two sub-bands because of the effect of magnetic splitting, analogous to the Zeeman effect. Therefore, this makes it possible to observe the slowly drifting feature in the dynamic spectrum. It also widely known that the radio emission itself occurs as a final step in a series of physical processes: initiation of the shock, particles acceleration, generation plasma waves (p_f), and finally conversion of plasma waves into electromagnetic waves.

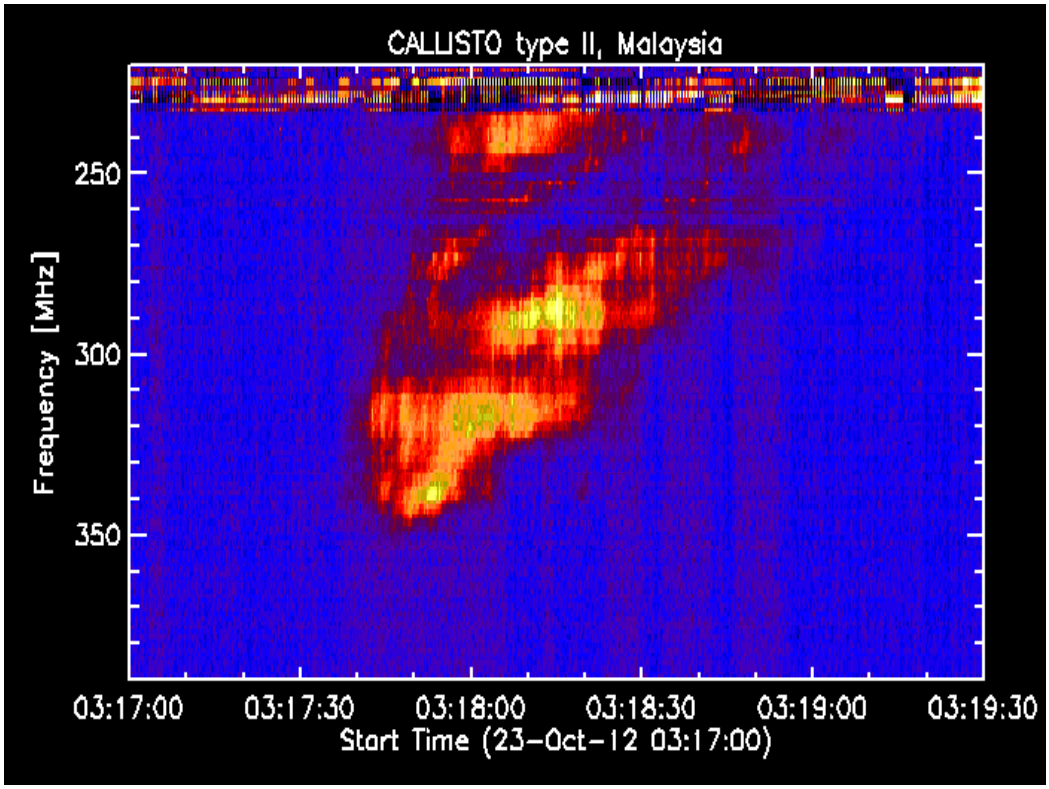

Figure 31. Type II burst with band splitting of fundamental and harmonic emission on 23rd October 2012.

The main feature of the burst is illustrated in Figure 31. It is clearly observed a group and individual solar radio burst type III before the formation of solar radio burst type II. Based on analysis, the drift rate of this burst is 2.116 MHz s^{-1}, which is considering as a slow drift rate. These drifting bands are approximately having a frequency ratio 2:1. The burst also accompanied by a group of solar radio burst type III since 00:00 UT. It means that it takes almost 3 hours and 17 minutes to form solar radio burst type II. In this case, a burst of charged solar particles expelled from the Sun, and is related to GOES–15 light curve showing an X 1.8 solar flare explosion and was the 3rd significant flare from AR1598 since it emerged over the south-eastern limb only three days ago. The duration of the formation of the burst is long lasting until 3 minutes. Band splitting of the order of 10 MHz can also be seen in the harmonic backbone at times around 3:17:45UT to 3:18:45 UT with the peak of flux exceeds up to 620 sfu. This splitting is associated with the rising phase of the flare. The times profiles of data X-ray of solar flare for the period 22:00 UT to 4:00 UT.

Significant results of the flaring becoming more intense at 3:00 UT were also determined. The highest peak of the solar flare can be observed during that time. Despite this, the bursts show wide varieties of dynamic spectra probably because of the solar plasma inhomogeneity through which parts of the shock wave travel. The simplest is sharp-featured and continue their curved sweep towards decreasing frequencies as far as the lower frequencies observable, their duration increasing with decreasing frequency. There is also an extreme ultraviolet flash observed by SDO. Radiation from the flare created waves of ionization in the upper atmosphere over Asia and Australia and possibly HF radio blackouts at high latitudes. The blast did not, however, produce a significant Coronal Mass Ejections (CMEs) [283].

Present understanding of solar burst phenomena is still very limited and here possible ways, in which the emission could be generated, will be discussed accordingly. These results suggest that, although there might exist a causal relationship between superimposed pulses observed at radio bursts, they are probably produced at different physical locations and/or by different emission mechanisms [284].

The relationship of solar radio burst type II and CME has been a long controversy. Sometimes solar radio burst type II is associated with CMEs, but sometimes not. Still, there are many factors that need to be considered. The structure of individual active region itself also should not be neglected. Overall, each event will give a unique characteristics and the dynamic structure of the burst could be understood with a longer period of observation by looking the starting point of the evolution of solar flare or CMEs event. In this case, the solar burst type II is formed as an alternative of a blast wave from a solar flare. Data for the October 23rd, 2012 event are particularly meaningful, because they were obtained with the best atmosphere transmission conditions at the site (Malaysia) and it is hoped that there will be more solar radio burst type II that can be detected from our site.

6. 2. 2. Observation during 30th March 2013

The latest event solar radio burst type II associated with CMEs event during 30th March 2013 is highlighted. It implies that the outward-travelling disturbance responsible for the type II band is a source which ejects rapidly travelling disturbances. There was a CME event between 13:22 and 13:33 UT due to region AR 1708. This event is successfully detected from a few e-CALLISTO networks such as Glasgow, Royal Observatory of Belgium and BIR observatory, Ireland.

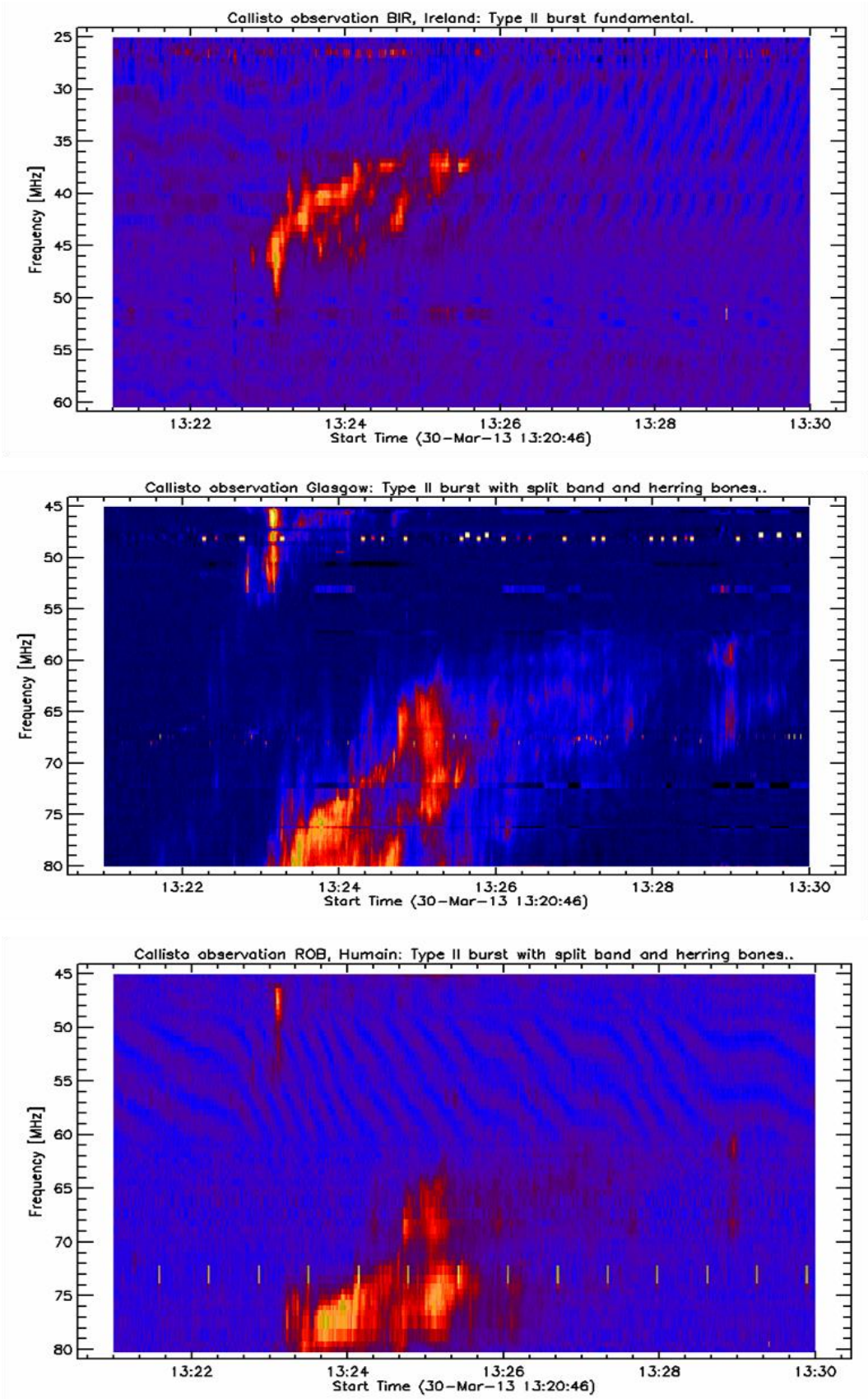

Figure 32. Solar radio burst type II at different sites (a) BIR Ireland, (b) Glasgow and (c) Humain.

The burst began as a fairly typical harmonic type II, but after the burst had been in progress for approximately 3 minutes, rapidly drifting elements suddenly appeared extending from the low frequency side of each of the harmonic bands.

A type II solar radio burst with a split and herring bones is occurred at 13:23 UT from 36 MHz till 50 MHz. During that day, a stream of solar wind from a coronal hole on the sun has disturbing Earth's magnetosphere creating a minor geomagnetic storm, G1 on the NOAA scale of G1-G5. Detail illustration of solar radio burst type II is presented in Figure 32.

Before the formation of solar radio burst type II, it has been observed a continuous solar radio burst type III since 10:36 UT which means that it take about 3 hours to form SRBT II. However, the group of type III is intermittently and sometimes it form as an individual type III.

In this case, the solar flare is not very high but CME is responsible to form a SRBT II. Overall, based on seven days observation beginning from 25th March 2013, the solar activity is considered as very low. The highest solar flare can be observed within 7 days is only a B8 type flare.

Although the solar flare event is at a lower stage, it is still possible to form the SRBT II which is associated with CME event. This SRBT II formation is the first event that successfully detected by e-CALLISTO network in this year and it is hoped that there will more SRBT II associated with CMEs and solar flares can be observed [285].

6. 3. CONCLUSION

A preliminary correlation study of the both solar burst of has been made. On the basis of this study and in combination with the observation in radio emission, an interpretation of the mechanism of the occurrence of this event has been proposed.

From the selected events, although theoretically solar radio burst type II is associated with CMEs, there is no compelling SRBT II without a flare. The only difference is the dynamic structure and the intensity and speed of both phenomena (solar flares and CMEs) which depend on the active region. Nevertheless, understanding how energy is released in solar flares is one of the central questions in astrophysics. The morphology of thermal and non-thermal flare plasma is of particular significance because it holds many important signatures of the energy release process. To this point of discussion, the onsets of solar flares and Coronal Mass Ejections (CMEs) have been studied as well.

CONCLUSION AND FUTURE WORK

The Sun is the predominant source of energy input to the Earth [286]. Both long- and short-term variations in solar intensity are known to affect global climate. Scientific discussions about the possible role of solar activity variations in climate have suffered from the lack of a precise physical mechanism that could account for the vast number of reported correlations. There are also various manifestations of solar activity driven by the total amount of magnetic flux emerging through the photosphere into the chromosphere and corona, and its temporal and spatial distribution. For reasons not clearly understood, solar activity flows over a cycle of more than 11 years [287].

Along the process of carrying out the research, many works have been done to fulfil the objectives of this dissertation. It started from understanding the principle of solar flare and CMEs phenomena associated with all types of solar radio bursts. During the experimental method's progress, a construction of Log Periodic Dipole Antenna and identifying the RFI in the wide region was also required in this study.

Until now, the number of people interested to pursue research in this field is increasing. The data of solar activity associated with solar burst also become much more relevant. Especially toward 24th year cycle, there are more sun activities that will be observed. In this case, the role of radio region monitoring is very important. We could possible to detect a large flare and Coronal Mass Ejections (CMEs) for instance if we alert on it. Therefore a 24 hour solar monitoring is very significant to fulfil this work. In addition, with international collaboration, there are many advantages that we could gain. We can compare the data, and choose a high quality data if there are a site that polluted by interference for instance.

7. 1. FUTURE WORK

With the implementation of 45 MHz – 870 MHz CALLISTO systems and development of solar burst monitoring network, a new wavelength regime is becoming available for solar radio astronomy. Solar activities potentially affect the heliosphere in the short term (space weather) and in the long term (space climate) through numerous physical processes that exhibit similarities in various spatial domains of the heliosphere. Understanding the nature of the motions associated with non-thermal line represents one of the major challenges of high resolution solar studies [288]. Monitoring the Sun reveals a variety of fascinating and complex physical phenomena which are being studied mainly by analyzing its emission. Hopefully, these observations can bring upon large scale impact by illuminating the nature of the evolution of the solar burst and the role of that evolution in generating solar activity.

7. 2. FURTHER PROSPECTS ON SOLAR FLARES AND CMES

It is well-known that high energy CMEs can propagate further into the interplanetary medium and have serious consequences throughout the heliosphere. The radio data provides valuable information on the structure of the solar atmosphere above the minimum

temperature. To this end reliable absolute measurement of the brightness of the temperature is required. The scatter could be due to inherent difficulties in the measurements and/or solar cycle variations, although the latter is not expected to be very important at the relevant atmospheric layers. In any case, there is an obvious need for more consistent observations and these can only be obtained with single-dish instruments. Observations from space would be the ideal since they are not hindered by the terrestrial atmosphere.

On the basis of these work, we suggest that:

1. Future low-frequency imaging arrays are expected to greatly advance our understanding of the bursts and their relation to CMEs.
2. Observations for 24 hours on solar radio burst monitoring by e-CALLISTO, which will make it possible in a short period of time to make a new study focusing on modelling the solar radio data.

With the present level of the international collaboration, it is believed that the potential involvement of local and international scientist in solar astrophysics will increase. In conclusion, the study of solar radio burst is very important as it is a key element in defining the actual caused of Coronal Mass Ejections (CMEs) phenomena has been summarized.

BIOGRAPHY

Dr. Zety Sharizat Hamidi is currently a senior lecturer and focused in Solar Astrophysics research specifically in radio astrophysics at the School of Physics and Material Sciences, Faculty of Sciences, MARA University of Technology, 40450, Shah Alam, Selangor, Malaysia. Involve a project under the International Space Weather Initiative (ISWI) and also a lecturer in School of Physics and Material Science, at MARA University of Technology, Shah Alam Selangor, Malaysia

BIBLIOGRAPHY

[1] J.S. Hey, S.J. Parsons, J.W. Phillips, *Monthly Notices of the Royal Astronomical Society* 108 (1948) 354-371.

[2] J.P. Wild, Smerd S.F., Weiss, A.A., *Ann. Rev. Astron. Astrophysicsv* 10 (1972).

[3] J.P. Wild, Smerd S.F., Weiss, A.A., *Australian J. Sci. Res* 12 (1959) 369.

[4] S. Maxwell, Thomas, Proc.I.R.E. 46 (1958) 142.

[5] V.V. Grechnev, *ApJ* 566 (2002).

[6] D. Herdiwijaya, M. Makita, B. Anwar, *Publications of the Astronomical Society of Japan* 49 (1997) 14.

[7] A.O. Benz, *Sol. Phys.* 96 (1985).

[8] P. Messmer, Benz, A. O., *A&A* 354 (2000).

[9] M.J. Aschwanden, Güdel M., *ApJ* 401 (1992) 736-753.

[10] G.D. Fleishman, Melnikov V. F., *ESA* 448 (1999).

[11] M.J. Aschwanden, Benz A. O., ApJ 480 (1997).

[12] P.A. Robinson, *Sol. Phys.* 134 (1991).

[13] A.O. Benz, Messmer P., Monstein C., *A&A* 366 (2001).

[14] N. Gopalswamy, Energetic Particle and Other Space Weather Events of Solar Cycle 24, (2012).

[15] D. Herdiwijaya, On The Prediction of Solar Cycle 24, Proceeding of the Conference on Earth and Space Science, Bandung, Indonesia, 2010, pp. 6.

[16] M.J. Aschwanden, *Space Science Reviews* 101 (2002).

[17] N.M. Vilmer,Energy Conversion and Particle Acceleration in the Solar Corona, Lecture Notes in Physics, Springer, Berlin, 2003.

[18] M. Stix, The sun: an introduction, (2004).

[19] Z. Hamidi, N. Shariff, F.Z. Ulum, Z. Abidin, Z. Ibrahim, *International Journal of Astronomy* 1 (2012) 101-104.

[20] J.G. Andrews, *J. Inst. Maths. Applic.* 15 (1976).

[21] A.G. Emslie, H. Kucharek, B.R. Dennis, N. Gopalswamy, G.D. Holman, G.H. Share, A. Vourlidas, T.G. Forbes, P.T. Gallagher, G.M. Mason, T.R. Metcalf, R.A. Mewaldt, R. J. Murphy, R.A. Schwartz, T.H. Zurbuchen, *Journal of Geophysical Research* 109 (2004) 15.

[22] N. Gopalswamy, M.R. Kundu, *Solar Physics* 143 (1993) 327-343.

[23] D. Herdiwijaya, S. Imelda, *Jurnal Matematika dan Sains* 11 (2006) 7.

[24] Joel C. Allred, Suzanne L. Hawley, William P. Abbett, M. Carlsson, *ApJ* 630 (2005).

[25] A.O. Benz, Solar and Stellar Coronae, Kluwer Academic Publishers, 2002.

[26] G.D. Fleishman, Gary, D. E., Nita, G. M., *ApJ* 593 (2003).

[27] C.H. Mandrini, P. Démoulin, J.C. Hénoux, M.E. Machado, *Astron. Astrophys.* 325 (1991) 305-317.

[28] D. Herdiwijaya, On the relation of type II solar radio burst with X-ray flares and Coronal Mass Ejections (CMEs) during year 2004-2009, Proceedings of the Third International Conference on Mathematics and Natural Sciences (ICMNS 2010), Bandung Indonesia, 2010, pp. 7.

[29] J.P. Wild, Smerd S.F., Weiss A.A., Solar Burst, *Ann. Rev. Astron. Astrophysics* 1 (1963) 291-366.

[30] K.A. Marsh, Hurford G.J., *Ann. Rev. Astron. Astrophysics* 20 (1982) 497.

[31] G.A.G. Dulk, *Astron. Astrophys* 124 (1983) 103.

[32] S.W. Kahler, *J. Geophys. Res.* 87 (1992) 3439-3448.

[33] S.K. Haisch, B. Rodono M., *Annu.Rev. Astron. Astrophys.* 29 (1991) 275-324.

[34] J. Hudson, H. Ryan, *Ann. Rev. Astron. Astrophysics* 35 (1995) 239-282.

[35] J.A. Miller, P. J. Cargill, e.a. G. Emslie, *J. Geophys. Res.* (1997) 4631-4660.

[36] G.D. Holman, M.R. Kundu, *ApJ* 292 (1985).

[37] S.G. Benka, G.D. Holman, *ApJ* 435 (1994).

[38] V. Petrosian, High-Energy Solar Phenomena, in: J.M. Ryan, W.T. Vestrand (Eds.), AIP Conf. Proc. 294, New York: AIP, 1994.

[39] V. Petrosian, High Energy Solar Physics, in: R. Ramaty, N. Mandzhavidze, X.-M. Hua (Eds.), Woodbury: AIP, 1996.

[40] A.O. Benz, Plasma Astrophysics, Springer, Dordrecht, 2002.

[41] T. Takakura, *Nature* 302 (1983) 317-319.

[42] J. Lim, *Sol. Phys.* 140 (1992).

[43] P. Kaufmann, *Sol. Phys.* 84 (1983) 311-319.

[44] A.V.R. Silva, H. Wang, D.E. Gary, *Astrophys. J.* 545 (2000).

[45] R. Tousey, The solar corona, in: M.J. Rycroft, S.K. Runcorn (Eds.), Space Research XIII, Proceedings, Akademie-Verlag, Berlin, Madrid, Spain, 10-24 May, 1972, pp. 713-730.

[46] D.N. Baker, R. Balstad, J.M. Bodeau, E. Cameron, J.F. Fennell, G.M. Fisher, K.F. Forbes, C.A. Gruber, Severe Space Weather Events – Understanding Societal and Economic Impacts, The National Academies Press, Washington DC, 2008.

[47] R. Schwenn, *Living Rev. Solar Phys.* 3 (2006).

[48] T. Pulkkinen, *Living Rev. Solar Phys.* 4 (2007).

[49] D.M. Rust, D.F. Webb, *Solar Phys.* 54 (1977) 403-417.

[50] N. Gopalswamy, *Geophysical Monograph Series* 165 (2006).

[51] K.P. Dere, G.E. Brueckner, R.A. Howard, M.J. Koomen, C.M. Korendyke, R.W. Kreplin, D.J. Michels, J.D. Moses, N.E. Moulton, D.G. Socker, O.C. St Cyr, J.P. Delaboudini`ere, G.E. Artzner, J. Brunaud, A.H. Gabriel, Hochedez, M. J.F., S. F., X.Y., J.P. Chauvineau, J.P. Marioge, J.M. Defise, C. Jamar, P. Rochus, R.C. Catura, J.R. Lemen, J.B. Gurman, W. Neupert, F. Clette, P. Cugnon, E.L. van Dessel, P.L. Lamy, A. Llebaria, R. Schwenn, G.M. Simnett, *Sol. Phys.* 175 (1997) 601-612.

[52] P.F. Chen, *Living Rev. Solar* 8 (2011).

[53] N. Gopalswamy, M.R. Kundu, *Astrophys. J.* 390 (1992) 37-39.

[54] Y.J. Moon, G.S. Choe, H. Wang, Y.D. Park, N. Gopalswamy, G. Yang, S. Yashiro, *The Astrophysical Journal* 581 (2002) 694-702.

[55] N. Gopalswamy, S. Yashiro, Y. Liu, G. Michalek, A. Vourlidas, M.L. Kaiser, R.A. Howard, *Journal of Geophysical Research: Space Science* 110 A09S15-JA010958.

[56] B. Vrsnak, D. Ruzdjak, D. Sudar, N. Gopalswamy, *Astron. Astrophys.* 423 (2004) 717-728.

[57] N. Gopalswamy, *Journal of Astrophysics and Astronomy* 27 (2006) 243-254.

[58] B. Schmieder, L. van Driel-Gesztelyi, Coronal and Stellar Mass Ejections, in: J.W. K. Dere, Y. Yan (Eds.), Cambridge University Press, Cambridge 2005, pp. 149-160.

[59] A.G. Emslie, H. Kucharek, B.R. Dennis, N. Gopalswamy, G.D. Holman, G.H. Share, A. Vourlidas, T.G. Forbes, P.T. Gallagher, G.M. Mason, T.R. Metcalf, R.A. Mewaldt, R.J. Murphy, R.A. Schwartz, T.H. Zurbuchen, *Journal of Geophysical Research* 109 (2004) 15.

[60] D.Herdiwijaya, J. Hermawan, On the Correlation of Solar Energetic Particles Shock Wave, Magnetic Cloud and Geomagnetic Storm, The 3rd Asian Physics Symposium Bandung, Indonesia, 2009, pp. 5.

[61] R.A. Howard, Sheeley Jr, N.R., Michels, D.J. Koomen, M.J., *J. Geophys. Res.* 90 (1985) 8173-8191.

[62] O.C. St Cyr, S.P. Plunkett, D.J. Michels, S.E. Paswaters, M.J. Koomen, G.M. Simnett, B.J. Thompson, J.B. Gurman, R. Schwenn, D.F. Webb, E. Hildner, P.L. Lamy, *J. Geophys. Res.* 18 (2000) 169-186.

[63] N. Gopalswamy, A Global Picture of CMEs in the Inner Heliosphere, in: G. Poletto, Suess, S.T. (Ed.), *Astrophysics and Space Science* (2004) 201-251.

[64] R.M.E.a.H. Illing A.J., *J. Geophys. Res.* 90 (1985) 275-282.

[65] Y.J. Moon, G.S. Choe, Haimin Wang, Y.D. Park, N. Gopalswarmy, G. Yang, S.Yashiooro, A statistical Study of Two Classes of Coronal Mass Ejections, *The Astrophysical Journal* 581 (2002) 8.

[66] N. Gopalswamy, *Advances in Space Research* 31 (2003) 869-881.

[67] N. Gopalswamy, S. Yashiro, R.A.Howard, M.L.Kaiser, J.L.Bougeret, *Astrophysical Journal* 548 (2001) 4.

[68] J.T. Gosling, McComas P.D.J., S.J.J.L. Bame, *J. Geophys. Res.* 96 (1991) 7831-7839.

[69] V. Yurchyshyn, S. Yashiro, V. Abramenko, H. Wang, N. Gopalswamy, *The Astrophysical Journal* 619 599.

[70] N. Gopalswamy, A. Lara, S. Yashiro, M. L.Kaiser, R. A.Howard, Predicting the 1-AU Arrival Times of Coral Mass Ejections, *Journal of Geophysical Research* (2001).

[71] N. Gopalswamy, *A&A* 27 (2006).

[72] D.F. Webb, From Solar Min to Max: Half a Solar Cycle with SOHO, ESA, A. Wilson, Noordwijk, Netherlands, 2002, pp. 409.

[73] S.W. Kahler, in: N.G.a.J. Torsti (Ed.), Chapman Conference on Solar Energetic Plasmas and Particles, AGU GM, Washington, DC, 2006.

[74] A.J. Hundhausen, Coronal Expansion and Solar Wind, *Physics and Chemistry in Space* 5 (1972).

[75] O.C. St Cyr, J.T. Burkepile, A.J. Hundhausen, A.R. Lecinski, *J. Geophys. Res.* 104 (1999).

[76] N. Gopalswamy, H. Xie, S. Yashiro, I.G. and Usoskin, Coronal mass ejections and ground level enhancements, in: B.e.a. Sripathi Acharya (Ed.), 29th International Cosmic Ray Conference, Pune, India, 2005, pp. 169-172.

[77] N. Gopalswamy, S. Akiyama, S. Yashiro, P. and Makela, Coronal mass ejections from sunspot and non-sunspot regions, in: S.S. Hasan, Rutten, R.J. (Ed.), Astrophysics and Space Science, pringer, Berlin; Heidelberg, 2010a, pp. 289-307.

[78] A. Vourlidas, R.A. Howard, E. Esfandiari, S. Patsourakos, S.A.M. Yashiro, G., *Astrophys. J.* 722 (2010) 1522–1538.

[79] A.J. Hundhausen, *J. Geophys. Res.* 98 (1993) 13177-13200.

[80] R. A. Howard, N. R. Sheeley Jr., M.J. Koomen, A.D.J. Michels, *J. Geophys. Res.* 90 (1985) 8173-8191.

[81] T.A. Howard, D.F. Webb, S.J. Tappin, D.R.a.J. Mizuno, *J. Geophys. Res.* 111 (2006).

[82] N. Gopalswamy, P. Makela, H. Xie, S.a.Y. Akiyama, S., CME interactions with coronal holes and their interplanetary consequences, *J. Geophys. Res.* (2009a).

[83] N. Gopalswamy, M. Shimojo, W. Lu, S. Yashiro, K. Shibasaki, R.A. Howard, Prominence Eruptions and Coronal Mass Ejection: A Statistical Study Using Microwave Observations, *The Astrophysical Journal* 586 (2003).

[84] H.S. Hudson, E.W. Cliver, *J. Geophys. Res.* 106 (2001) 199-213.

[85] Webb R.A., *J. Geophys. Res.* 99 (1994) 4201-4220.

[86] J.T. Burkepile, A.J. Hundhausen, A.L. Stanger, O.C.a.S. St Cyr, J.A., *J. Geophys. Res.* 109 (2004).

[87] I.S. Kim, I. Alexeyeva, Magnetic Field Observations of Active Region Prominences, in Solar Active region Evolution: Comparing Models with Observations, in: A.C. Ser. (Ed.), 1994, pp. 403.

[88] A. Vourlidas, D. Buzasi, Howard E., Mass and energy properties of LASCO CMEs, in: A. Wilson (Ed.), ESA Conference Proceedings, 2002a, pp. 91-94.

[89] A. Ciaravella, J.C. Raymond, S.W. Kahler, *The Astrophysical Journal* 652 (2006) 774-792.

[90] R.A. Harrison, *A&A* 304 (1995).

[91] N. Gopalswamy, M. Shimojo, W. Lu, S. Yashiro, K. Shibasaki, R.A. Howard, *The Astrophysical Journal* 586(1) (2003).

[92] T.G. Forbes, J.A. Linker, J. Chen, Cid,, K. C., L. J., M.A., , G. Mann, Z. Mikić, M.S. Potgieter, J.M. Schmidt, G.L. Siscoe, R. Vainio, S.K.a.R. Antiochos, P., *Space Sci. Rev.* 123 (2006).

[93] J.A. Klimchuk, Theory of Coronal Mass Ejections, in: P. Song, Singer, H.J., Siscoe, G.L. (Ed.), Space Weather, American Geophysical Union, Washington, DC, 2001.

[94] M. Zhang, B.C. Low, The Hydromagnetic Nature of Solar Coronal Mass Ejections, *Annu. Rev. Astron. Astrophys.* 43 (2005) 103-137.

[95] B. Vršnak, *Ann. Geophys.* 26 (2008).

[96] T.G. Forbes, *J. Geophys. Res.* 105 (2000) 153-166.

[97] M. Zhang, Flyer N. Low B.C., *Astrophys. J.* 644 (2006) 575-586.

[98] S.F. Martin, *Sol. Phys.* 182 (1998).

[99] V. Gaizauskas, D.H. Mackay, Harvey K. L., *ApJ* (2001).

[100] Y. Wang Zhang, *Astrophys. J.* 665 (2007) 1428-1438.

[101] A.G. Emslie, H. Kucharek, B.R. Dennis, N. Gopalswamy, G.D. Holman, G.H. Share, A. Vourlidas, T.G. Forbes, P.T. Gallagher, G.M. Mason, T.R. Metcalf, R.A. Mewaldt, R.J. Murphy, Schwartz T.H., *J. Geophys. Res.* 109 (2004).

[102] N. Gopalswamy, S. Yashiro, M. Kaiser, R. Howard, J.-L. Bougeret, *The Astrophysical Journal Letters* 548 (2001) 91.

[103] J. Zhang, I.G. Richardson, D.F. Webb, N. Gopalswamy, E. Huttunen, J.C. Kasper, N.V. Nitta, W. Poomvises, B.J. Thompson, C.C. Wu, S. Yashiro, A.N. Zhukov, *Journal of Geophysical Research* 112 (2007) 19.

[104] Z. Hamidi, U. Ibrahim, U.F. Salwa, Z. Abidin, Z. Ibrahim, N. Shariff, *International Journal of Fundamental Physical Sciences* 3 (2013).

[105] A. Kruger, Introduction to Solar Radio Astronomy and Radio Physics, D. Reidel, Publ. Co., Dordrecht, Holland, 1979.

[106] D.J. McLean, a.N.R. Labrum, Solar Radiophysics, Cambridge University Press, Cambridge, 1985.

[107] Z. Hamidi, U.F.S.U. Ibrahim, Z. Abidin, Z. Ibrahim, N. Shariff, *International Journal Physical Fundamental Sciences* 3 (2013) 20-23.

[108] M.R. Kundu, Solar Radio Astronomy, John Wiley, 1965.

[109] V.V. Zheleznyakov, Radio Emission of the Sun and Planets (1970).

[110] E.Y. Zlotnik, *Soviet Astron.* 12 (1968).

[111] S.M. White, Kundu, M. R., *Sol. Phys.* 174 (1997).

[112] W. Kundu, Solar and Space Weather Radiophysics, Dordrecht: Kluwer, 2004.

[113] J.W. Brosius, White S. M., *ApJ* 601 (2004).

[114] S.M. White, *Sol. Phys.* 190 (1999).

[115] Kundu, Alissandrakis, *Nature* 257 (1975).

[116] C.E. Alissandrakis, Kundu M. R., Lantos P., *A&A* 82 (1980).

[117] S.M. White, S. Krucker, R.P. Lin, Corona, *Ap. J. Lett* 40 (2007).

[118] J. Lee, S.M. White, N. Gopalswamy, M.R. Kundu, *Sol. Phys.* 174 (1997).

[119] J. W.Brosius, *The Astrophysical Journal* 601 (2004) 22.

[120] D. Herdiwijaya, The characteristics of solar wind parameters during minimum periods of solar cycle 24 and impact on Geoeffectiveness, ICAMP 2011, AIP Conf. Proc., Bandung Indonesia, 2011, pp. 4.

[121] Z.S. Hamidi, N.N.M. Shariff, Z.A. Ibrahim, Z.Z. Abidin, Solar Studies in Radio Emision and Oprtical Photometry, University of Malaya Publisher, 2013.

[122] V.V. Zheleznyakov, *Astrophys. J.* 155 (1969).

[123] A. Boichot, A.C. Riddle, J.B. Pearce, J.W. Warwick, *Solar Phys.* 65 (1980).

[124] T.B. Veronese, R.R. Rosa, M.J.A. Bolzan, F.C. Rocha Fernandes, H.S. Sawant, M. Karlicky, Fluctuation analysis of solar radio bursts associated with geoeffective X-class flares, *Journal of Atmospheric and Solar-Terrestrial Physics* (2010).

[125] A. Nindos, S.M. White, M.R. Kundu, D.E. Gary, *Astrophys. J.* 533 (2008) 1053-1062.

[126] J.P. Wild, *J. Sci. Res* 3 (1950a).

[127] L.J. Lanzerotti, Solar and Solar Radio Effects on Technologies, 2004.

[128] A.P. Cerruti, P.M. Kintner, D.E. Gary, Mannucci, M. A. J., D. R. F., P., A.J. Coster, Effect of intense December 2006 solar radio bursts on GPS receivers, *Space Weather* 6 (2008).

[129] K. Akabane, *PASJ* 173 (1956).

[130] A.E. Covington, *JRASC* 45 (1951).

[131] H.W. Dodson, E.R. Hedeman, A.E. Covington, *ApJ* 119 (1954).

[132] T. Kakinuma, T. Yamashita, S. Enome, *Proc. Res. Instit. Atmospherics* 16 (1969).

[133] T. Takakura, Kai, K., *PASJ* 18 (1966).

[134] K. Kai, *PASJ* 20 (1968).

[135] J.P. Castelli, D.A. Guidice, *AFCRL* 72 (1972) 49.

[136] D.A. Guidice, Castelli J.P., *Sol. Phys.* 44 (1975).

[137] E.W. Cliver, McNamara L. F., Gentle L. C., *AFGL* 85 (1985).

[138] G.M. Nita, Gary D. E., Lanzerotti L. J., Thomson D. J., *ApJ* 570 (2002).

[139] Y.D. Park, Y.-J. Moon, I. Kim, Y. S., *Astrophys. Space Sci.* 279 (2002).

[140] Y.I. Yermolaev, M.Y. Yermolaev, *Cosmic Res.* 40 (2002) 3.

[141] Y.I. Yermolaev, Yermolaev M.Yu., Statistical relationships between solar, interplanetary, and geomagnetic disturbances, 1976–2000, Cosmic Res. 41.

[142] S.R. Cranmer, J.T. Hoeksema, J.L. Kohl, Understanding a Peculiar Solar Minimum, SOHO-23:, *ASP Conference Series* 428 (2010).

[143] N. Gopalswamy, N. Nitta, P.K. Manoharan, A. Raoult, M. Pick, *Astronomy and Astrophysics* 347 (1999) 684-695.

[144] R. Payne-Scott, D.E. Yabsley, J.G. Bolton, *Nature* 160 (1947) 256-257.

[145] Boischot, *C.R* 244 (1957).

[146] N. Gopalswamy, E. Aguilar-Rodriguez, S. Yashiro, S. Nunes, M.L. Kaiser, R.A. Howard, *Journal of Geophysical Research* 110 (2005).

[147] J.P. Wild, J.D. Murray, W.C. & Rowe, *Australian J. Phys.* 7 (1954).

[148] Nelson, a. Melrose, Solar Radiophysics Cambridge Univ. Press, New York, 1985.

[149] G. Mann, A. Klassen, *Astron. Astrophys.* 441 (2005) 319-326.

[150] N. Gopalswamy, A. Lara, M.L. Kaiser, J.L. Bougeret, *J. Geophys. Res.* 106 (2001a) 25261-25278.

[151] N. Gopalswamy, S. Yashiro, M.L. Kaiser, R.A. Howard, J.-L. Bougeret, *Journal of Geophysical Research: Space Physics* 106 (2001) 29219-29229.

[152] N. Gopalswamy, A. Lara, M.L. Kaiser, J.-L. Bougeret, *Journal of Geophysical Research: Space Physics* 106 25261-25277.

[153] H.T. Classen, Aurass H., *A&A* 384 (2002).

[154] A. Shanmugaraju, Y.-J. Moon, K.-S. Cho, M. Dryer, Umapathy S., *Sol. Phys.* 233 (2006).

[155] H.S. Hudson, Warmuth A., *ApJ* 614 (2004).

[156] K.S. Cho, Y.J. Moon, M. Dryer, et al., *JGR* 110 (2005).

[157] K.S. Cho, J. Lee, Y.J. Moon, et al., *A&A* 461 (2007).

[158] S. Pohjolainen, Lehtinen, N.J., *A&A* 449 (2006).

[159] M.J. Reiner, Krucker S., Gary D.E., et al., *ApJ* 657 (2007).

[160] B. Vrˇsnak, Warmuth, A., Temmer, M., et al., *A&A* 448 (2006).

[161] C. Dauphin, N. Vilmer, S. Krucker, *A&A* 455 (2006).

[162] Y. Liu, Luhmann,, B. J.G., S.D., R.P. Lin, *ApJ* 691 (2009).

[163] R.M. Evans, M. Opher, Manchester, I. W. B., T.I. Gombosi, *ApJ* 687 (2008).

[164] Vrˇsnak B, H. Aurass, J. Magdalenic, N. Gopalswamy, *Basic properties Astron. Astrophys.* 377 (2001) 321-329.

[165] E. Aguilar-Rodriguez, N. Gopalswamy, R.J. MacDowall, S. Yashiro, M.L. Kaiser, *Solar Wind* 11/SOHO (2005) 393-396.

[166] N. Gopalswamy, S. Akiyama, S. Yashiro, Major solar flares without coronal mass ejections, in: N. Gopalswamy, D.F. Webb (Eds.), Universal Heliophysical Processes, 2009a, pp. 283-286.

[167] N. Gopalswamy, et al., *Sol. Phys.* 259 (2009b) 227-254.

[168] B. Vrˇsnak, *JGR* 106 (2001a).

[169] Gopalswamy, R. N., J. P.,, M.R. Kundu, N. Nitta, J.R. Lemen, R. Herrmann, D. Zarro, T. Kosugi, *ApJ* 455 (1995).

[170] W.J. Wagner, R.M. & MacQueen, *A&A* 120 (1983).

[171] G.A. Harvey, *JGR* 70 (1965).

[172] A. Klassen, H. Aurass, K.-L. Klein, A. Hofmann, Mann, G., *A&A* 343 (1999).

[173] J. Zhang, K.P. Dere, R.A. Howard, M.R. Kundu, & White, S.M., *ApJ* 559 (2001).

[174] J. Zhang, K.P. Dere, R.A. Howard, & Vourlidas, A., *ApJ* 604 (2004).

[175] M. Temmer, A.M. Veronig, B. Vrˇsnak, et al., *ApJ* 673 (2008).

[176] N. Gopalswamy, H. Xie, P. M¨akel¨a, S. Akiyama, S. Yashiro, M.L. Kaiser, R.A. Howard, J.L. Bougeret, *Astrophys. J.* 710 (2010b) 1111-1126.

[177] K. Kai, *Sol. Phys.* 11 (1970).

[178] A.F. Kuckes, Sudan R.N., *Sol. Phys.* 17 (1971).

[179] P. Lantos, *Sol. Phys.* 22 (1972).

[180] G.B.a.L. Gelfreikh, B. I. , *Soviet Astron.* 23 (1979).

[181] A. Vourlidas, Bastian, T. S., Nitta, N., Aschwanden, M. J., *Sol. Phys.* 163 (1996).

[182] S.M.a.K. White, M. R., *Sol. Phys.* 174 (1997).

[183] D.E.K. Gary, C. U., Solar and Space Weather Radiophysics Current Status and Future Developments Dordrecht: Kluwer, 2004.

[184] V.L. Ginzburg, V.V. Zheleznyakov, On the possible mechanisms of sporadic solar radio emission (radiation in an isotropic plasma), *Sov. Astron.* 2 (1958).

[185] W.C. Erickson, *J. Geophys. Res.* 68 (1963).

[186] M.V. Goldman, D.F. Smith, Physics of the Sun, Dordrecht: Reidel, 1986.

[187] D.B.Melrose, *Australian J. Phys.* 23 (1970) 885-903.

[188] P.A. Sturrock, *Phys. Rev. Lett.* 16 (1966).

[189] A.O. Benz, C. Monstein, a.H. Meyer, *Solar Phys.* 226 (2005) 143-151.

[190] R.P. Lin, W.K. Levedahl, W. Lotko, D.A. Gurnett, F.L. Scarf, *ApJ* 308 (1986).

[191] P.H. Yoon, *Phys. Plasmas* 2 (1995).

[192] P.H. Yoon, *Phys. Plasmas* 4 (1997).

[193] G.B. Field, *ApJ 1*24 (1956).

[194] D.B. Melrose, Plasma Astrophysics., Gordon and Breach, New York, 1980.

[195] P.A. Sturrock, in: W.N. Hess (Ed.), AAS-NASA Symposium on the Physics of Solar Flares, Washington: Sci. and Tech. Information Division, 1964.

[196] S.A. Kaplan, V.N. Tsytovich, Plasma Astrophysics (1973).

[197] K.D. Papadopoulos, M.L. Goldstein, R.A. Smith, *ApJ* 190 (1974).

[198] M. Karlický, Kosugi T., *A&A* 419 (2004).

[199] L.A.a.G. Frank D.A., *Solar Phys.* 27 (1972).

[200] H. Alvarez, F.T. Haddock, Lin R. P., *Sol. Phys.* 26 (1972).

[201] J. Fainberg, L.G. Evans, Stone R.G., *Science* 178 (1972).

[202] D.A. Gurnett, R.R. Anderson, *Science* 194 (1976).

[203] D.A. Gurnett, R.R. Anderson, *J. Geophys. Res.* 82 (1977).

[204] S. Bardwell, M.V. Goldman, *ApJ* 209 (1976).

[205] P.A. Robinson, L.H. Cairns, D.A. Gurnett, *ApJ* 407 (1993).

[206] P.A. Robinson, A. Willes, I.H. Cairns, *ApJ* 408 (1993b).

[207] R.A. Smith, M.L. Goldstein, K. Papadopoulos, *ApJ* 234 (1979).

[208] A.J. Willes, P.A. Robinson, D.B. Melrose, *Phys. Plasmas* 3 (1996).

[209] M. Pick, A. Kerdraon, F. Auch`ere, G. Stenborg, A. Bouteille, E. Soubri´e, *Sol. Phys.* 256 (2009) 101.

[210] D. Oberoi, et al., *Astrophysical Journal Letters* (2010b).

[211] B.V. Jackson, K.V. Sheridan, Proceedings of the Astronomical Society of Australia, 1979.

[212] K.a.V.d. Burg, *Sol. Phys.* 77 (1982).

[213] A. Klassen, S. Pohjolainen, K.-L. Klein, *Sol. Phys*. 218 (2003).

[214] d. Jager, Sol. Phys. 2 (1967).

[215] Z. Hamidi, Z. Ibrahim, Z. Abidin, M. Maulud, N. Radzin, N. Hamzan, N. Anim, N. Shariff, Designing and Constructing Log Periodic Dipole Antenna to Monitor Solar Radio Burst: e-Callisto Space Weather Project, 2nd International Conference on Applied Physics and Mathematics, AICIT Press, 2011, pp. 1-4.

[216] Mittra, K.E. Jones, Theoretical brillouin diagrams for monopole and dipole arrays and their applications to log-periodic antennas, IEEE Trans. Antennas Propag, 1964, pp. 533-540.

[217] W.H. G.H. Zhai, K. Wu, Z.Q. Kuai *Antennas Propag.* 4 (2010) 899-905.

[218] D.E.Isbell, Antenna Propagate (1960) 260-267.

[219] R.L.Carrel, *IRE Conv. Rec.* 1 (1961) 61-75.

[220] Z. Hamidi, Z. Ibrahim, Z. Abidin, M. Maulud, N. Radzin, N. Hamzan, N. Anim, N. Shariff, Designing and Constructing Log Periodic Dipole Antenna to Monitor Solar Radio Burst: e-Callisto Space Weather Project, (2012).

[221] Z.S. Hamidi, C. Monstein, Z.Z. Abidin, Z.A. Ibrahim, N.N.M. Shariff, Modification and Performance of Log Periodic Dipole Antenna, *International Journal of Engineering Research and Development* 3 (2012) 36-39.

[222] Z. Hamidi, N. Anim, N. Hakimi, N. Hamzan, A. Mokhtar, N. Syukri, S. Rohizat, I. Sukma, Z. Ibrahim, Z. Abidin, *International Journal of Fundamental Physical Sciences* 2 (2012).

[223] Z. Hamidi, N. Shariff, C. Monstein, The Different Between the Temperature of the Solar Burst at the Feed Point of the Log Periodic Dipole Antenna (LPDA) and the CALLISTO Spectrometer, (2014).

[224] Z. Hamidi, N. Shariff, *International Journal of Science and Mathematics* 2 (2014) 3.

[225] Z.S. Hamidi, Z. Ibrahim, Z. Abidin, M. Maulud, N. Radzin, N. Hamzan, N. Anim, N. Shariff, *International Journal of Applied Physics and Mathematics* 2 (2011) 3.

[226] Z.S.Hamidi, Z. Abidin, Z. Ibrahim, N. Shariff, C. Monstein, *International Journal of Engineering Research and Development* 3 (2012) 36-39.

[227] Z.S.Hamidi, N.M.Anim, N. N.S.Hakimi, N.Hamzan, A.Mokhtar, N.Syukri, S.Rohizat, I.Sukma, Z.A. Ibrahim, Z.Z.Abidin, N.N.M.Shariff, C.Monstein, *International Journal of Fundamental Physical Sciences* 2 (2012) 4.

[228] Z. Hamidi, N. Shariff, Evaluation of signal to noise ratio (SNR) of log periodic dipole antenna (LPDA), Business Engineering and Industrial Applications Colloquium (BEIAC), 2013 IEEE, IEEE, 2013, pp. 434-438.

[229] Z. Hamidi, N. Shariff, *International Letters of Chemistry, Physics and Astronomy* 7 (2014) 21-29.

[230] S.-C. Bon, Y.-H. Kim, H. Roh, K.-S. Cho, S. Choi, J.-H. Baek, C. Monstein, A.O. Benz, Y.-J. Moon, S.S. Kim., *Journal of The Korean Astronomical Society* 42 (2009) 7.

[231] Z.S.Hamidi, S. Chumiran, A. Mohamad, N. Shariff, Z. Ibrahim, N. Radzin, N. Hamzan, N. Anim, A. Alias, *American Journal of Modern Physics* 2 (2013) 4.

[232] Z. Hamidi, S. Chumiran, A. Mohamad, N. Shariff, Z. Ibrahim, N. Radzin, N. Hamzan, N. Anim, A. Alias, *American Journal of Modern Physics* 2 (2013).

[233] Z.S.Hamidi, N.N.M.Shariff, Evaluation of Signal to Noise Ratio (SNR) of Log Periodic Dipole Antenna (LPDA) Business Engineering and Industrial Applications Colloquium 2013, IEEE, Langkawi, Malaysia, 2013, pp. 434-438.

[234] C. Monstein, R. Ramesh, C. Kathiravan, *Bull. Astr. Soc. India* 35 (2007) 473-480.

[235] Z.S. Hamidi, N.N.M. Shariff, C. Monstein, *The International Journal of Engineering* 1 (2012) 3.

[236] A.O. Benz, C. Monstein, H. Meyer, P.K. Manoharan, R. Ramesh, A. Altyntsev, A. Lara, J. Paez, *Solar Phys.* 55 (2004) 121-134.

[237] A.O. Benz, M. Guedel, H. Isliker, S. Miszkowicz, W. Stehling, *Sol. Phys.* 133 (1991) 385-393.

[238] P. Messmer, A.O. Benz, C. Monstein, *Sol. Phys.* 187 (1999) 335-345.

[239] Z. Hamidi, Z. Abidin, Z. Ibrahim, N. Shariff, Effect of light pollution on night sky limiting magnitude and sky quality in selected areas in Malaysia, Sustainable Energy & Environment (ISESEE), 2011 3rd International Symposium & Exhibition in, IEEE, 2011, pp. 233-235.

[240] Z. Hamidi, N. Shariff, C. Monstein, *International Letters of Chemistry, Physics and Astronomy* 10 (2014) 38-45.

[241] Z. Hamidi, N. Shariff, Z. Abidin, Z. Ibrahim, C. Monstein, *Middle-East Journal of Scientific Research* 12 (2012) 893-898.

[242] Z.S. Hamidi, N. Shariff, Z. Abidin, Z. Ibrahim, C. Monstein, *Middle-East Journal of Scientific Research* 12 (2012) 6.

[243] A.O. Benz, C. Monstein, H. Meyer, P.K. Manoharan, R. Ramesh, A. Altyntsev, A. Lara, J. Paez, K.-S. Cho, *Earth Moon and Planets* 104 (2009) 277-285.

[244] Z.S. Hamidi, Z.Z. Abidin, Z.A. Ibrahim, N.N.M. Shariff, Indication of radio frequency interference (RFI) sources for solar burst monitoring in Malaysia, AIP Conference Proceedings 1454 (2012) 43.

[245] Z. Hamidi, N.Shariff, Z. Abidin, Z. Inrahim, C. Monstein, *Malaysian Journal of Science and Technology Studies* 9 (2013) 15-22.

[246] Z.S.Hamidi, Z. Abidin, Z. Ibrahim, C. Monstein, N. Shariff, *International Journal of Fundamental Physical Sciences* 2 (2012) 32-34.

[247] V.V. Lobzin, I.H. Cairns, P.A. Robinson, G. Steward, G. Patterson, *The Astrophysical Journal Letters* 710 (2010) 58-62.

[248] Z. Hamidi, N. Shariff, R. Umar, *Thailand Journal of Physics* 3 (2012) 6.

[249] Z.S.Hamidi, N.N.M.Shariff, R.Umar, *Malaysia Thailand Journal of Physics* 3 (2012) 6.

[250] R. Umar, Z. Abidin, Z. Ibrahim, N. Gasiprong, K. Asanok, S. Nammahachak, S. Aukkaravittayapun, P. Somboopon, A. Prasit, N. Prasert, *Middle East Journal of Scientific Research* 14 (2013).

[251] R. Umar, Z.Z. Abidin, Z.A. Ibrahim, M.S.R. Hassan, Z. Rosli, Z.S. Hamidi, *American Institute of Physics (AIP) Proceedings* 1454 (2012) 39-42.

[252] N. Anim, Z. Hamidi, Z. Abidin, C. Monstein, N. Rohizat, Radio frequency interference affecting type III solar burst observations, 2012 NATIONAL PHYSICS CONFERENCE: (PERFIK 2012), American Institute of Physics Proceedings, 2013, pp. 82-86.

[253] Z. Hamidi, Z. Abidin, Z. Ibrahim, N. Shariff, *AIP Conference Proceedings-American Institute of Physics* 1454 (2012).

[254] Z. Hamidi, Z.Z. Abidin, Z.A. Ibrahim, M.F. Zabedi, M.A. Yaacob, F. Khallaf, N. Shariff, Investigations of Radio Frequency Interference (RFI) Profile Analysis, (2012).

[255] Z. Hamidi, Z.Z. Abidin, Z.A. Ibrahim, M.F. Zabedi, M.A. Yaacob, F. Khallaf, N. Shariff, *Science of Structure Formation - Light, Energy, Material, and Space* 3 (2011) 33-36.

[256] Z. Hamidi, Z. Abidin, Z. Ibrahim, N. Shariff, U.F.S.U. Ibrahim, R. Umar, Preliminary analysis of investigation Radio Frequency Interference (RFI) profile analysis at Universiti Teknologi MARA, Space Science and Communication (IconSpace), 2011 IEEE International Conference on, IEEE, 2011, pp. 311-313.

[257] Z.S.Hamidi, Z. Abidin, Z. Ibrahim, N. Shariff, Indication of radio frequency interference (RFI) sources for solar burst monitoring in Malaysia, ICPAP 2011, AIP Publisher, Indonesia, 2012, pp. 6.

[258] Z. Hamidi, N. Shariff, *International Letters of Chemistry, Physics and Astronomy* 5 (2014) 43-49.

[259] Z. Hamidi, N. Shariff, C. Monstein, Evaluation of Spectral Overview and Radio Frequency Interference (RFI) Sources at Four Different Sites in CALLISTO Network at the Narrow Band Solar Monitoring Region, (2014).

[260] Z. Hamidi, N. Shariff, *Thermal Energy and Power Engineering* 3 (2014).

[261] Z. Hamidi, N. Shariff, C. Monstein, *International Letters of Chemistry, Physics and Astronomy* 13(2) (2014) 144-154.

[262] Z. Hamidi, N. Shariff, *International Letters of Chemistry, Physics and Astronomy* 4 (2014) 29-36.

[263] Z. Hamidi, Z. Abidin, Z. Ibrahim, C. Monstein, N. Shariff, M. Sabaghi, *International Journal of Fundamental Physical Sciences* 2 (2012).

[264] Z. Hamidi, N. Shariff, *International Letters of Chemistry, Physics and Astronomy* 5 (2014) 32-42.

[265] Z. Hamidi, Z. Abidin, Z. Ibrahim, C. Monstein, N. Shariff, *International Journal Physical Fundamental Sciences* (2012).

[266] Z.S. Hamidi, N. Anim, N.N.M. Shariff, Z.Z. Abidin, Z.A. Ibrahim, C. Monstein, Dynamical structure of solar radio burst type III as evidence of energy of solar flares, in: R.Shukor (Ed.), PERFIK 2012, American Institute of Physics, Malaysia, 2013, pp. 11-15.

[267] Z. Hamidi, N. Anim, N. Shariff, Z. Abidin, Z. Ibrahim, C. Monstein, Dynamical structure of solar radio burst type III as evidence of energy of solar flares, Persidangan Fizik Kebangsaan (PERFIK) 2012, Universiti Kebangsaan Malaysia, 2012, pp. 11-15.

[268] Z. Hamidi, C. Monstein, N. Shariff, Radio Observation of Coronal Mass Ejections (CMEs) Due to Flare Related Phenomenon on 7 th March 2012, (2012).

[269] Z. Hamidi, N. Shariff, C. Monstein, First Light Detection of A Single Solar Radio Burst Type III Due To Solar Flare Event, (2014).

[270] Z. S. Hamidi, N. N. M. Shariff, C. Monstein, W. N. A. Wan Zulkifli, M. B. Ibrahim, N. S. Arifin, N. A. Amran, *International Letters of Natural Sciences* 5 (2014) 10-17

[271] Z. Hamidia, Z. Abidina, Z. Ibrahima, N. Shariffa, C. Monsteinc, Observations of Coronal Mass Ejections (CMEs) at Low Frequency Radio Region on 15th April 2012, *AIP Conf. Proc* 1528 (2013) 55-60.

[272] Z. Hamidi, N. Shariff, C. Monstein, *The International Journal of Engineering* 1 (2012) 3.

[273] Z. Hamidi, N. Shariff, C. Monstein, *International Letters of Chemistry, Physics and Astronomy* 10 (2014) 81-90.

[274] Z. Hamidi, N. Shariff, M. Ali, C. Monstein, W.W. Zulkifli, M. Ibrahim, N. Arifin, N. Amran, *International Letters of Chemistry, Physics and Astronomy* 9 (2014) 84-92.

[275] Z. Hamidi, N. Shariff, C. Monstein, W.W. Zulkifli, M. Ibrahim, N. Arifin, N. Amran, *International Letters of Chemistry, Physics and Astronomy* 8 (2014) 13-19.

[276] Z. Hamidi, N. Shariff, C. Monstein, W.W. Zulkifli, M. Ibrahim, N. Arifin, N. Amran, *International Letters of Chemistry, Physics and Astronomy* 9 (2014) 8-15.

[277] Z. Hamidi, N. Shariff, C. Monstein, Fundamental and Second Harmonic Bands of Solar Radio Burst Type II Caused by X1. 8-Class Solar Flares, (2014).

[278] Z. Hamidi, N. Shariff, C. Monstein, Statistical Study of Nine Months Distribution of Solar Flares, (2014).

[279] Z. Hamidi, N. Shariff, *International Letters of Chemistry, Physics and Astronomy* 7 (2014) 30-36.

[280] Z. Hamidi, N. Shariff, C. Monstein, Disturbances of Solar Eruption From Active Region AR1613, (2014).

[281] Z. Hamidi, N. Shariff, The Propagation of An Impulsive Coronal Mass Ejections (CMEs) due to the High Solar Flares and Moreton Waves, (2014).

[282] Z. Hamidi, N. Shariff, C. Monstein, The Tendencies and Timeline of the Solar Burst Type II Fragmented, (2014).

[283] Z. Hamidi, N. Shariff, C. Monstein, Scenario of Solar Radio Burst Type III During Solar Eclipse on 14 th November 2012, (2014).

[284] Z. Hamidi, N. Shariff, C. Monstein, *International Letters of Chemistry, Physics and Astronomy* 13 (2014) 104-111.

[285] N. Hashim, Z. Abidin, U. Ibrahim, R. Umar, M. Hassan, Z. Rosli, Z. Hamidi, Z. Ibrahim, Radio Astronomy in Malaysia: Current Status and Outreach Activities, Astronomical Society of the Pacific Conference Series, 2011, pp. 355.

[286] Z. Hamidi, N. Shariff, C. Monstein, Z. Ibrahim, *International Letters of Chemistry, Physics and Astronomy* 7 (2014) 37-44.

[287] Z. Hamidi, N. Shariff, C. Monstein, Z. Abidin, Z. Ibrahim, N. Hashim, R. Umar, N. Aziz, *International Journal of Fundamental Physical Sciences* 3 (2013).

[288] Z. S. Hamidi, N. N. M. Shariff, C. Monstein, *International Letters of Natural Sciences* 8(1) (2014) 9-16.

(Received 29 April 2014; accepted 01 June 2014)